



Virginia Commonwealth University
VCU Scholars Compass

Theses and Dissertations


Graduate School

2021

Development of SAM-based Chemical Probes for Methyltransferases

Daniel V. Mongeluzi
Virginia Commonwealth University

Follow this and additional works at: <https://scholarscompass.vcu.edu/etd>

 Part of the [Medicinal and Pharmaceutical Chemistry Commons](#)

© The Author

Downloaded from

<https://scholarscompass.vcu.edu/etd/6782>

This Thesis is brought to you for free and open access by the Graduate School at VCU Scholars Compass. It has been accepted for inclusion in Theses and Dissertations by an authorized administrator of VCU Scholars Compass. For more information, please contact libcompass@vcu.edu.

Daniel Mongeluzi 2021

All rights reserved

Development of SAM-based Chemical Probes for
Methyltransferases

Daniel Mongeluzi

June 1, 2021

Thesis Director's name title and department

A thesis/dissertation submitted in partial fulfillment of the requirements for the degree of (list degree, for example, Master of Science, Doctor of Philosophy) at Virginia Commonwealth University.

Acknowledgement

I would first like to thank my supervisor Dr. Yana Cen for all of the help and expertise she has provided me throughout my time in her lab. I feel very fortunate to have been a part of her research laboratories. Thank you so much for always giving me words of encouragement that allowed me to complete my masters. With your help I was given every opportunity to succeed.

In addition to this, I would like to acknowledge my committee members, Dr. Li and Dr. Aberg. I would like to thank you all for the guidance you have given me while working on my project.

I would like to thank all of my lab mates Dr. Dawanna White, Alyson Curry, Dickson Donu, Dr. Wenjia (Ivy) Kang, and Rosalie Hoyle. Thank you for all of the help you have given me while working on this project. I would like to specifically thank Dr. Dawanna White for taking the time to work with me in the lab and answer all of the questions I have had.

I would like to express my gratitude to my parents, grandparents, and sisters. Thank you for raising me too always push me to achieve greater things. Also, thank you for all of the support you have given me, and calming me down when I was stressed. Dad, thank you for reminding me about your report card every time something didn't go perfect. Mom, thank you for starting my love for learning that has led me to this point. Pop-pop, thank you for talking to me for being an amazing mentor and friend to me throughout my entire life.

I would like to thank all of the friends I have made while going through graduate school. Specifically, I would like to thank Jeremy, Rawan, and Akua for taking time outside of school to explore Richmond and eating tons of great food around the city.

Table of Contents

Abstract	6-8
1. Introduction	9-30
1.1 Epigenetic regulation of gene expression	9-11
1.2 Epigenetic modification protein and enzymes and their roles in disease.....	11-12
1.3 Methyltransferase	12-17
1.3.1 DNA Methyltransferases	12-14
1.3.2 Histone Methyltransferases	14-17
1.4 Small molecule MTase probes	17-19
1.5 MTase inhibitors	19-21
1.6 Activity-Based Protein Probes	21-29
1.6.1 ABPP probes	23-26
1.6.2 Comparative ABPP	26-27
1.6.3 Competitive ABPP	27-29
1.7 Goal of the current research	29-30
2. Experimental section	31-56
2.1 Specific aims	31-35
2.1.1 Aim 1: design and synthesis of the SAM-based chemical probes for MTase profiling	31-33
2.1.2 Aim 2: Biochemical characterization of SAM-based chemical probes	34-35
2.1.2.1 Aim 2.1: establishment and optimization of recombinant MTase labeling and enrichment using SAM-based chemical probes	34-35
2.1.2.2 Aim 2.2: cell lysate labeling using ABPP probes	35
2.2 Methods	35-55
2.2.1 Synthesis	35-50
2.2.2 Protein purification	50-55
2.2.2.1 Plasmid prep	50-51
2.2.2.2 PCR	51-53

2.2.2.3 Transforming cells	53
2.2.2.4 Protein purification	53-54
2.3 Noncompetitive protein pull-down assay	55-56
2.4 Competitive protein pull-down assay	56
3. Results and Conclusions	57-73
3.1 Synthesis of probe 1	57-60
3.2 EHMT1 expression and purification	60-62
3.3 Photoaffinity labeling and affinity enrichment of EHMT1 assay	62-69
3.3.1 Optimization of irradiation time	62-63
3.3.2 Optimization of probe concentration	63-64
3.3.3 Improvement of enrichment assay	64-66
3.3.4 Pull-down assay lacking filtration step	66-67
3.3.5 Optimized pull-down assay	67-69
3.4 Pull-down assay using an adenosine binding protein	69-70
3.5 competitive labeling assay	70-71
3.6 spiked in cell lysate	71-72
3.7 Conclusion	72-73
NMR Spectrums	74-85
References	86-99

position with NaN_3 . The biotin tag was tethered to the C6-position of the adenine ring through a 1,6-hexadamine linker.^{9,11} The 5'-OH can then be selectively deprotected to afford the photocrosslinkable adenosine derivative probe 4 (Fig. 2B). The later stage of the synthesis focuses on the installation of the “warhead”. The 5'-OH was activated as a mesylate, which can then be replaced by a methylamino group.⁶ The subsequent reductive amination with *tert*-butyl (*S*)-2-[*N*-(*tert*-butoxycarbonyl) amino]-4-oxobutanoate allowed the “warhead” to be fully incorporated into the structure. Finally, the global deprotection should provide the desired SAM analog, probe 1. We are still in the process of finalizing the last step of the synthesis.

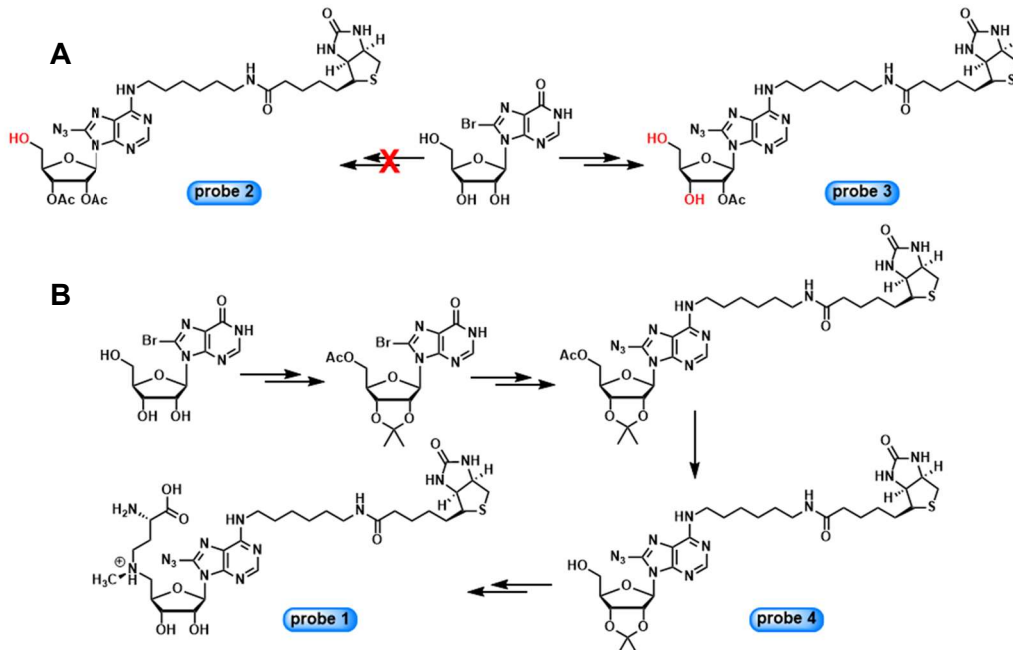


Fig.2. Synthetic plans for probe 1. **A.** Original plan involves the tri-*O*-acetylation of the hydroxyl groups on the ribose ring. However, the selective deprotection of 5'-OH was challenging; **B.** Revised plan features the selective protection/deprotection of 5'-OH.

In parallel to the synthetic effort, we also established and optimized the photoaffinity labeling and affinity capture assays. Recombinantly expressed and purified human euchromatin histone lysine methyltransferase 1 (EHMT1) was used for the initial assay development. Several parameters such as irradiation time, probe dosage, and elution conditions were fine-tuned to ensure accurate profiling of active enzymes. The protein was incubated with probe 3, followed by UV irradiation to trigger the covalent conjugation (Fig. 3A).^{8,12} The unbound free probes were then filtered off. Subsequently, streptavidin beads were introduced to the sample to capture the biotinylated protein. Ultimately, EHMT1 was eluted off the beads and analyzed by western blot using anti-biotin antibody. EHMT1 was only strongly labeled by probe 3 at high micromolar concentrations (Fig. 3B, left). We reasoned that probe 3 is an adenosine analog rather than a SAM analog. It may demonstrate selectivity towards adenosine-binding proteins.

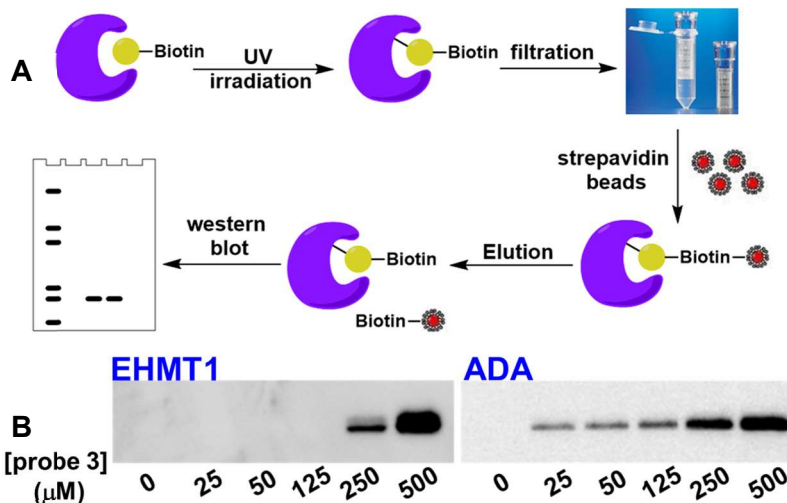


Fig.3. Photoaffinity labeling and affinity capture of recombinant proteins using synthetic probe. **A.** Schematic representation of the labeling and enrichment protocols; **B.** Western blots showing the labeling of EHMT1 (left) and ADA (right) with probe 3. The biotinylated proteins were detected with anti-biotin antibody.

Indeed, probe 3 labeled adenosine deaminase (ADA) in a concentration-dependent manner (**Fig. 3B, right**). Even at the lowest probe concentration, ADA can still be labeled and enriched. The labeling can be competed off using a known ADA inhibitor, suggesting the on-target effect of the probe.

The labeling strategy was also applied to cell lysates. It has the advantage of enriching the active enzymes independently of protein abundance, allowing the capture of dynamic enzyme activity changes in response to environmental or cellular stimuli.

In the current study, the facile synthesis of SAM analogs was developed. Photoaffinity labeling and affinity enrichment protocols were developed. The probes were able to label recombinant proteins, and demonstrated target selectivity. The synthesis of probe 1 will be completed. These innovative chemical probes will be used to profile MTase activity in their native matrix to better understand their roles in different cellular events.

1. Introduction and Background

1.1 Epigenetic regulation of gene expression

Epigenetics, a term first used by C.H. Waddington in 1942, is defined as the changes in gene expression without changing the genetic code of the organism.¹³ These changes are achieved through epigenetic modifications as well as chromatin remodeling, which regulate the accessibility of specific genes to the transcriptional machinery.¹⁴ The three major epigenetic changes include: 1) covalent modifications at the DNA level, namely, DNA methylation; 2) covalent modifications of the histone N-terminal tails such as methylation, acetylation or phosphorylation; and 3) non-coding RNA regulations such as siRNA and miRNA.¹⁵ All of these changes orchestrate the access of DNA, which serves as the main interface between environmental cues and transcription activation/suppression. For the scope of the current study, the following discussion will focus on DNA methylation and histone modifications.

In eukaryotic cells, DNA is wrapped around histone proteins to form nucleosomes, which are considered the basic units of chromatin.^{16,17} The packaging of DNA into chromatin controls the accessibility of genetic materials. DNA methylation, more specifically, the methylation of cytosine residues in the promoter region of genes has profound consequences in gene transcription. Simple methylation at the 5-position of cytosine at CpG islands prevents the binding of transcription factors to the promoter region, ultimately leading to gene silencing.¹⁸ The significance of 5-methylcytosine (5mC) in transcription silencing, genomic imprinting and cellular differentiation has been well established.^{19,20} This is why sometimes 5mC is referred to as “the fifth base” of the genome.

The histone octamer is composed of two copies of each of the core histones H2A, H2B, H3, and H4.^{16,17,21} The N-terminal tails of histones are prone to posttranslational modifications (PTMs)

including, but not limited to, methylation, acetylation, phosphorylation and SUMOylation.²² Accumulating evidence suggested that the N-terminal tails of histones interact with neighboring nucleosomes to affect the overall chromatin structure.²¹ In addition to regulating the binding affinity of DNA to histones,²³ the PTMs also serve as the docking sites to recruit effector proteins resulting in chromatin remodeling, transcription regulation, and DNA repair.^{24,25} Among all the histone PTMs, lysine acetylation was the first to be reported.²⁶ The addition of acetyl group to lysine side chain ϵ -amino group, which is positively charged under normal physiological conditions, neutralizes the positive charge and weakens the interactions between histone and negatively charged DNA backbone. Consequently, chromatin relaxation occurs to allow transcription activation.²⁷ The acetylation can be reversed for chromatin condensation, which is closely associated with transcription silencing.

Histone methylation, in contrast, is more complex than acetylation. It occurs on lysine and arginine residues. Methylation does not change the charges of these amino acids. To make it more complex, lysines can be mono-, di- or tri-methylated, and arginines can be mono- or di-methylated (either symmetrically or asymmetrically).^{28,29} Furthermore, the functional consequences of histone methylation rely on the methylation degree and methylation site. For example, the trimethylation of histone H3 lysine 27 (H3K27me3) by polycomb group proteins is closely associated with transcription silencing.³⁰ On the contrary, the trimethylation of histone H3 lysine 4 (H3K4me3) is a hallmark of transcription activation *via* the recruitment of RNA polymerase II elongation factors.^{31,32}

Epigenetic changes are heritable and affected by various factors such as development, exposure to environmental chemicals, administration of drugs and other pharmaceuticals, aging, and diet.^{33,34} For example, during the Dutch famine of 1944-1945, malnutrition ran rampant through

population of the Netherlands. When examined at the DNA levels, it was noticed that there appeared to be dysregulation of the DNA methylation patterns in the survivors due to prenatal exposure to the famine.³⁵

1.2 Epigenetic modification proteins and enzymes and their roles in diseases

The dynamic and reversible epigenetic landscape is maintained by a group of proteins and enzymes including “writers”, “erasers” and “readers”.^{36,37} The “writer” enzymes are responsible for the introduction of covalent modifications to DNA nucleobase or histone amino acids. DNA methyltransferases (DNMTs) and histone acetyltransferases (HATs) are examples of the “writers”. “Erasers”, on the other hand, are dedicated for the removal of chemical modifications from DNA or histone proteins. Histone deacetylases (HDACs) and histone lysine demethylases (KDMs) represent the “eraser” enzymes.²³ “Reader” proteins specialize in the recognition and interpretation of epigenetic marks. Specialized domains in chromatin modifiers act as “readers” such as bromodomains (BRDs)³⁸ and plant homeodomains (PHDs).³⁹

Growing evidence demonstrated that the epigenetic proteins work coordinately to regulate gene transcription, and defects of these proteins play important roles in disease initiation and development. On one hand, altered functions caused by mutations or altered protein abundance of an epigenetic regulator protein may directly impact gene expression, leading to diseases such as cancers. Alternatively, an aberrant gene expression may be driven by an upstream factor, and epigenetic proteins serve as mediators in this signaling cascade.⁴⁰ The reversible nature of epigenetic modifications suggest that any dysregulation can be restored by drugs targeting the epigenetic regulators.^{37,41}

The last few decades witnessed tremendous efforts in pursuing “writers”, “erasers”, and “readers” as viable therapeutic targets. However, the success stories were scarce. The DNMT

inhibitor, azacitidine, was the first epigenetic drug to be approved by FDA for the treatment of myelodysplastic syndrome.⁴² Vorinostat, a small molecule HDAC inhibitor, was approved for cutaneous T-cell lymphoma.⁴³ It is important to point out that these success relied solely on phenotypic observations before the mechanism of action (MOA) was discovered. Several DNMT and HDAC inhibitors have been marketed later on, most of which are analogs of azacitidine or vorinostat.⁴⁴ Since then, the drug discovery focus has been shifted to other epigenetic targets. For example, the once considered “undruggable” BRDs became the highly sought-after targets for epigenetic drug discovery, owing to their implications in cancers and other diseases.⁴⁵ A handful of BRD inhibitors have become clinical candidates for cancers,^{46,47} diabetes,⁴⁶ and atherosclerosis.⁴⁸ The current bottlenecks for epigenetic drug discovery include isoform-selectivity, substrate selectivity, and combination therapy, among the others.^{44,49,50} With the rapid progress of “oimcs” analysis, phenotypic assays as well as structural biology studies, it is anticipated the discovery and development of epigenetic drugs will be greatly accelerated.^{44,51,52}

1.3 Methyltransferases

Methyltransferases (MTases) are a group of epigenetic writer enzymes that are responsible for the methylation of nucleobases and histone protein amino acids. Methyltransferases most often methylate lysine and arginine of histone proteins, and cytosines in DNA. In the process of methylation MTases transfer a methyl group to their target from *S*-adenosyl-L-methionine (SAM) transforming it into *S*-adenosyl-L-homocysteine (SAH).

1.3.1 DNA Methyltransferases

DNA methyltransferases (DNMTs) are a family of enzymes that are responsible for the methylation of the 5 position of cytosines into 5-methylcytosine (Fig. 1).⁵³ The mammalian

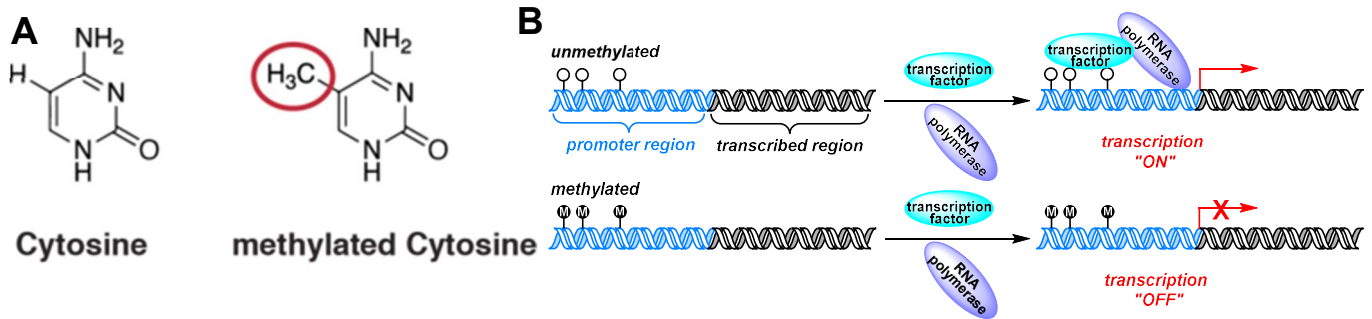


Figure 1. A. DNMTs methylate the 5 position of cytosine. B. DNA that is unmethylated on the promoter region easily allows transcription factors to interact and transcribe the gene. When methylation occurs on the promoter region the transcription factors cannot easily interact with the DNA and prevents transcription of the gene.

DNMT family is comprised of DNMT1, DNMT2, DNMT3A, DNMT3B, and DNMT3L. If the methylation to the DNA occurs on a cytosine that is located in the promoter region of a gene could cause the gene to be silenced.

DNMT1, DNMT3A, and DNMT3B are responsible for the methylation of cytosines in the DNA.¹⁹ DNMT1 functions by selectively hemimethylating DNA. Hemimethylation is methylation of just one of the two complementary strands of DNA. DNMT3A/3B are *de novo* DNA MTases,⁵⁴ which is attributed to their activity in methylation during embryogenesis. An up regulation of any one of these three DNMTs can lead to hypermethylation of the genome. Hypermethylation of the p16 tumor suppressor gene has been linked to non-small cell lung cancer (NSCLC).⁵⁵ The upregulation of the three above-mentioned DNMTs have been observed in myeloid leukemia.^{39,52} Hypermethylation of tumor suppressor gene p15 was suggested as the cause for the myeloid leukemia. Mice embryos that have the gene for DNMT1, DNMT3A, or DNMT3B deleted become unviable and expire before development.

Instead of methylating DNA, DNMT2 specifically methylates the 38th cytosine on tRNA.³⁵ DNMT2 is primarily localized in the cytoplasm of mammalian cells, instead of the nucleus like

other DNMTs. DNMT2 knock out mice tRNAs have a higher rate of amino acid substitutions, leading to the incorrect codon recognition.^{54,55}

The DNMT family is round out by DNMT3L,⁵⁶ which lacks the same C-terminal domain that gives DNMT3A and DNMT3B their activity. DNMT3L does not methylate DNA or RNA like the rest of the DNMTs. It has no catalytic activity all by itself. It has been reported that the activity of DNMT3A or DNMT3B is increased when they interact with DNMT3L.⁵⁴

1.3.2 Histone Methyltransferases

There are 2 classes of histone MTases, lysine MTase (KMT) and arginine MTase (PRMT).⁵⁷ Both of these MTases are responsible for the methylation of specific lysine or arginine residues in histone proteins' tails. Lysine can be mono, di, or trimethylated by KMTs (Fig. 2.), while arginine can only be mono or dimethylated by PRMTs. Methylating histone tails does not always lead to suppressed gene transcription like it does for DNA methylation. Methylation of histone tails can activate or suppress gene expression. The change in gene expression is dependent on the degree and location that the methylation occurs to.

Some residues, such as H3K4, H3K9, H3K27, H3K36, H3K79, and H4K20 are more likely to be methylated by KMTs. Euchromatin Histone Methyltransferase 1 (EHMT1), also known as

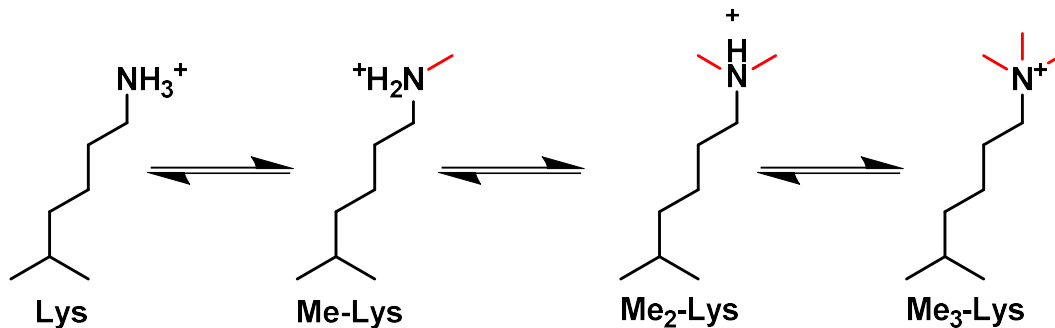


Figure 2. KMTs with methylate the amine on Lysine. This methylation can occur in monomethylation, demethylation, or trimethylation. This methylation does not change the charge of the lysine residue, instead location and degree of methylation lead to the change in gene expression.

G9a-like protein (GLP),¹ is a well-studied KMT that most often mono- or dimethylates H3K9. EHMT1 has been observed to methylate other proteins, such as H3K27 and even itself. Mono methylation of the K370 has been linked to the suppression of tumor suppressor gene p53.⁵⁸ Esophageal cancer specifically has been linked to an overexpression of EHMT1, and levels of EHMT1 present have been linked to physical characteristics of the tumors.⁵⁹

Enhancer of Zeste Homolog 2 (EZH2) is a KMT that when up regulated has been linked to poor prognosis of colorectal cancer.^{57,60} EZH2 is the core part of Polycomb Repressor Complex 2 (PRC2), a group of enzymes that aid in the methylation of H3K27. (Fig. 3. A.) Trimethylation of H3K27 has been linked to gene silencing due to a subsequent recruitment of DNMTs that perform *de novo* methylation in cancer cells.^{57,60} Because of this, EZH2 has also been linked to many other cancers such as pancreatic cancer, prostate cancer, lung cancer, and breast cancer.⁶⁰

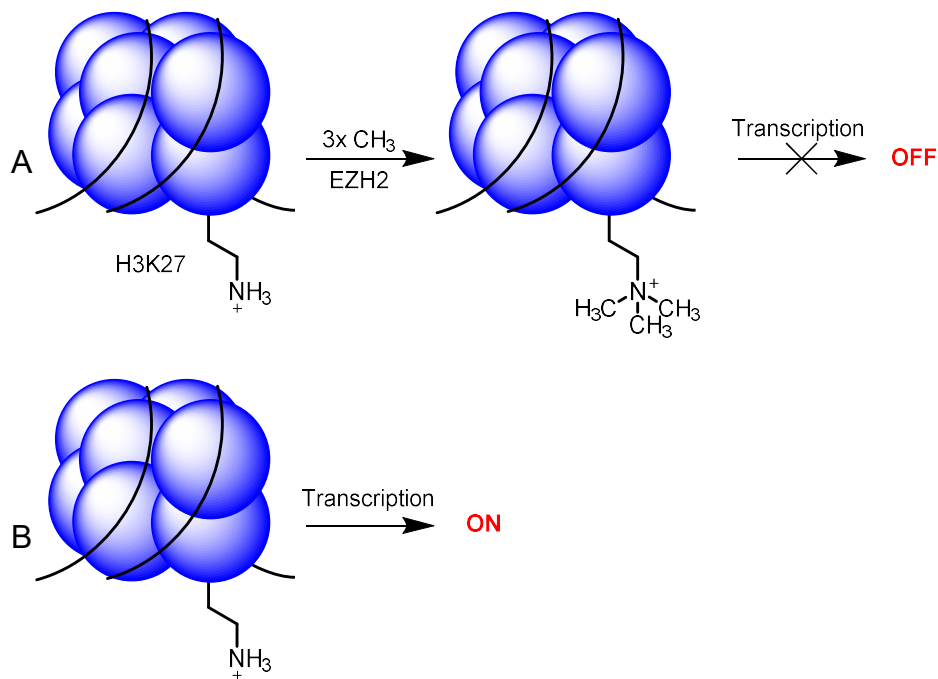


Figure 3. A. Methylation of H3K27 by EZH2 leads to the suppression of the genes. B. In the absence of EZH2 methylation of H3K27 cannot occur, this leaves the genes active.

Labs like Wei Qi et al have worked on synthesizing small molecule inhibitors to prevent hypermethylation of H3K27 caused by EZH2 as a treatment for colorectal cancer.⁶¹

Another important KMT is the Disruptor of Telomeric silencing 1-Like (DOT1L).⁶² DOT1L gene knock out has been observed in yeast, flies, mice, and humans, a commonality between all of these samples is that H3K79 is always unmethylated.^{1,63} This leads to the conclusion that DOT1L is the only KMT that can mono, di, or trimethylate H3K79. This is important to know because dysregulation of DOT1L leads to hypermethylation of H3K79 and can lead to Mixed Lineage Leukemia (MLL). In addition to a link to MLL, DOT1L is partially responsible for recruiting DNA repair proteins such as tumor suppressor p53-binding protein 1 (53BP1).³⁸ If there are lower levels of H4K20me present in the cells then 53BP1 will rely on H3K79me for recruitment. If DOT1L is downregulated then the 53BP1 no longer can repair the DNA.

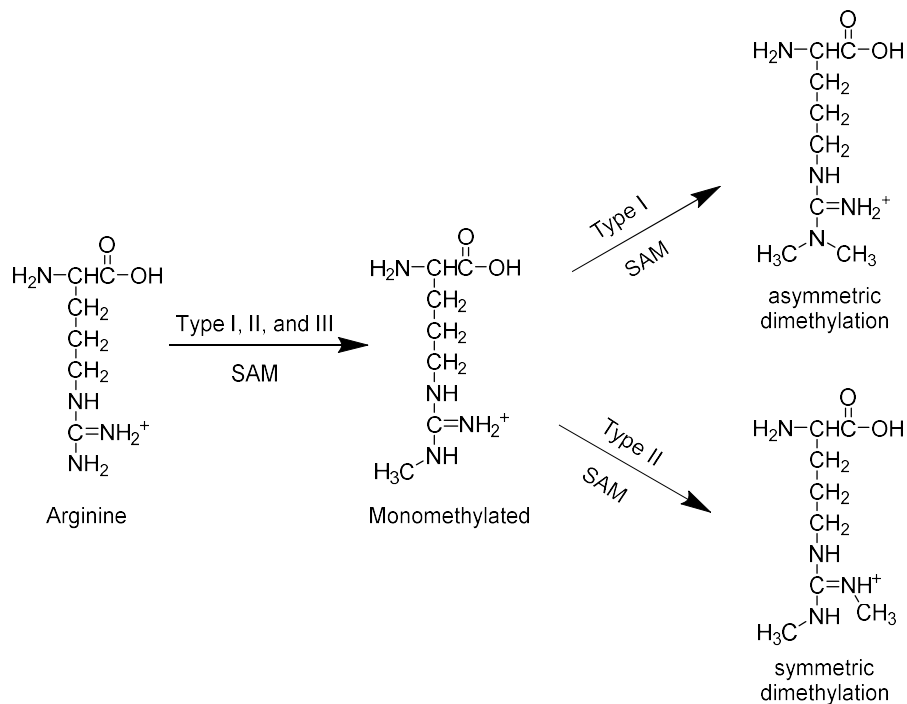


Figure 4. Type I, II, and III RMTs can perform the monomethylation of an arginine residue on a histone tail. Type I RMTs can also perform the asymmetric dimethylation reaction while Type II performs the symmetric dimethylation reaction.

PRMTs are a family of eleven MTases that are placed into three groups. The first is Type I which contains Protein arginine MTase 1 (PRMT1), PRMT2, PRMT3, PRMT4, PRMT6, and PRMT8.⁶² Type I PRMTs catalyze the formation of monomethylated arginine as well as asymmetric demethylated arginine (Fig. 4.). The second group, Type II, contains PRMT5 and PRMT9; which catalyze the formation of monomethylated arginine as well as symmetric demethylated arginine. The final group of PRMT is Type III which contains PRMT7 with a selectivity for the formation of monomethylated arginine over the formation of symmetric demethylated arginine.⁶⁴ Non-Hodgkin's Lymphoma, as well as other various cancers, have been linked to an upregulation in PRMT5.⁶⁵ In early stage clinical trials, GSK3326595, a potent PRMT5 inhibitor developed by GSK, has shown the ability to inhibit tumor growth.^{1,35}

1.4 Small Molecule MTase Probes

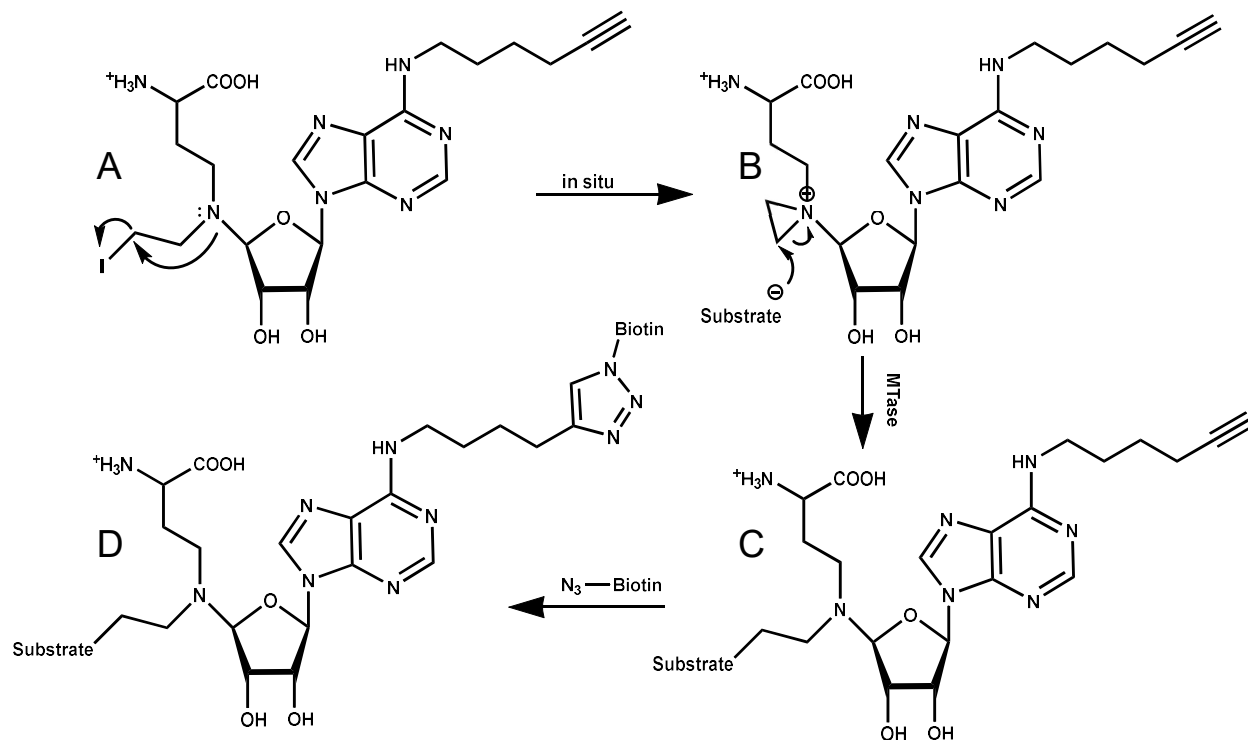


Figure 5. A. L. Comstock lab's probe B. Cyclized probe product C. Substrate-probe complex D. Substrate-probe-biotin reaction.

SAM based probes have been developed for a better understanding of MTases. Many of the probes currently available target substrates of MTases instead the MTases themselves. These powerful small molecule probes have greatly expanded the substrate range of various MTases.

Van Mai et al created a SAM based MTase probe (Fig. 5. A.) that was used in a proof-of-concept study to label MTase substrates.^{66,5} The probe has 2 functionalities that separate it from SAM. The first is an ethyl iodide functional group that replaces the methyl group on the warhead, and the second is the long linker group with an alkyne group on it. The ethyl iodide group has the iodine that is a good leaving group. The departure of iodine causes an intramolecular cyclization reaction to form an aziridine ring. When the cyclized probe interacts with a MTase and its target substrate, instead of adding a methyl group to the substrate, the entire probe is covalently connected to the substrate. Following this the substrate-probe complex can be reacted with biotin-azide *via* a click reaction. The substrate-probe-biotin complex can then be separated from the cell lysate using streptavidin beads. The captured protein can then be analyzed by mass spectrometry to determine what targets a specific MTase would have.

In the proof-of-concept study Van Mai et al tested if the probe could covalently bind to AcH4-21, a known target of PRMT1, in the presence of this MTase. The probe was incubated with AcH4-21 in a buffer solution. PRMT1 was added to the solution then given time to catalyze the addition of the probe to AcH4-21. The reaction could be quenched, then the PRMT1 could be denatured with heat, and then biotin-azide could be conjugated to the probe-AcH4-solution for separation. Following the click reaction, the probe-AcH4-21-biotin complex would be separated from the solution and then analyzed. Van Mai et al concluded that this probe could be used to study MTase's substrates.

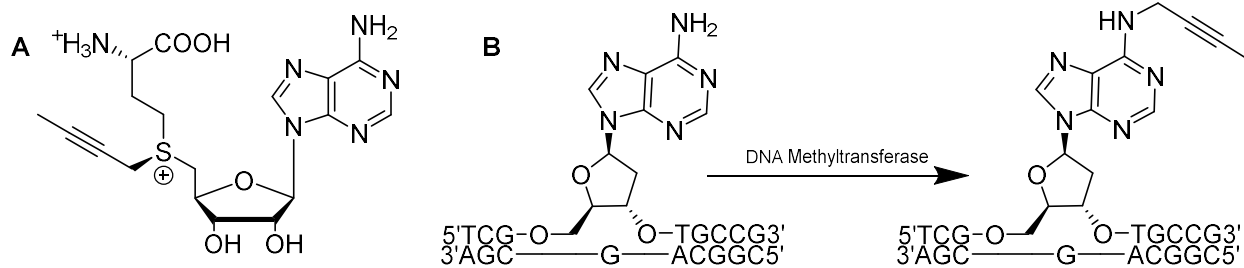


Figure 6. A. The SAM based probe created by E. Weinhold lab. B. How the probe modifies the DNA. The Methyltransferase used in this study was M.TaqI which selectively Methylates adenines that are located in TCGA regions of DNA.

Another SAM based probe was developed by Christian Dalhoffl et al (Fig. 6. A.), this probe was created to study DNMTs.⁷ Instead of acting like the previous probe and adding the entire probe to the substrate, this probe works by adding an acetyl group instead. This probe is SAM aside from one functional group change, the methyl is changed to a 2-butyne. The goal of this probe is to acetylate the DNA instead of methylating it. (Fig 5. B.) A proof-of-concept study was run with this probe, again M.TaqI and R.TaqI were used to determine if this probe could modify the DNA. Christian Dalhoffl et al tested this probe by incubating one sample with the probe, DNA, and M.TaqI and then denatured the M.TaqI and incubated the sample with R.TaqI. In the second sample DNA was incubated with M.TaqI, then the M.TaqI was denatured and it was then incubated with R.TaqI. Following this the samples were run on SDS page gels. Christian Dalhoffl et al found that these probes were successful at modifying the DNA and that the M.TaqI was able to accommodate a larger group than a methyl.

1.5 MTase Inhibitors

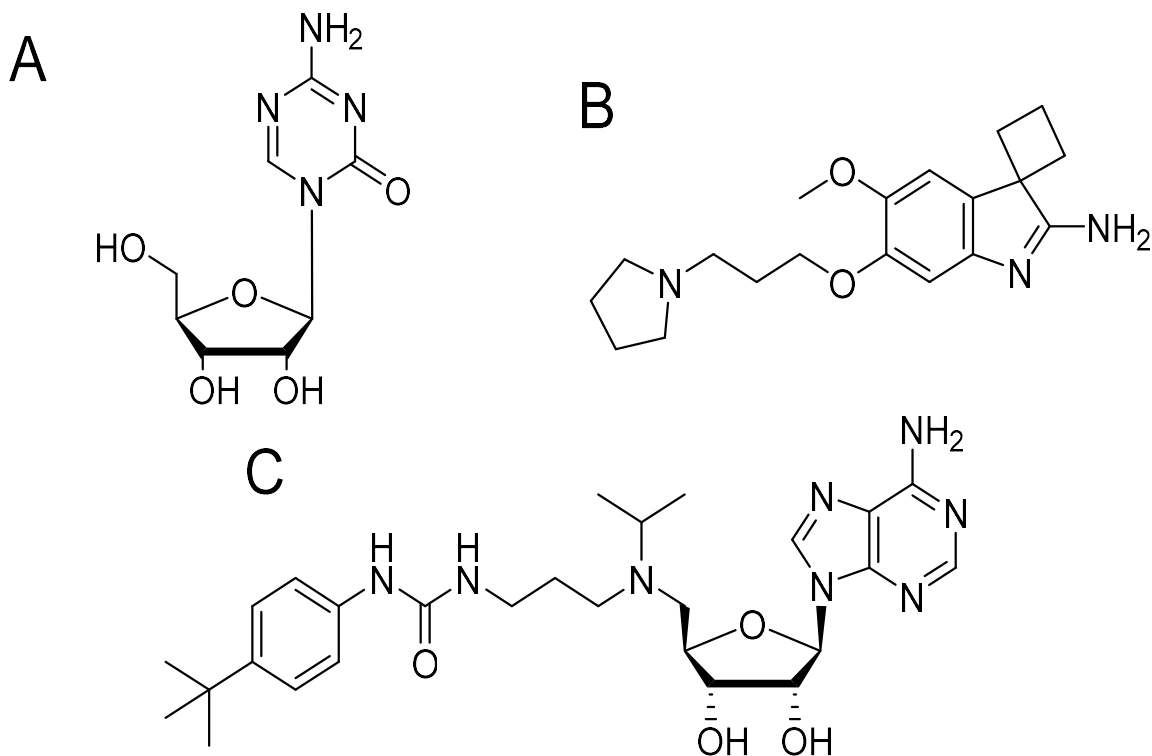


Figure 7. A. A-366 a selective EHMT1 inhibitor made by Abbvie. B. Azacitidine is an FDA approved DNMT1 inhibitor for the treatment of Myelodysplastic Syndrome. C. EPZ004777 a DOT1L inhibitor created by Epizyme as a treatment for Mixed Lineage Leukemia (MLL).

Inhibitors have been developed to overcome the dysregulation of MTases in specific disease states. MTase inhibitors have been developed to knock down or knock out specific MTases to attempt to treat specific diseases. Examples of some of these inhibitors are Azacitidine, A-366, and EPZ004777.

On May 19th, 2004, Azacitidine (Figure 7A),⁶⁷ a DNMT1 inhibitor, was approved by FDA for the treatment of myelodysplastic syndrome as well as myeloid leukemia.⁵¹ As a cytidine analog prodrug, azacitidine can be incorporated into DNA to become active. When DNMT1 attempts to methylate the azacitidine that have been incorporated into the DNA, a coupling reaction will occur to covalently tethered the DNMT1 in place. DNMT1 being covalently bound to azacitidine prevents DNMT1 from further performing its function. The inactivation of DNMT1 corrected the dysregulation that otherwise leads to hypermethylation of the tumor suppressor genes. (reference?)

A-366 is an inhibitor that was discovered by AbbVie, through high throughput screening. A-366 binds with selectivity to Euchromatin methyltransferase 1 (EHMT1) and Euchromatin methyltransferase 2 (EHMT2) (Fig. 7. B.).⁶⁸ A-366 specifically has been used in early studies as a treatment for leukemia. Being able to selectively inhibit specific MTase makes A-366 a good drug candidate. In this study A-366's ability to inhibit the dimethylation of H3K9 was compared with UNC0638. H3K9me2 was chosen because the level of this epigenetic mark is highly linked to the action of EHMT1/2. UNC0638 was selected because it was a proven EHMT1/2 inhibitor with unfavorable off target. Both compounds were incubated with MCF-7 and MDA-MB-231 cells, two breast cancer cell lines. Subsequently, the level of H3K9me2 was evaluated by western blot. Both inhibitors demonstrated comparable ability to reduce the level of H3K9me2, primarily through the inhibition of EHMT1/2.

EPZ004777 (Fig. 7. C.) is a DOT1L inhibitor that was discovered by Epizyme to prevent H3K79 methylation. DOT1L is the only known MTase to methylate H3K79.⁶³ When DOT1L is dysregulated, it can lead to the hypermethylation of H3K79 which has been linked to Mixed Lineage Leukemia (MLL).^{38,57} MLL is an aggressive cancer that accounts for 70% of infant leukemias. In this study varying concentrations of EPZ004777 were given to MLL cells, and the level of H3K79me2 was assessed by western blot. With increasing concentrations of EPZ004777, the level of H3K79me2 was gradually decreased.

1.6 Activity-based Protein Profiling

The human genome encodes 20,000~25,000 genes.⁶⁹ Based on alternative promoters or alternative splicing as well as mRNA editing, it is estimated that the transcriptome harbors ~100,000 transcripts.⁷⁰ The complex increases exponentially *via* Post Translational Modifications (PTMs). The proteomes may contain more than 1,000,000 proteins.⁷¹ The functional assignment

of these proteins in the so-called “post-genomic era” can be challenging.⁷² The classical method to study protein function involves the recombinant expression and purification of the protein target, followed by characterization using *in vitro* assays. Although useful, it is only applicable to proteins that can be expressed recombinantly. Furthermore, some proteins exist in large protein complex endogenously. Upon isolation, they may lose activity entirely. And for some proteins, activity assays are not readily available.

Proteomic analysis has been increasingly recognized as a powerful approach to investigate protein abundance on a large scale.⁷³ In cells, the protein function can be regulated by several factors such as PTMs, endogenous protein binding partners, and endogenous inhibitors.⁷⁴ It is critical to point out that these above-mentioned factors may alter protein function/activity without changing protein abundance. Thus, abundance-based proteomic studies may only provide indirect information about protein function.

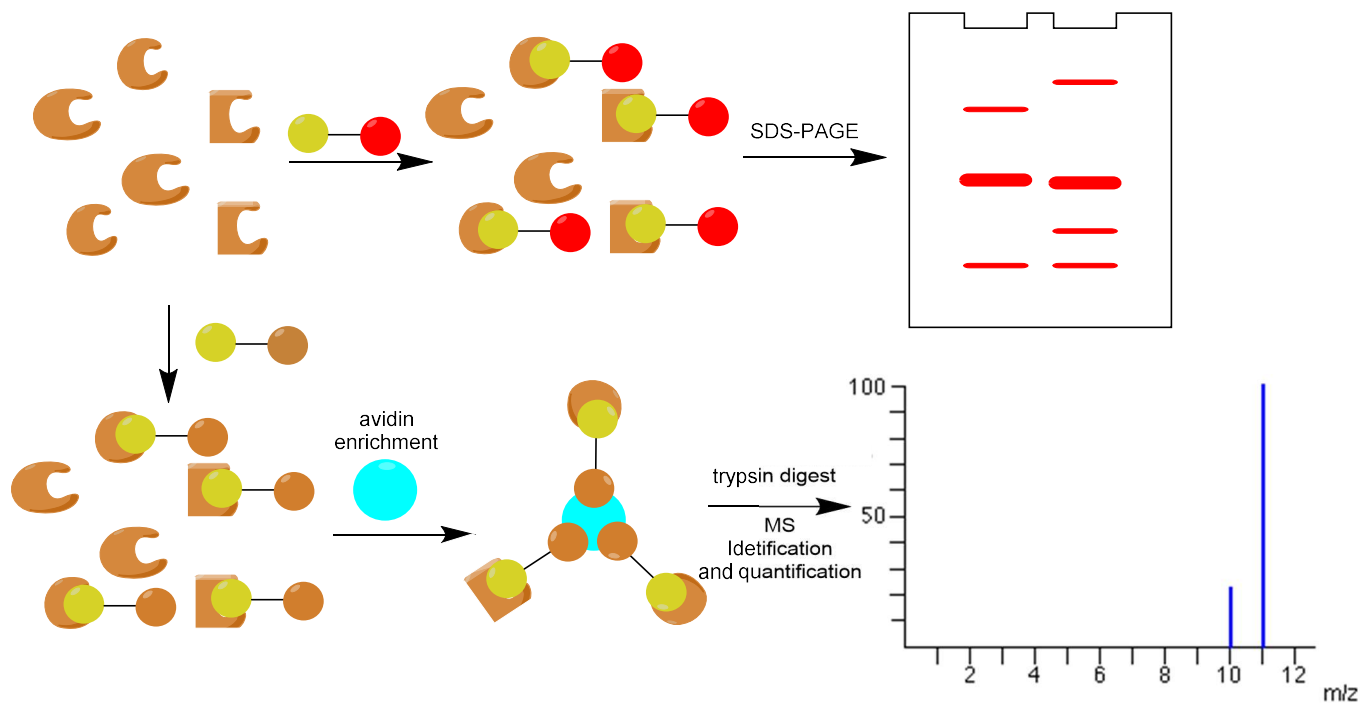


Figure 8. Proteome can be incubated with ABPP probe to selectively target active enzymes only. ABPP probes can have a fluorescent group on them to visualize active enzymes. ABPP could also have a biotin group on them to allow for binding to streptavidin beads to separate bound proteins from cell lysate and then MS analysis can be run to determine which enzymes were active.

Recent studies suggested that the functional interrogation of enzymes in complex native matrix can be accomplished by activity-based protein profiling (ABPP), pioneered by Ben Cravatt's group at the Scripps Research Institute.⁷⁵ ABPP utilizes active site-directed small molecule probes to directly confer the functional state of a particular enzyme in a complex biological sample.^{76,77} The key player in ABPP is the small molecule probe which normally has three major components: 1) a reactive group (or "warhead") that targets the active site of an enzyme; 2) a tag that allows the visualization or affinity capture of the active enzyme; 3) a linker that connects the "warhead" with the tag. The ABPP probes label the active enzyme, but not the inactive or inhibitor-bound ones. Comparison of the labeling intensity and labeling pattern in normal cells/tissues *vs* disease cells/tissues will reveal the role a specific protein plays in certain physiological or pathophysiological process, and may also suggest potential therapeutic targets for drug discovery (Fig. 8.). The past two decades have witnessed an ever-growing interest in developing ABPP probes for functional proteomics analysis.⁷⁶⁻⁷⁹ These probes greatly expanded our scope of the "druggable" proteomes and led to the discovery of some potent and selective enzyme inhibitors.^{77,80}

1.6.1 ABPP Probes

Like mentioned earlier, a typical ABPP probe comprise a "warhead", a tag, and a linker. "Warheads" are usually small molecules with high affinity against the active site of an enzyme. They can form covalent linkages with the amino acid residues (AAs) in the active site. Some

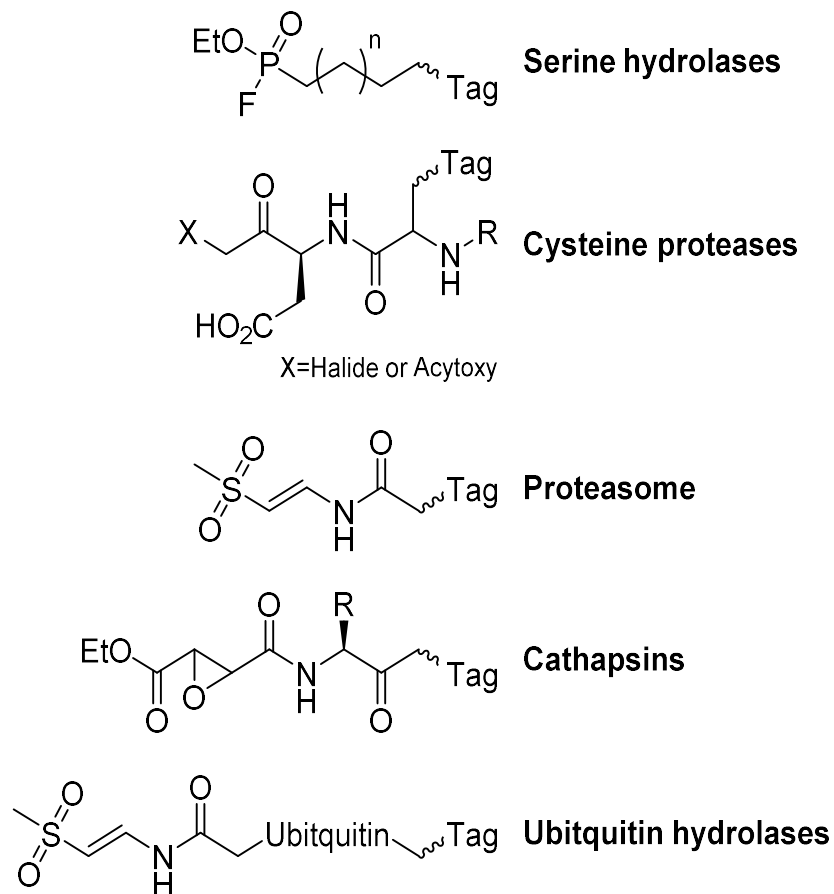


Table 1. ABPP warhead groups on the left and the proteins that the probes targeted.

representative “warheads” are listed in Table 1.⁷⁴ Most ABPP probes use electrophilic “warheads” to covalently interact with nucleophilic AAs.

In the case when nucleophilic AAs are not available in the active site, photoaffinity groups such as benzophenone, diazirine or azide can be incorporated into the probe. Upon UV irradiation, these photoactivatable groups can form covalent bond with the AAs in their vicinity (Fig. 9. B.).⁷⁴

In ABPP probes, the tag can either be a fluorophore for visualization or a biotin for the subsequent affinity enrichment.⁷⁴ Special attention is given to the size of the tags because large tags may interfere with the cell-permeability and cellular distribution of the ABPP probes. Alternatively, “click” chemistry can be used to append a tag to the ABPP probes. “Click” chemistry refers to the reaction between terminal alkyne and azide,⁸¹ two bioorthogonal functional

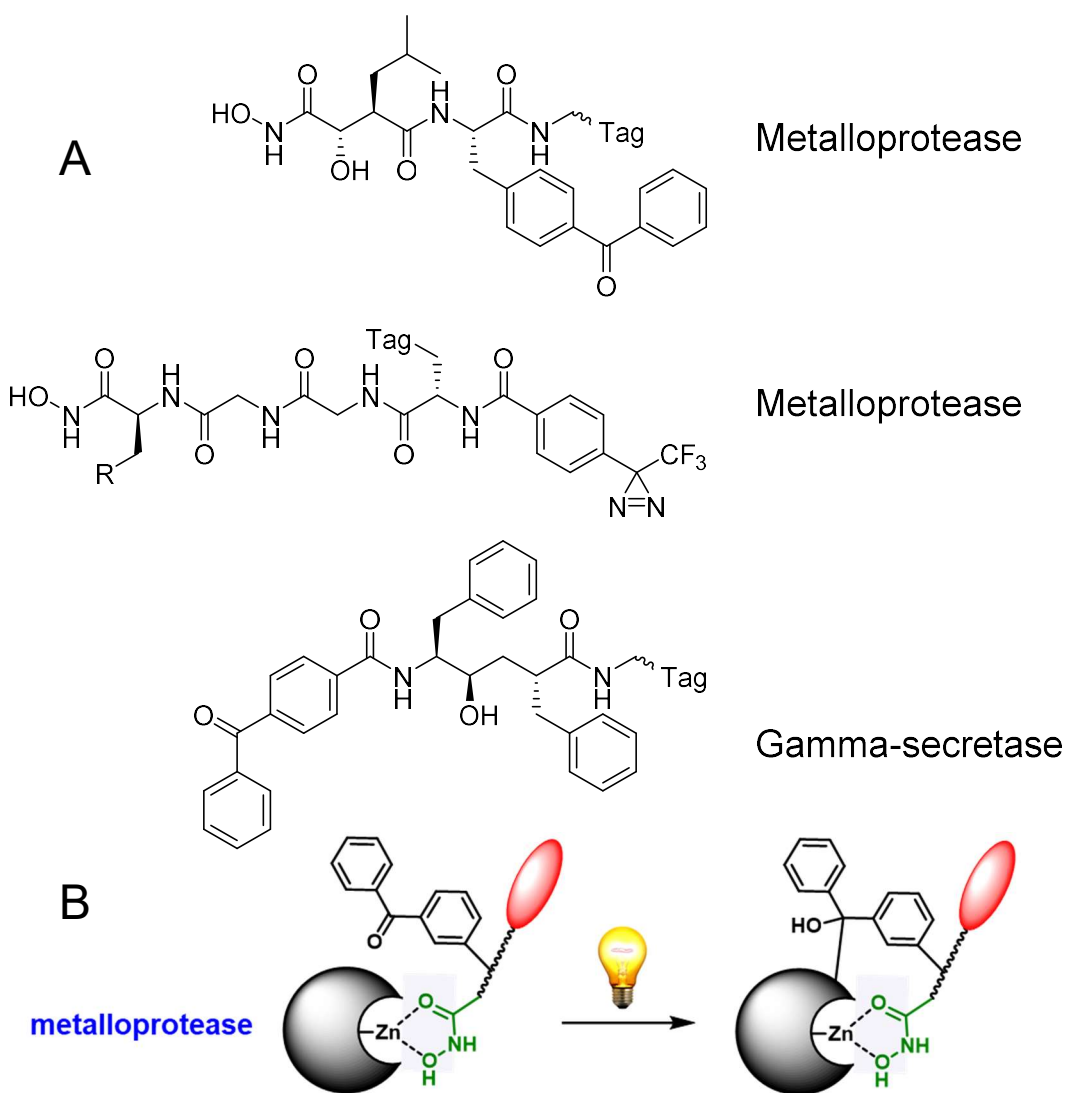


Figure 9. A. Photocrosslinking groups on ABPP probes allow for probes to covalently bind to their target enzymes. B. Schematic representation of benzophenone photocrosslinking reaction to a metalloprotease

groups. These functional groups do not exist in the native biological system. However, the presence of these groups will not interfere with the native cellular events. With the presence of copper (I) catalyst, terminal alkyne and azide undergo intermolecular cycloaddition reaction to form 1,4-disubstituted 1, 2, 3-triazole derivatives *via* the “click” chemistry.⁸¹ This reaction is spontaneous and quantitative, and is very selective between alkyne and azide.⁸¹ It demonstrates broad functional group tolerance, and has been widely utilized to investigate various biological

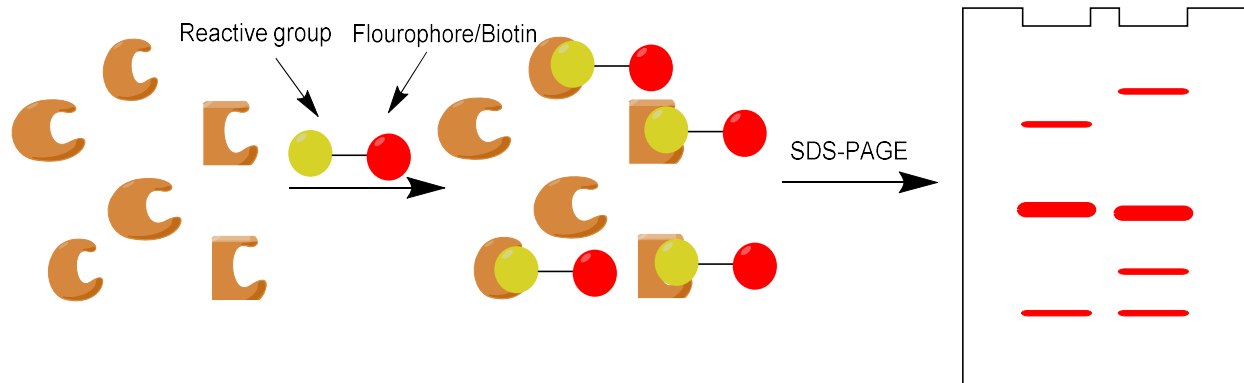


Figure 10. Schematic representation of comparative ABPP.

processes.^{82,83}

The linker of an ABPP probe tethers the “warhead” and the tag together. The presence of the linker reduces the potential steric hindrance from the tags. The linker length and composition can be varied to sample the adequate proximity, favorable solubility and cell permeability.⁷⁴ Alkyl linkers and polyethylene glycol (PEG)-based linkers are commonly used in ABPP probes. Linkers can also provide selectivity/specificity for the ABPP probes. For example, in some protease probes, the linker inherits the substrate peptide sequence that is specific for the protease target.⁸⁴

1.6.2 Comparative ABPP

In comparative ABPP, the functional states of enzymes are compared in normal and disease states. It aims to discover enzyme activities closely associated with distinct physiological or pathophysiological conditions.^{85,86} In the recent effort to uncover potential biomarkers for cancer therapy, comparative ABPP was carried out for serine hydrolase (SH).^{87,88} SHs are a large group of proteases that play critical roles in the regulation of a myriad of cellular events such as angiogenesis, hormone processing,⁸⁹ and inflammatory response.⁹⁰ More importantly, the dysregulation of SH activity has been implicated in diseases such as cancers.⁹¹ Despite the strong physiological relevance of SHs, the cellular functions of many of them remained elusive. There is a highly conserved catalytic triad including a serine, a histidine, and an aspartate in the active site

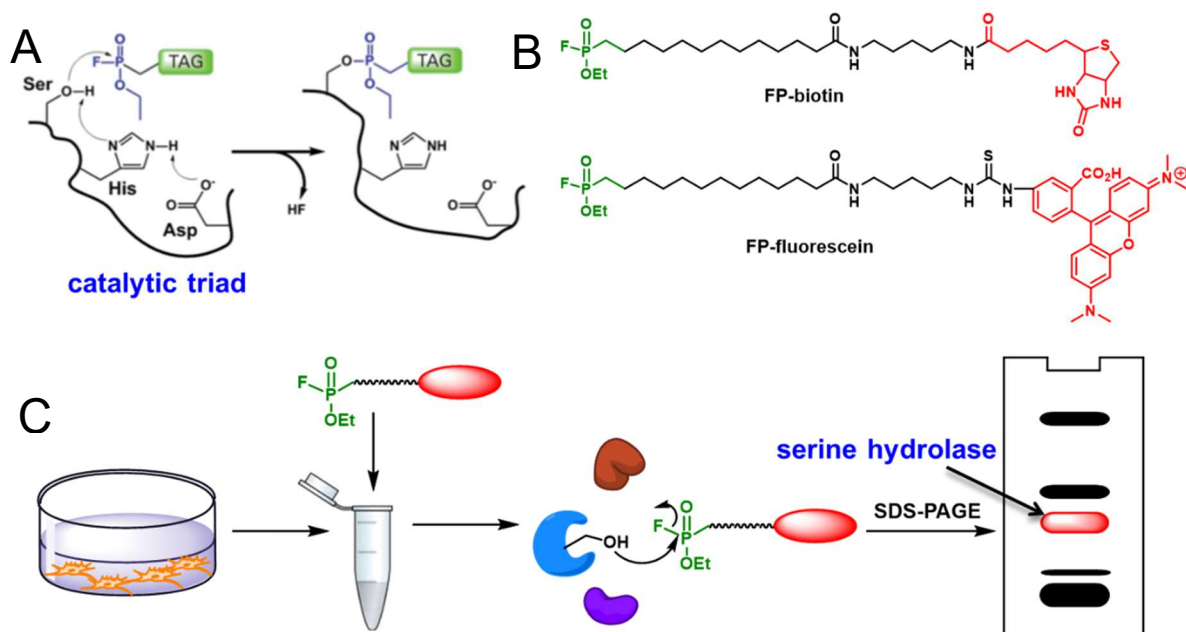


Figure 11. ABPP of serine hydrolases (SH). A. The catalytic triad in the active site of SHs. B. The chemical structures of ABPP probes for SHs. C. Schematic representation of the labeling protocol using the fluorescent ABPP probe.

of SHs (Fig. 11. A.). Targeting the nucleophilic serine residue, a couple of fluorophosphonate (FP)-based ABPP probes have been developed.⁸⁷ Both probes harbor the fluorophosphonate “warhead” which will form covalent interaction with the active site serine (Fig. 11. B.). FP-biotin carries the affinity tag, biotin, where FP-fluorescein bears a fluorophore (Fig. 11. C.). illustrates the work flow of ABPP using FP-fluorescein.

SH activity was then profiled in a panel of breast cancer and melanoma cell lines using FP-fluorescein.⁸⁸ KIAA1363 was found to be significantly upregulated in the membrane proteomes of the most invasive cancer cells. The ABPP result correlated well with the gene expression pattern, suggesting that KIAA1363 could act as a biomarker for the invasiveness of cancer cells.

1.6.3 Competitive ABPP

ABPP technology has been adapted for inhibitor discovery, namely, competitive ABPP (Fig. 12.). This type of study is normally performed in a parallel fashion in multi-well plates. To each of the wells, same concentrations of target protein and identical buffer condition will be

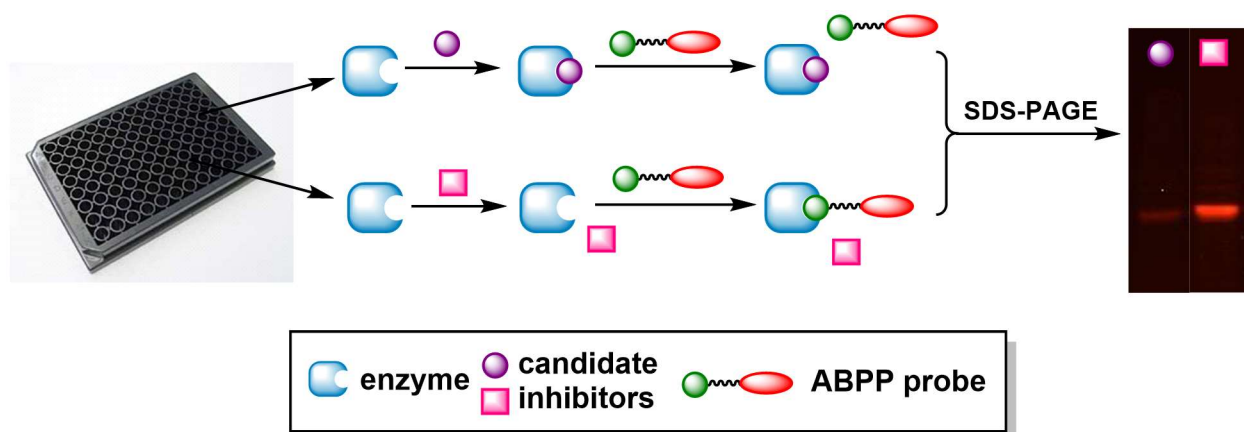


Figure 12. Competitive ABPP. In the top scheme the inhibitor prevents the ABPP probe from labeling the enzyme leading to a dull signal. In the bottom scheme the inhibitor does not bind to the active site, allowing the ABPP probe to bind more easily leading to a more intensely fluorescent band.

introduced. Subsequently, a different inhibitor candidate will be added to each well, followed by the addition of an ABPP probe. There are two possible scenarios: on one hand, if the candidate compound is indeed an inhibitor, it is going to block the active site of the enzyme to prevent the ABPP from interacting with the target, leading to reduced or complete loss of labeling (Fig. 11. top). Alternatively, the candidate compound may not be an inhibitor for the protein target. Then the active site is still available for the normal labeling by the ABPP probe to occur (Fig. 11. bottom). This method can be applied to cell lysates, so there is no need to recombinantly express and purify the protein target. It does not require the use of substrate, which renders this approach suitable for enzymes without known substrates. The competitive ABPP has been used for the discovery of inhibitors for SHs, cysteine proteases, and lipases.⁹²

A study completed by Andrea Zuhl et al used competitive ABPP to identify selective inhibitors for SHs.^{75,88} In this study fluorophosphonate probes were used in a competitive assay to determine if aza- β -lactams (ABLs) could be used as selective SH inhibitors. This idea that ABLs

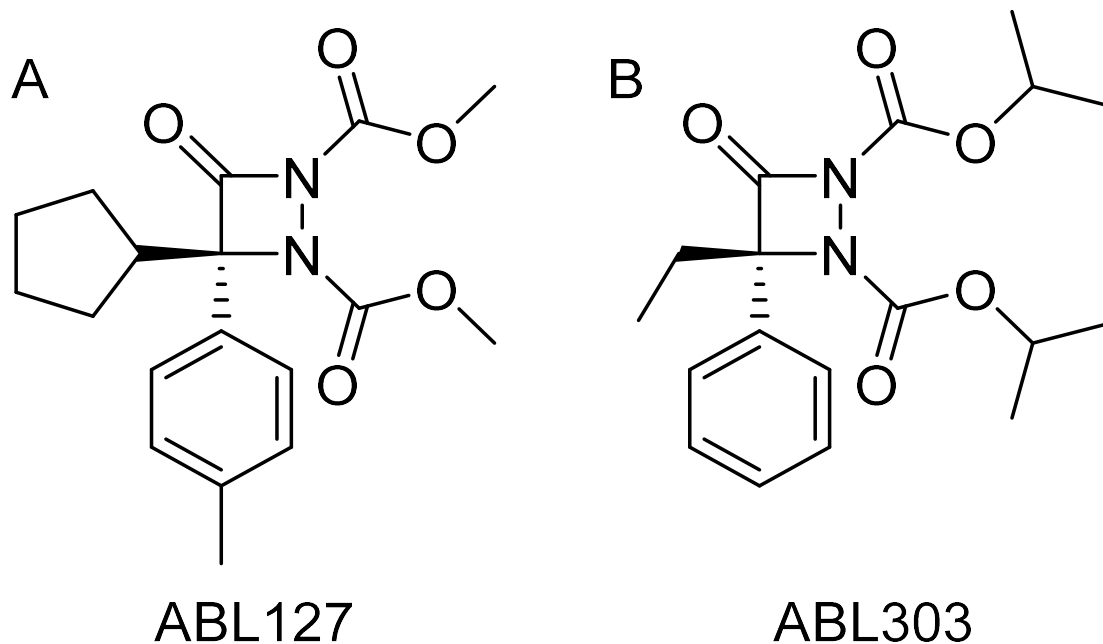


Figure 13. A. ABL127 a known inhibitor for Protein Phosphatase Methyltransferase 1 (PME1). Was discovered from high throughput screening. B. ABL303 is a selective ABHD10 inhibitor that was discovered using competitive ABPP.

might make for selective SH came from the discovery of ABL127 from high throughput screening. (Fig. 13. A.) ABL127 is a selective inhibitor for Protein Phosphatase Methyltransferase 1 (PME-1). In the study a mouse brain proteome was treated with both the fluorophosphonate probes tagged with biotin as well as prospective ABL inhibitors. This led Andrea Zuhl et al to ABL303, a selective inhibitor of ABHD10 with nanomolar potency. (Fig. 13. B.) Looking at the differences between ABL127 and ABL303 Andrea Zuhl et al concluded that minor alterations to ABLs could lead to other selective inhibitors of SHs.

1.7 Goals of the current research

Short term goal:

1. To develop activity-based chemical probes for the profiling of MTase activity in their native environment.
2. To apply the ABPP probes to the labeling and enrichment of recombinant MTases, endogenous MTases in cell lysates.

Long term goal:

Our group has a long-standing interest in generating creative chemical probes to study enzymatic mechanisms, and developing novel therapeutics for diseases with unmet medical needs. Recently, we have been using a highly integrative chemical biology approach to interrogate the functional state of epigenetic modification enzymes in their native matrix. The current project is in collaboration with Dr. Stanley Stevens at the University of South Florida. The project will examine the impact of ethanol on the brain with specific focus on epigenetic regulation of microglia through histone methylation and its influence on activation phenotype after ethanol exposure. Although a growing body of data demonstrates the ability of ethanol to influence changes in epigenetic modifications in various cell/tissue types, the ethanol-induced epigenetic code and mechanisms underlying cell type-specific changes in this code are far from being deciphered. The *central hypothesis* of the project is that alteration of the histone methylation code could be a major regulatory event associated with various microglial activation phenotypes at different stages of ethanol exposure. Our group is responsible for the synthesis and characterization of ABPP probes targeting SAM-dependent MTases. Ethanol-induced activity changes of MTases in microglia will be quantified by Dr. Stevens' team using the ABPP probes in combination with MS approaches. It is expected that changes in MTase activity through ethanol is important to define a complete mechanistic network involved in microglia activation mediated by histone methylation.

2. Experimental Section

2.1 Specific Aims

2.1.1 Aim 1: Design and synthesis of SAM-based chemical probes for MTase profiling.

The human proteome encoded more than 200 MTases. Despite the intense pursuit of MTases as potential therapeutic targets, the endogenous substrates and biological functions of many MTases remain elusive. The need for innovative chemical probes to evaluate MTase activity in the native biological matrix becomes apparent. In this aim, we will develop an ABPP probe to enable the subsequent profiling of MTase activity in native biological samples. This probe (probe 1, Fig 14.) is a structural analog of SAM with several major components: 1) a methylated nitrogen “warhead” mimics the positively charged sulfur in SAM; 2) a photocrosslinkable azido group for the covalent modification of the target enzyme; and 3) a biotin tag for the subsequent affinity capture by streptavidin beads.

SAM is a universal methyl donor for MTases. The SAM analog, probe 1, should be readily recognized by the MTase family members. To enhance the small molecule-protein interaction, a

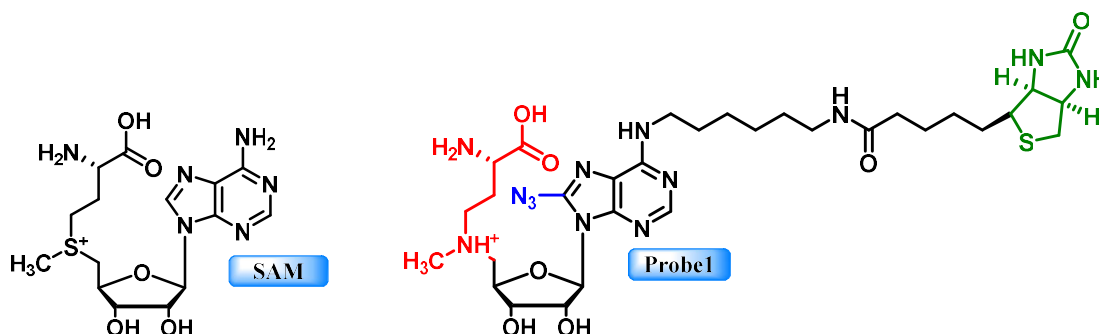


Figure 14. Chemical structure of SAM and probe 1. In red we see the modified SAM warhead group. Instead of a sulfur group in SAM we instead see an amine group. This makes the methyl a poor leaving group and should allow the probe to spend more time in the binding pocket. In blue we see the azide photocrosslinking group. When exposed to a specific wavelength of light in close proximity to a protein it will covalently bond the probe to the protein. The final group is green, the biotin tag. The biotin tag will allow the probe to bind to streptavidin beads, and be separated from cell supernatant.

photoactivatable azido group is introduced at the 8-position of the adenine ring. Upon photo irradiation, it is expected that this group will form an irreversible, covalent adduct with the AAs in its vicinity. Azido group is chosen as the photoaffinity group because of its small size and good quantum yield. And there is ample literature precedent on the installation of azido groups on nucleobases. Careful inspection of the crystal structures of several MTases suggests that the exocyclic amino group at the C6 position of the adenine ring is solvent accessible and can easily accommodate a biotin tag. The biotin tag is tethered to the adenine ring through a hexadamine linker to reduce the potential steric hindrance.

Figure 15 illustrates the synthetic plan for probe 1. Commercially available 8-bromoinosine can be protected using acetic anhydride and DMAP in anhydrous CH_2Cl_2 to generate 2', 3', 5'-*O*-triacetyl-8-bromoinosine. Subsequently, the azido group can be readily installed at 8-position with sodium azide in DMF furnishing intermediate 3. Mono-*N*-Boc-1,6-diaminohexane will be coupled to the 6-position with PyBOP in the presence of DIPEA to generate *N*⁶-substituted adenosine 4. The deprotection of the *N*-Boc group in intermediate 4 will be accomplished with trifluoroacetic acid (TFA) yielding intermediate 5. Biotin can then be coupled to the primary amino group using EDCI/DMAP to form the *N*⁶-biotinylate-8-azido-adenosine 6. Finally, the 5'-hydroxy group will be selectively deprotected in ammonia in methanol at -40°C to afford the photocrosslinkable adenosine derivative probe 2.

The later stage of the synthesis will focus on the installation of the “warhead” onto the 5'-position of probe 2 (Fig. 15). The 5'-hydroxy group can be activated with methanesulfonyl chloride to obtain mesylate 7. Intermediate 7 can then be treated with methylamine, during which the installation of the methylamino functionality and the deprotection of 2' and 3'-hydroxy groups will be accomplished simultaneously. The subsequent reductive amination between intermediate

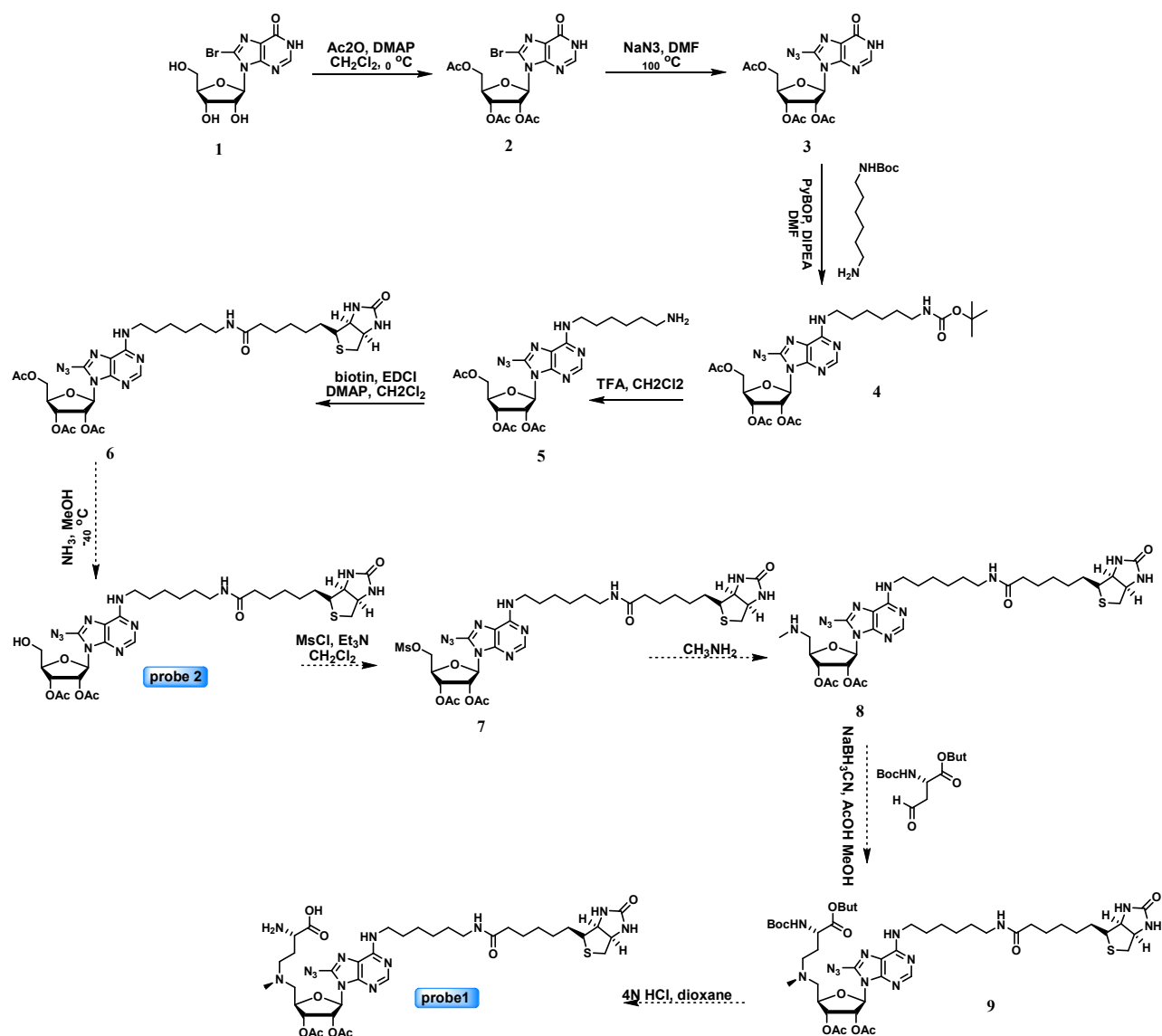


Figure 15. Synthetic scheme 1

8 and *tert*-butyl (*S*)-2-[*N*-(*tert*-butoxycarbonyl) amino]-4-oxobutanoate in the presence of NaBH₃CN and acetic acid will lead to the formation of intermediate 9. Finally, the global deprotection with 4N HCl in dioxane will provide the desired photocrosslinkable SAM analog, probe 1.

Most of the reactions listed above have literature precedent, and some of them have been tested out on small scales in Dr. Cen's lab to confirm feasibility. All the new compounds synthesized will be fully characterized by ¹H NMR, ¹³C NMR and HRMS.

2.1.2 Aim 2: Biochemical characterization of SAM-based chemical probes.

2.1.2.1 Aim 2.1 Establishment and optimization of recombinant MTase labeling and enrichment using SAM-based chemical probes.

Photoaffinity labeling and the subsequent affinity enrichment of recombinant MTase with the synthetic probes serves as the model study. Recombinant protein has the advantage of being ample in amount and free of background noise. Important labeling parameters can be easily optimized to enable accurate profiling of active enzymes. Technical details will be fine-tuned to achieve fast, selective, and efficient labeling. The optimized protocols will then be applied to proteome labeling using cell lysates.

Euchromatin histone lysine methyltransferase 1 (EHMT1) belongs to the lysine methyltransferase subfamily. Extensive studies on EHMT1 have revealed its role in epigenetic silencing of gene transcription and DNA repair. It has also been closely associated with genetic Alzheimer's disease and various cancers. The plasmid of human EHMT1 is commercially available from Addgene. We plan to purchase the plasmid and recombinantly express and purify the protein using a published protocol. The identity of the protein will be confirmed by tryptic digestion followed by LC-MS/MS analysis performed at the Vermont Biomedical Research Network Proteomics Facility.

The purified protein will then be subjected to the photoaffinity labeling and affinity capture process. EHMT1 will be incubated with the ABPP probe, followed by UV irradiation to affect the covalent conjugation. Subsequently, streptavidin beads will be introduced to the sample to capture the biotinylated EHMT1. Ultimately, EHMT1 will be eluted off the beads and analyzed by western blot. Several parameters such as irradiation time, probe dosage, and elution conditions will be further optimized. It is expected that probe 1, a close analog of SAM, can efficiently label EHMT1.

One of the major challenges in photoaffinity labeling is the non-specific labeling, which may create false positive results. To rule out the possibility of off-target effect, competition labeling experiments will also be performed. The introduction of excess amount of a known EHMT1 inhibitor should out-compete the labeling of EHMT1 by probe 1, confirming the on-target effect of the ABPP probe.

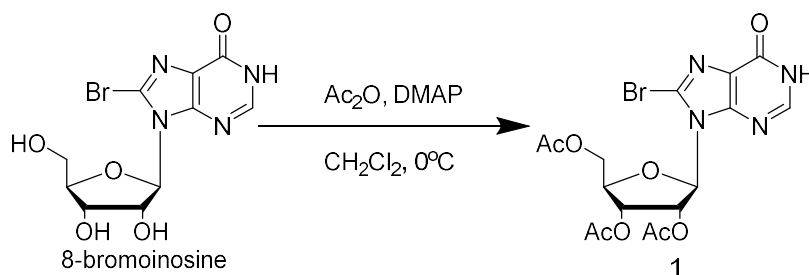
2.1.2.2 Aim 2.2 Cell lysate labeling using ABPP probes.

Probe 1 will be applied to the labeling of MTases in cell lysate. The identities of the labeled proteins can be further verified by either western blot or Mass Spectrometry (MS). This strategy has the advantage of enriching for the active enzymes independently of protein abundance, allowing the capture of dynamic enzyme activity changes in response to environmental and cellular stimuli.

2.2 Methods

2.2.1 Synthesis

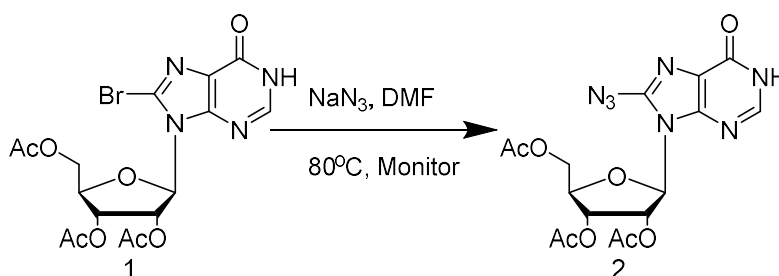
All reagents and solvents were purchased from Fisher Scientific (Somerville, NJ) or Sigma-Aldrich (St. Louis, MO) and used without additional purification.



Scheme 1. the protection of the 2, 3, and 5 positions of the ribose sugar ring on 8-bromoinosine.

In a 100 mL 24/40 flame dried round bottom flask and a solution of 8-bromoinosine (1 g, 2.881 mmol) and DMAP (35.2 mg, 0.288 mmol) in dry dichloromethane (10 mL) was cooled at 0°C for 5-7 mins. To the cooled reaction mixture acetic anhydride (2.72 mL, 28.808 mmol) was slowly

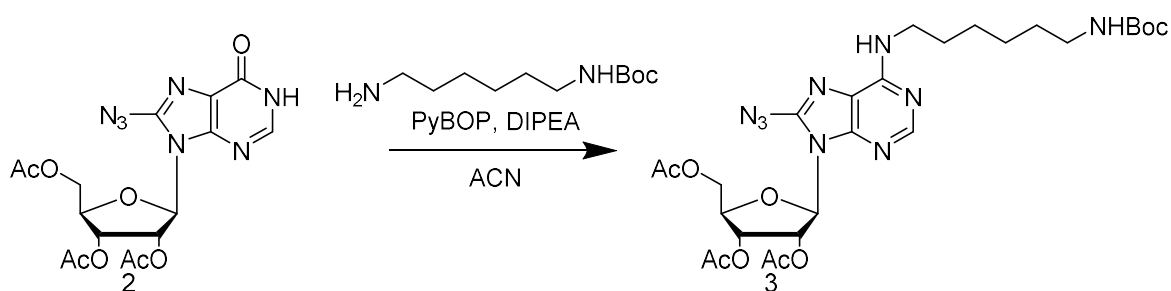
added. After 2 hours of stirring at 0°C, while ice was continuously added, the mixture was taken off of ice and stirred at room temperature overnight. The next morning the reaction mixture was quenched with ice water mixture and the ice was allowed to melt before extraction. The reaction mixture was washed with DCM (3 x 10 mL) before the organic layer was pooled and washed with saturated solution of sodium bicarbonate (3 x 10 mL) followed by brine. The dichloromethane layer was dried over anhydrous sodium sulfate and concentrated to a pale-yellow oil and subjected to flash column chromatography (5% MeOH/DCM).⁶ 68.7% isolated yield. ¹H NMR (400 MHz, CDCl₃) δ 12.43 (s, 1H), 8.09 (s, 1H), 6.23 (t, J = 5.2 Hz, 1H), 6.10 (dd, J = 4.6, 2.3 Hz, 1H), 5.78 (t, J = 6.0 Hz, 1H), 4.60 – 4.03 (m, 2H), 2.16 (s, 1H), 2.11 (s, 1H), 2.07 (s, 1H). ¹³C NMR Mass Spec HRMS (ESI) C₁₆H₁₇BrN₄O₈ Calc. 413.2322, found 414.1113.



Scheme 2. The addition of the photo crosslinking azide group to intermediate 1.

Add NaN₃ (403.1 mg, 6.201 mmol) to a solution of 2',3',5'-O-triacetyl-8-bromoinosine (733.6 mg, 1.550 mmol) in 3 mL of anhydrous DMF in a 50 mL flame dried 24/40 round bottom flask. The reaction was stirred at 80°C while being monitored by TLC until the consumption of starting material. The reaction was cooled down to room temp and the solvent was removed under reduced pressure. Water (5 mL) was added to the reaction mixture and the product was extracted with dichloromethane (3 times). The combined organic layer was washed with sat. NaHCO₃, water and brine and dried over Na₂SO₄ before being filtered and concentrated down.⁶⁶ 60.2% isolated yield.

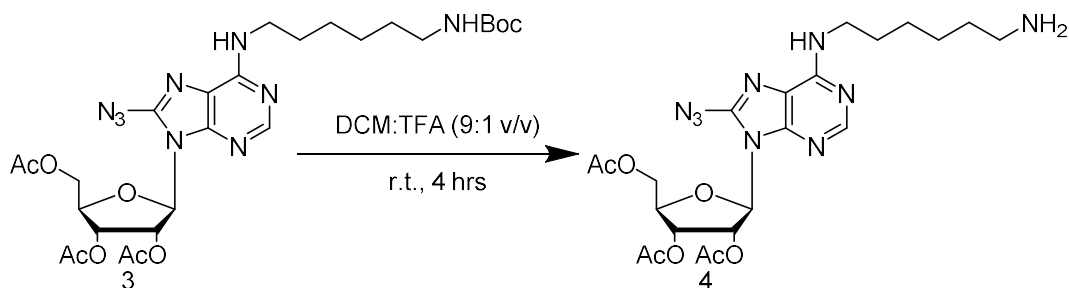
¹H NMR (400 MHz, CDCl₃) δ 12.43 (s, 0H), 8.09 (s, 0H), 6.23 (t, J = 5.2 Hz, 0H), 6.10 (dd, J = 4.6, 2.3 Hz, 1H), 5.78 (t, J = 6.0 Hz, 1H), 4.60 – 4.03 (m, 2H), 2.16 (s, 1H), 2.11 (s, 1H), 2.07 (s, 1H). ¹³C NMR (101 MHz, CDCl₃) δ 206.82, 170.41, 169.48, 169.35, 157.65, 148.77, 145.08, 144.09, 123.20, 85.76, 79.89, 77.32, 77.21, 77.00, 76.69, 71.97, 70.32, 63.02, 30.88, 20.65, 20.47, 20.38. NMR Mass Spec HRMS (ESI) C₁₆H₁₇N₇O₈ Calc. 458.1032, found 458.1012.



Scheme 3. A PyBOP coupling reaction is completed to add the Boc protected linker region.

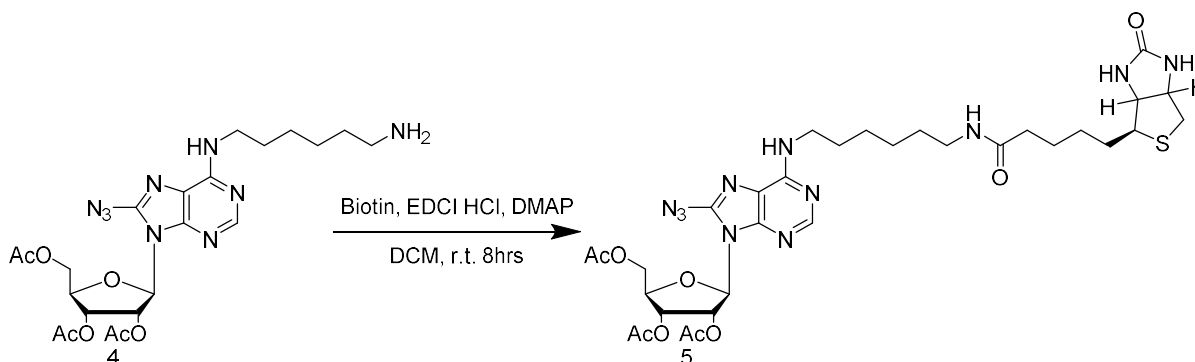
N, N-Diisopropylethylamine (23 μ L, 0.134 mmol) was added to a solution of 2',3',5'-O-triacetyl-8-azidoinosine (29.1 mg, 0.067 mmol) and PyBOP (2.341 g, 4.5 mmol) in 2.0 mL HPLC grade acetonitrile and stirred until the solution turned clear, this took 15 minutes. Mono-N-Boc-1,6-hexandiamine (6.0 mmol) was added drop wise and the reaction was stirred overnight at room temperature. The reaction was diluted with Et₂O and washed twice each with 1 M acetic acid, saturated NaHCO₃, and brine. The organic layer was dried over Na₂SO₄ and concentrated. The crude residue was purified by silica gel column chromatography, using a mobile phase that is 4:1 to 1:2 Hexane/EtOAc.⁶ 55.0% isolated yield. ¹H NMR (400 MHz, CDCl₃) δ 8.27 (s, 1H), 6.18 – 6.11 (m, 1H), 5.98 (d, J = 4.5 Hz, 1H), 5.81 (t, J = 5.5 Hz, 1H), 4.54 – 4.43 (m, 2H), 4.37 – 4.25 (m, 2H), 3.64 (s, 2H), 3.11 (q, J = 6.8 Hz, 3H), 2.13 (s, 3H), 2.08 (s, 3H), 2.06 (s, 3H), 1.50 (q, J = 7.1 Hz, 2H), 1.45 (s, 4H), 1.38 (q, J = 8.6, 7.6 Hz, 1H). ¹³C NMR (101 MHz, CDCl₃) δ 206.78, 170.50, 169.49, 169.39, 155.99, 144.20, 85.43, 79.83, 77.32, 77.21, 77.01, 76.69, 72.00, 70.47,

63.05, 53.39, 30.87, 30.02, 29.78, 28.42, 26.48, 26.44, 20.65, 20.49, 20.41.. Mass Spec HRMS (ESI) C₁₅H₁₇N₇O₆Na⁺ Calc. 414.1138, found 414.1113.



Scheme 4. Boc deprotection of intermediate 3.

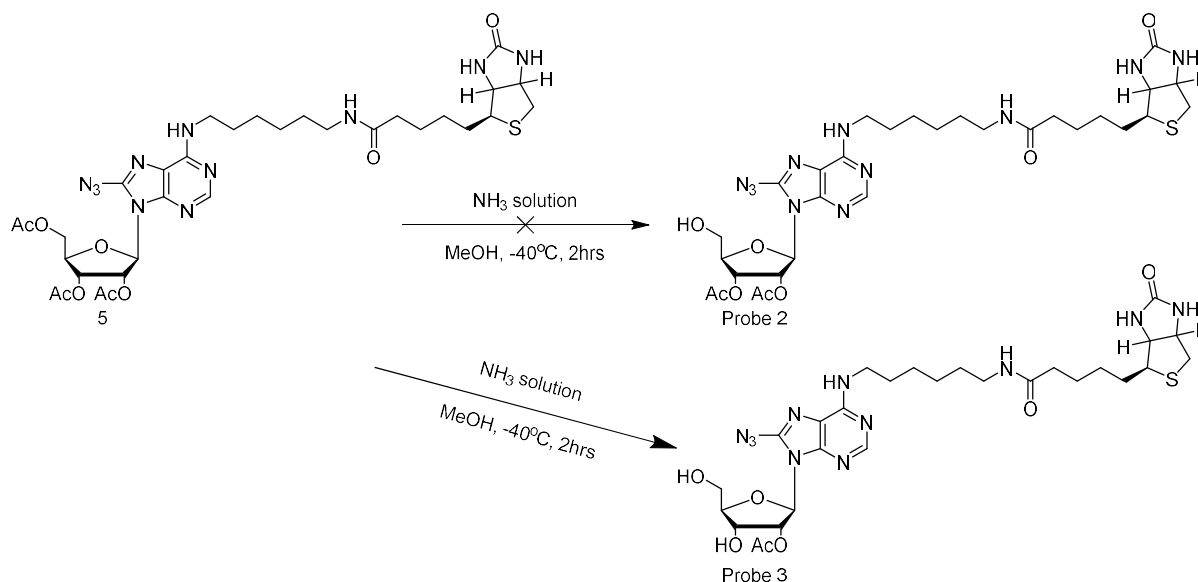
A solution of 2',3',5'-Tri-O-acetyl-8-azido-6-(N6-tert-butoxycarbonyl-6-amino-1002D`hexylamino)-purine riboside (451.2 mg, 0.712 mmol) in 9:1 dry DCM:TFA (8 mL) was stirred at room temperature for 4 hours. The reaction was followed by TLC for complete deprotection of N-Boc group and formation of the desired product. The TFA was removed by rotovap. Next 100 μ L of TEA was added along with additional DCM and water. The aqueous layer was rinsed and extracted with DCM 3 \times . The DCM was dried over anhydrous sodium sulfate and concentrated to pale yellow solid.⁶ 79.5% isolated yield. ¹H NMR (400 MHz, CDCl₃) δ 8.22 (s, 1H), 6.15 (t, J = 5.3 Hz, 1H), 5.96 (d, J = 4.7 Hz, 1H), 5.80 (t, J = 5.6 Hz, 1H), 4.46 (dd, J = 10.9, 2.6 Hz, 1H), 4.35 – 4.23 (m, 2H), 3.59 (s, 2H), 2.91 (t, J = 7.7 Hz, 2H), 2.11 (s, 3H), 2.06 (s, 3H), 2.03 (s, 3H), 1.63 (p, J = 7.1 Hz, 5H), 1.38 (p, J = 3.4 Hz, 6H). ¹³C NMR (101 MHz, CDCl₃) δ 206.94, 170.61, 169.58, 169.50, 162.94, 162.58, 162.23, 153.18, 152.13, 144.14, 120.76, 117.86, 117.76, 114.96, 112.07, 85.41, 79.79, 77.34, 77.23, 77.03, 76.71, 71.99, 70.47, 63.06, 40.77, 39.81, 30.86, 29.67, 29.41, 27.28, 26.06, 25.86, 20.62, 20.48, 20.39. HRMS (ESI) C₂₆H₄₀N₉O₇Na⁺ Calc. 612.2870, found 612.2901.



Scheme 5. EDCI coupling of the biotin tag to the linker region of intermediate 4.

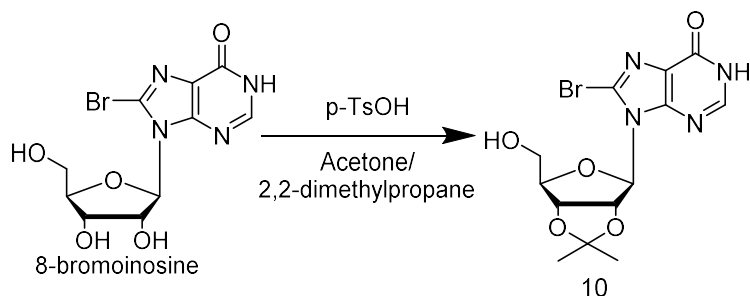
To a solution of biotin (6.5 mg, 0.027 mmol), EDCI·HCl (5.1 mg, 0.027 mmol), and DMAP (4.9 mg, 0.040 mmol) in dry DMF (2 mL), a solution of crude 2',3',5'-Tri-O-acetyl-8-azido-6-(N6-tert-butoxycarbonyl-6-amino-1-hexylamino)-purine riboside (14.3 mg, 0.027 mmol) in dry DCM (2 mL) was slowly added; the solution was stirred at room temperature for 8 hours. Water (8 mL) was added the reaction and the aqueous layer was extracted 3x with DCM. The organic layers were pooled together and washed with brine solution (1 × 10 mL). The DCM extract was dried over anhydrous sodium sulfate and concentrated to a pale yellow solid and subjected to reversed-phase column chromatography (30-100% acetonitrile in H₂O) to give 8 (256 mg, 72%) after freeze-drying.⁶ 62.0% isolated yield. ¹H NMR (400 MHz, CDCl₃) δ 8.24 (d, J = 3.4 Hz, 1H), 6.49 (d, J = 33.9 Hz, 1H), 6.28 – 6.12 (m, 2H), 5.95 (d, J = 4.4 Hz, 1H), 5.92 – 5.73 (m, 3H), 4.47 (dd, J = 8.1, 5.4 Hz, 2H), 4.29 (h, J = 5.9 Hz, 3H), 3.52 (d, J = 57.4 Hz, 2H), 3.22 – 3.05 (m, 3H), 2.87 (dd, J = 12.7, 4.6 Hz, 1H), 2.69 (d, J = 12.8 Hz, 1H), 2.17 (t, J = 7.4 Hz, 2H), 2.11 (s, 3H), 2.05 (dd, J = 11.5, 2.4 Hz, 7H), 1.78 – 1.57 (m, 7H), 1.49 (t, J = 7.0 Hz, 1H), 1.45 (s, 0H). ¹³C NMR (101 MHz, CDCl₃) δ 173.23, 170.63, 169.63, 169.55, 164.19, 153.45, 152.55, 144.11, 117.89, 85.56, 79.91, 77.48, 77.36, 77.16, 76.84, 72.12, 70.58, 63.18, 61.98, 60.27, 55.80, 50.72, 40.72, 39.51,

36.03, 29.73, 29.57, 28.24, 28.15, 26.69, 26.58, 25.73, 20.77, 20.60, 20.54. HRMS (ESI) C₃₃H₄₇N₁₁O₉Na⁺ Calc. 796.31, found 782.3022.



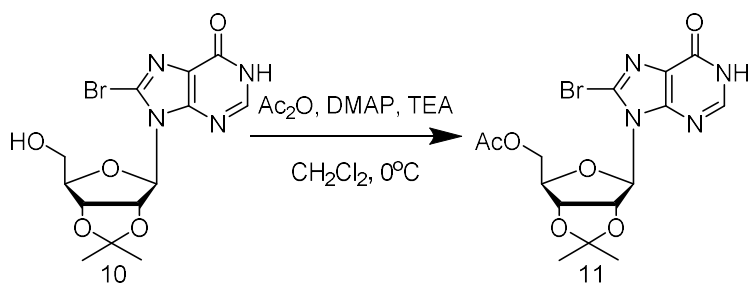
Scheme 6. Our goal was to selectively deprotect the 5-position acetyl group, but we realized that this would not be possible when we were left with the monoprotected product.

An ammonia solution was slowly added to a solution of 2',3',5'-Tri-O-acetyl-8-azido-6-(N6-biotinyl-6-amino-1-hexylamino)-purine riboside 3mg (0.067 mmol) in MeOH (1.5 mL) while being stirred at -40°C in a ice/salt water bath for 2 hours. The reaction mixture was diluted with MeOH and concentrated immediately under vacuum to give a foamy solid which was purified by HPLC chromatography (20-80% acetonitrile in H₂O) followed by freeze-drying to give 1 (57 mg, 61%) along with small amount of the monoprotected derivative. The goal of synthesizing the monodeprotected product (probe 2) was unsuccessful with this method, the product that was formed was the monoprotected compound (probe 3).⁶ 46.6% isolated yield. ¹H NMR (400 MHz, MeOD) δ 8.16 (s, 1H), 5.84 (d, J = 4.9 Hz, 1H), 5.08 (t, J = 5.2 Hz, 1H), 4.55 (t, J = 5.3 Hz, 1H), 4.49 – 4.40 (m, 2H), 4.29 (td, J = 7.0, 4.8 Hz, 2H), 4.18 – 4.10 (m, 1H), 3.59 (d, J = 15.8 Hz, 2H), 3.24 – 3.13 (m, 3H), 2.91 (dd, J = 12.8, 5.0 Hz, 1H), 2.71 (s, 1H), 2.01 (s, 3H), 1.80 – 1.37 (m, 16H). ¹³C NMR HRMS (ESI) C₂₉H₄₃N₁₁O₇Na⁺ Calc. 712.77, found 698.2789.



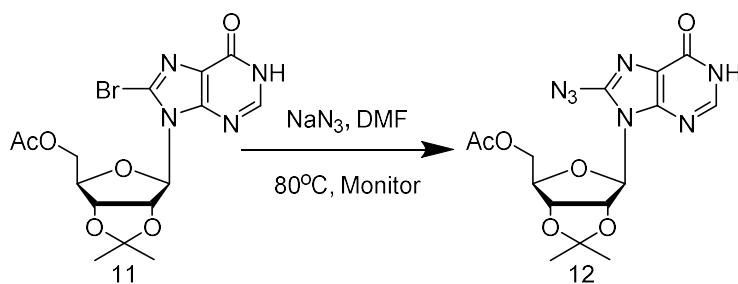
Scheme 7. the protection of the 2 and 3 position with 2,2-dimethylpropane.

In a flame dried round bottom flask add 8-bromoinosine (100 mg, 0.289 mmole) was dissolved in a 5 mL of a 4:1 v/v acetone:2,2-dimethoxypropane solution. Next p-TsOH (55.0 mg, 0.289 mmole) was added to the reaction mixture and the reaction was stirred at room temperature overnight. The reaction goes from a cloudy off white to a cloudy red orange. The solution was stirred overnight at room temperature before solid NaHCO₃ (24.3mg, 0.289 mmol) was added slowly in small portions, followed by saturated NaHCO₃ (932.3 μL). The reaction mixture was stirred for 1 hour before the salts were filtered off. After adding the sodium bicarbonate, the reaction changes from the cloudy red/orange to a cloud faint off white/yellow. The filtrate was concentrated down and purified by column chromatography on silica gel eluting with 10% MeOH/DCM (v/v).¹⁰ 83.5% isolated yield. ¹H NMR (600 MHz, CDCl₃) δ 12.98 (s, 2H), 8.37 (s, 1H), 6.09 (d, J = 4.7 Hz, 2H), 5.25 (t, J = 5.4 Hz, 2H), 5.06 (dd, J = 5.8, 2.0 Hz, 2H), 4.48 (dt, J = 4.0, 2.1 Hz, 2H), 3.93 (ddd, J = 12.8, 4.1, 2.0 Hz, 2H), 3.79 (d, J = 12.5 Hz, 2H), 1.66 (s, 5H), 1.38 (s, 5H). ¹³C NMR (101 MHz, CDCl₃) δ 157.75, 149.39, 146.55, 126.90, 126.50, 114.87, 93.74, 86.30, 83.32, 81.72, 77.79, 77.68, 77.48, 77.16, 63.47, 30.13, 28.04, 25.88. HRMS (ESI) C₁₃H₁₅BrN₄O₅Na⁺ Calc. 410.00, found 452.0362.



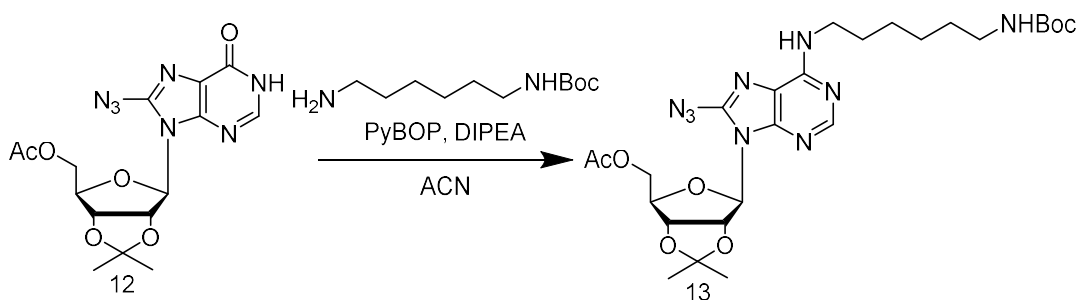
Scheme 8. the protection of the 5-position hydroxyl group with an acetyl group.

In a 50 mL 24/40 flame dried round bottom flask and a solution of 8-bromoinosine (50.0 mg, 7.202 mmol) and DMAP (3.2 mg, 0.0259 mmol) in dry dichloromethane (2 mL) was cooled at 0°C for 5-7 minutes. TEA (27.1 μ L, 0.1943 mmole) was added to the cooled reaction mixture followed by acetic anhydride (13.4 μ L, 0.1425 mmol). After 2 hours of stirring at 0°C, with ice continuously added, the mixture was taken off of ice and stirred at room temperature overnight. The next morning the reaction mixture was quenched with an ice water mixture, and the ice was given time to melt before extraction. The reaction mixture was washed with 10 mL of DCM 3 times before the organic layer was pooled and washed with saturated solution of sodium bicarbonate followed by brine. The dichloromethane layer was dried over anhydrous sodium sulfate and concentrated then subjected to flash column chromatography (5% MeOH/DCM).⁶ 99.4% isolated yield. ¹H NMR (400 MHz, CDCl₃) δ 13.10 (s, 1H), 8.35 (s, 1H), 6.22 (d, J = 1.9 Hz, 1H), 5.55 (d, J = 1.9 Hz, 1H), 5.12 (dd, J = 6.4, 4.2 Hz, 1H), 4.44 – 4.29 (m, 2H), 4.19 (dd, J = 11.6, 7.2 Hz, 1H), 2.04 (s, 3H), 1.62 (s, 3H), 1.40 (s, 3H). ¹³C NMR (101 MHz, CDCl₃) δ 170.53, 157.82, 149.56, 145.90, 126.58, 125.59, 114.90, 91.19, 85.32, 83.70, 81.70, 77.36, 77.24, 77.04, 76.72, 63.82, 29.69, 27.21, 25.43, 20.77. HRMS (ESI) C₁₃H₁₅N₇O₅Na⁺ Calc. 451.01, found 453.0163.



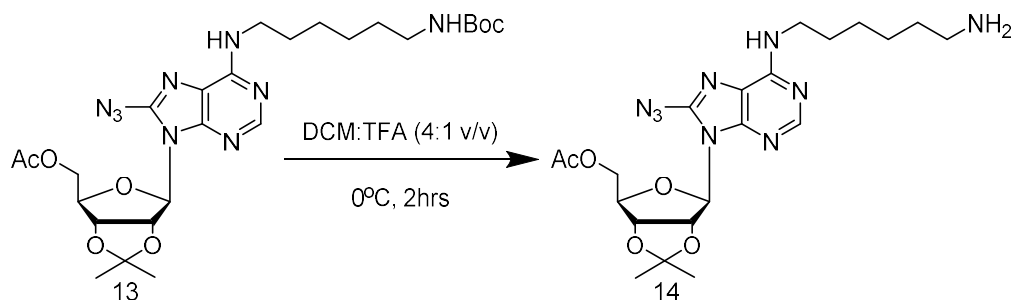
Scheme 9. The azide photocrosslinking group is added to intermediate 11.

To a solution of 2',3'-O-isopropylidene-5'-O-acetyl-8-bromoinosine (55.4 mg, 0.1294 mmol) in 6 mL of anhydrous DMF was added NaN_3 (33.7 mg, 0.5177 mmol) in a 50 mL flame dried 24/40 round bottom flask. The reaction was stirred at 80°C while being monitored by TLC until the consumption of starting material. The reaction was cooled down to room temp and the solvent was removed under reduced pressure. Water (5 mL) was added to the reaction mixture and the product was extracted with dichloromethane (3 times). The combined organic layer was washed with sat. NaHCO_3 , water and brine and dried over Na_2SO_4 before being filtered and concentrated down.⁶⁶ 82.9% isolated yield. ^1H NMR (400 MHz, CDCl_3) δ 13.36 (s, 1H), 8.26 (s, 1H), 6.01 (d, $J = 2.0$ Hz, 1H), 5.39 (dd, $J = 6.4, 2.0$ Hz, 1H), 5.01 (dd, $J = 6.6, 3.5$ Hz, 1H), 4.37 – 4.26 (m, 2H), 4.15 (dt, $J = 10.5, 4.6$ Hz, 1H), 2.01 (s, 3H), 1.57 (s, 3H), 1.35 (s, 3H). ^{13}C NMR (101 MHz, CDCl_3) δ 170.55, 162.67, 158.02, 148.57, 145.00, 144.94, 123.04, 114.85, 88.52, 85.00, 83.55, 81.63, 77.48, 77.36, 77.16, 76.84, 63.94, 36.55, 31.49, 27.20, 25.43, 20.77. $\text{C}_{15}\text{H}_{17}\text{N}_7\text{O}_6\text{Na}^+$ Calc. 414.10, found 414.0931.



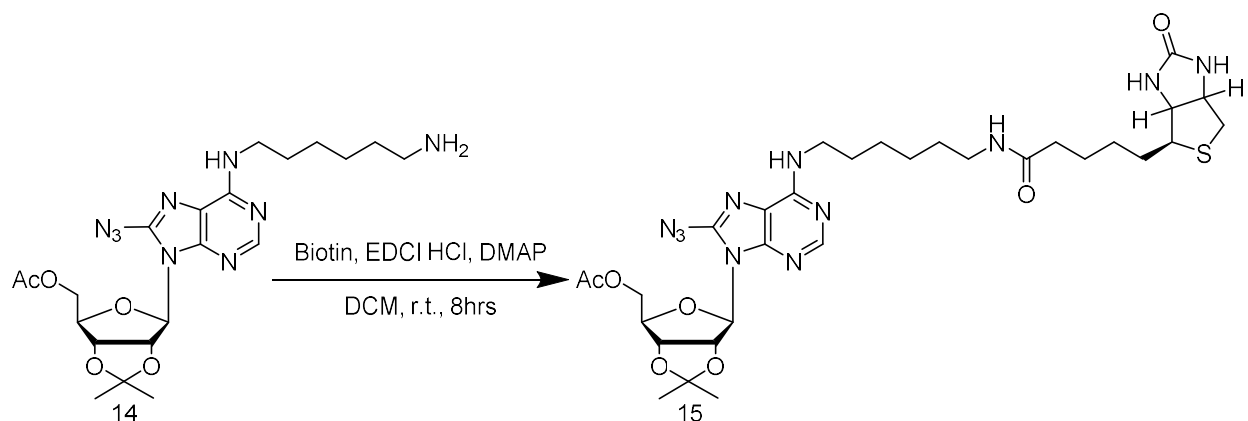
Scheme 10. The addition of the linker region to intermediate 12.

N, N-Diisopropylethylamine (22.5 μ L, 0.1293 mmol) was added to a solution of 2',3'-O-isopropylidene-5'-O-acetyl-8-azidoadenosine (25.3 mg, 0.0646 mmol) and PyBOP (50.5 mg, 0.0970 mmol) in 2.0 mL sealed dry HPLC grade acetonitrile and stirred until the solution turned clear (15 min). Mono-N-Boc-1,6-hexandiamine (29.0 μ L, 0.1293 mmol) was added drop wise and the reaction was stirred overnight at room temperature. The reaction was quenched with water and washed 3x with EtOAc. The organic layer was pooled together and washed once with brine. The organic layer was dried over Na₂SO₄ and concentrated. The crude residue was purified by column chromatography (silica gel, 7% MeOH in DCM).⁹ 81.9% isolated yield. ¹H NMR (400 MHz, CDCl₃) δ 8.24 (s, 1H), 6.00 (d, J = 1.9 Hz, 1H), 5.53 (dd, J = 6.4, 2.0 Hz, 2H), 5.11 (dd, J = 6.5, 3.2 Hz, 1H), 4.55 (s, 1H), 4.38 – 4.27 (m, 2H), 4.21 – 4.11 (m, 1H), 3.64 – 3.57 (m, 2H), 3.09 (q, J = 6.7 Hz, 2H), 2.01 (s, 3H), 1.66 (p, J = 7.1 Hz, 2H), 1.42 (s, 11H), 1.37 (s, 4H). ¹³C NMR (101 MHz, CDCl₃) δ 170.68, 156.12, 153.35, 152.31, 152.06, 151.66, 149.94, 148.86, 144.35, 142.90, 119.97, 118.53, 118.02, 114.54, 114.45, 110.15, 88.48, 88.41, 85.26, 83.53, 83.46, 82.11, 82.01, 79.15, 77.48, 77.36, 77.16, 76.84, 64.26, 64.16, 47.18, 47.13, 40.56, 30.12, 29.87, 28.54, 27.29, 26.60, 26.55, 26.50, 26.45, 26.41, 25.60, 25.57, 20.86. HRMS (ESI) C₂₆H₃₉N₉O₇Na⁺ Calc. 589.30, found 590.3062.



Scheme 11. The selective deprotection of the Boc group on the linker of intermediate 13.

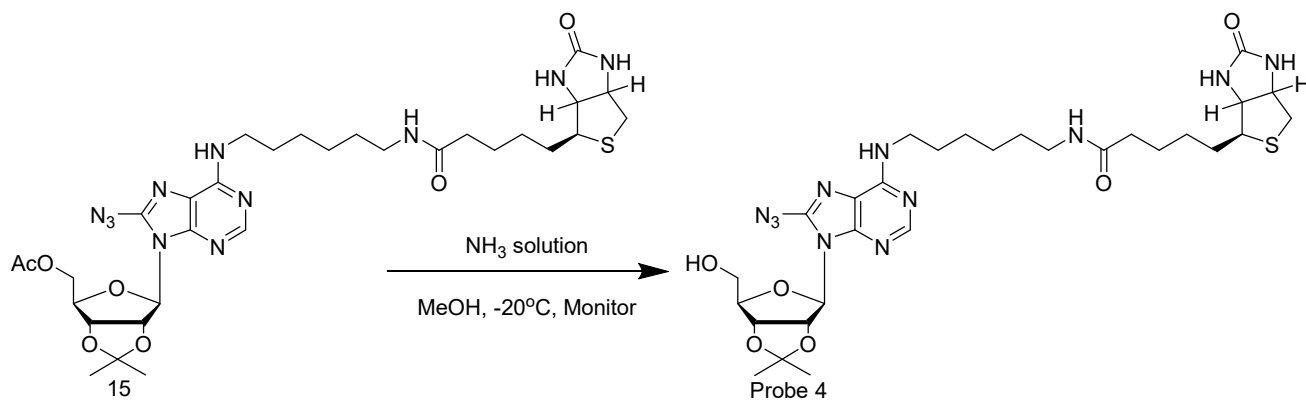
A solution of 2',3'-O-isopropylidene-1-5'-O-acetyl-N6-N-Boc-hexandiamine-8-azidoinosin (79.1 mg, 0.1342 mmol) in 4:1 dry DCM: TFA (2:0.5 mL) was stirred at 0°C in an ice/water bath for 2 hours. The reaction was followed by TLC for complete deprotection of N-Boc group and formation of the desired product. The TFA was removed by rotovaping. Next 100 μ L of TEA was added along with additional DCM and water. The aqueous layer was rinsed and extracted with DCM 3 times. The DCM was dried over anhydrous sodium sulfate and concentrated to pale yellow solid). ($\text{CH}_2\text{Cl}_2/\text{CH}_3\text{OH}$, 90/10, v/v).⁹³ 99.7% isolated yield. ^1H NMR (400 MHz, MeOD) δ 8.16 (s, 1H), 6.00 (d, $J = 1.9$ Hz, 1H), 5.57 (dd, $J = 6.3, 1.9$ Hz, 1H), 5.12 (dd, $J = 6.4, 3.5$ Hz, 1H), 4.36 – 4.15 (m, 4H), 3.57 (s, 2H), 3.36 (s, 1H), 3.32 (p, $J = 1.7$ Hz, 1H), 2.93 (t, $J = 7.7$ Hz, 2H), 1.98 (s, 3H), 1.68 (ddt, $J = 14.8, 11.0, 6.7$ Hz, 5H), 1.57 (s, 3H), 1.54 – 1.44 (m, 5H), 1.37 (s, 3H). ^{13}C NMR (101 MHz, MeOD) δ 172.30, 154.43, 152.89, 149.76, 145.87, 115.46, 89.75, 86.34, 84.55, 83.14, 65.01, 49.85, 49.64, 49.43, 49.28, 49.21, 49.07, 49.00, 48.79, 48.57, 48.36, 40.64, 28.48, 27.41, 27.36, 27.14, 25.52. HRMS (ESI) $\text{C}_{21}\text{H}_{31}\text{N}_9\text{O}_5\text{Na}^+$ Calc. 489.24, found 490.2504.



Scheme 12. The addition of the biotin tag to intermediate 14.

To a solution of biotin (21.5 mg, 0.0879 mmol), EDCI·HCl (16.8 mg, 0.0879 mmol), and DMAP (16.0 mg, 0.1310 mmol) in dry DMF (2 mL), a solution of 22',3'-O-isopropylidene-5'-O-acetyl-8-azido-6-(6-aminohexylamino)-purine riboside (43.0 mg, 0.0879 mmol) in dry DCM (4 mL) was slowly added; the solution was stirred at room temperature for 8 hours. Water (8 mL) was added to the reaction and the aqueous layer was extracted 3 times with DCM. The organic layers were pooled together and washed with 10 mL brine solution on time. The DCM extract was dried over anhydrous sodium sulfate and concentrated to a pale yellow solid and columned with silica in a mobile phase of (CH₂Cl₂/CH₃OH, 90/10, v/v).⁶ 60.6% isolated yield. ¹H NMR (400 MHz, CDCl₃) δ 8.23 (s, 1H), 6.45 (s, 1H), 6.22 (t, J = 5.7 Hz, 1H), 6.00 (d, J = 1.8 Hz, 1H), 5.79 (s, 1H), 5.53 (dd, J = 6.3, 1.9 Hz, 1H), 5.16 – 5.07 (m, 1H), 4.49 (dd, J = 7.8, 4.9 Hz, 1H), 4.37 – 4.28 (m, 3H), 4.16 (dt, J = 10.3, 4.7 Hz, 1H), 3.60 (s, 2H), 3.30 – 3.11 (m, 3H), 2.71 (d, J = 12.7 Hz, 1H), 2.18 (t, J = 7.3 Hz, 2H), 1.68 (ddp, J = 18.3, 13.3, 6.6 Hz, 7H), 1.58 (s, 4H), 1.50 (t, J = 7.2 Hz, 2H), 1.43 (q, J = 7.4 Hz, 5H), 1.38 (s, 5H), 1.24 (s, 5H). ¹³C NMR (101 MHz, CDCl₃) δ 173.15, 170.59, 164.06, 153.00, 144.29, 117.82, 114.49, 88.39, 85.14, 83.33, 81.87, 77.36, 77.24, 77.04, 76.72, 64.03, 61.87, 60.13, 55.70, 40.66, 39.38, 37.09, 36.47, 35.90, 32.74, 31.92, 31.43,

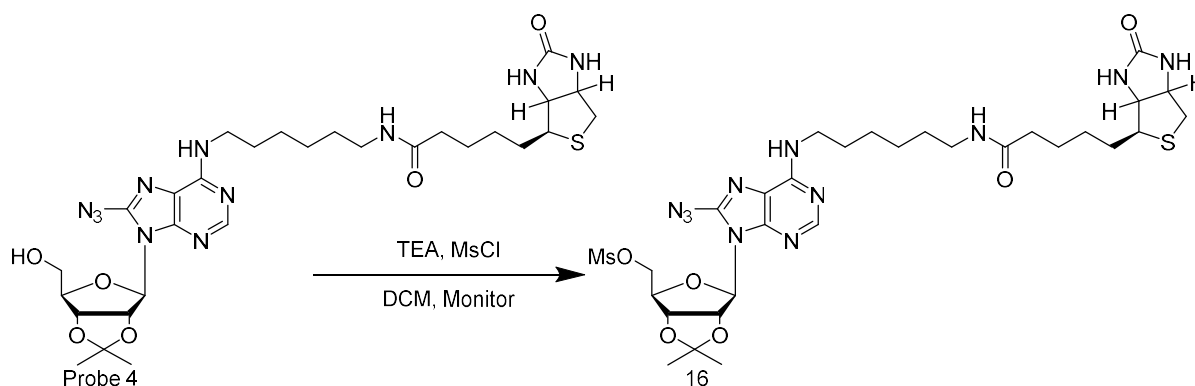
30.03, 29.69, 29.57, 29.44, 29.35, 28.09, 28.02, 27.18, 27.08, 26.55, 26.44, 25.63, 25.46, 22.68, 20.77, 19.73, 14.11. HRMS (ESI) C₃₁H₄₅N₁₁O₇SN⁺Na⁺ Calc. 715.83, found 716.3268.



Scheme 13. The selective deprotection of the 5-position acetyl group on intermediate 15 was completed giving us Probe 4.

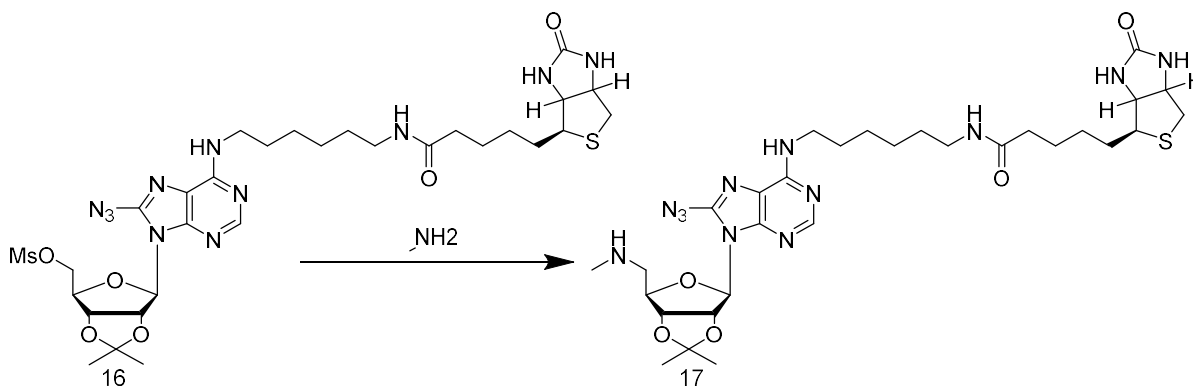
To a round bottom flask of 2',3'-O-isopropylidene-5'-O-acetyl-8-azido-6-(N6-biotinyl-6-amino-1-hexylamino)-purine riboside (23.1 mg, 0.0323 mmol) 1 mL of the ammonia 7 N in Methanol solution was slowly added. The argon line was removed and the reaction was monitored every 30 minutes while stirring at -20°C (ice/NaCl bath) monitoring for the consumption of starting material. The reaction mixture was diluted with MeOH and concentrated immediately under vacuum to give a foamy solid which was purified by silica column (DCM/MeOH, 90/10, (v/v)).⁶ 79.9% isolated yield. ¹H NMR (400 MHz, MeOD) δ 8.18 (s, 1H), 5.98 (d, J = 3.4 Hz, 1H), 5.44 (dd, J = 6.1, 3.4 Hz, 1H), 5.09 (dd, J = 6.1, 2.7 Hz, 1H), 4.51 (ddd, J = 7.9, 5.0, 1.0 Hz, 1H), 4.33 (tt, J = 4.8, 2.0 Hz, 2H), 3.82 (dd, J = 12.2, 4.0 Hz, 1H), 3.72 (dd, J = 12.2, 4.8 Hz, 1H), 3.63 (d, J = 12.0 Hz, 2H), 3.22 (ddd, J = 9.2, 5.6, 2.5 Hz, 3H), 2.94 (dd, J = 12.7, 5.0 Hz, 1H), 2.73 (d, J = 12.7 Hz, 1H), 2.23 (t, J = 7.3 Hz, 2H), 1.73 (dddd, J = 20.6, 17.6, 9.0, 6.7 Hz, 6H), 1.64 (s, 3H), 1.61 – 1.43 (m, 9H), 1.42 (s, 3H). ¹³C NMR (101 MHz, MeOD) δ 174.55, 151.44, 144.47, 113.87, 89.63, 86.73, 82.80, 81.53, 62.25, 61.98, 60.21, 55.60, 48.23, 48.02, 47.80, 47.59, 47.38, 47.17,

46.95, 39.61, 38.89, 35.41, 28.96, 28.36, 28.10, 26.32, 26.28, 26.21, 25.52, 24.17. HRMS (ESI) C₂₉H₄₃N₁₁O₆Na⁺ Calc. 673.31, found 696.2992.



Scheme 14. The addition of a good leaving group, a Mesylate, is added to the 5-position of the ribose ring of probe 4.

Triethylamine (6 μ L, 0.0431 mmol) and methanesulfonyl chloride (1.7 μ L, 0.0216 mmol) were added to a solution of the N6 substituted adenosine (12.1 mg, 0.0180 mmole) in 1 mL DCM. The reaction was stirred for 1 hour and then quenched with saturated NH₄Cl. The layers were separated and the organic layer. The aqueous layer was extracted twice with DCM, then the organic layers were pooled together, washed with brine, dried over Na₂SO₄ and concentrated. NMR crude if TEA is gone and looks right push forward. (Mohamed Ramadan, 2014) 35.6% isolated yield. ¹H NMR (400 MHz MeOD) δ 8.0736 (s, 1H), 5.8710 (d, J=2.7919 Hz, 1H), 5.3364 (dd, J=3.6294, 5.5837 Hz, 1H), 4.9959 (d, J=5.8629 Hz, 1H), 4.9404 (dd, J=6.1412, 8.9339 Hz, 1H), 4.4252 (t, J=5.3045 Hz, 2H), 4.2404 (d, J=3.9086 Hz, 2H), 3.7387 (tdd, J=3.6294, 12.005, 29.3145 Hz, 3H), 3.2952 (d, J=15.3552 Hz, 3H), 2.9169 (td, J=4.7462, 12.5634 Hz, 2H), 2.6363 (d, J=9.7715 Hz, 2H), 2.1501 (t, J=7.2588 Hz, 3H), 1.711 (ddt, J=7.2588, 13.4009, 34.3399 Hz, 8H), 1.5597 (dt, J=8.9339, 30.4313, 9H), 1.4057 (quintet, J=7.2588, 13H), 1.2482 (s, 1H). C₃₀H₄₅N₁₁O₈S₂Na⁺



Scheme 15. The mesyl group on the 5-position of the ribose ring is substituted for a methylamine group.

The N6 substituted mesylate (1.0 mmol) was brought up in 3mL of methylamine (50 mmol) and stirred for 3 days. The volatiles were evaporated off under high vacuum with gentle heating using a distillation apparatus. Upon addition of brine to the resulting material, the product was extracted with EtOAc, washed with brine, dried over Na₂SO₄ and concentrated. The crude residue was purified by column chromatography (silica gel, 9:1 to 7:3 DCM/MeOH).⁹ 26.6% isolated yield. ¹H NMR (400 MeOD) δ 8.1208 (s, 1H), 6.2779 (s, 1H), 5.5198 (s, 1H), 4.9868 (d, J=5.7904 Hz, 1H), 4.6811 (s, 1H), 4.6169 (d, J=5.6647 Hz, 1H), 4.5092 (dd, J=4.7425, 7.9042 Hz, 1H), 4.3254 (dd, J=4.4791, 7.9042 Hz, 1H), 3.5883 (t, J=6.9821 Hz, 2H), 3.5210 (quintet, J=1.5808 Hz, 1H), 3.4790 (dd, J=3.0300, 13.8324 Hz, 1H), 3.3796 (s, 1H), 3.2860 (d, J=1.5808 Hz, 1H), 3.2235 (td, J=6.7186, 2.1078 Hz, 4H), 3.1718 (quintet, J=1.5808 Hz, 1H), 2.9514 (dd, J=4.8743, 12.6468 Hz, 2H), 2.7317 (d, J=12.7785 Hz, 2H), 2.2331 (t, J=7.3773 Hz, 2H), 1.7424 (dd, J=7.1138, 13.8324 Hz, 2H), 1.6699 (d, J=2.2395 Hz, 1H), 1.6450 (dd, J=7.6408, 21.3415 Hz, 3H), 1.5454 (s, 5H), 1.5107 (dt, J=7.3773, 14.0959 Hz, 9H), 1.3587 (s, 4H), 1.3239 (s, 2H).
C₃₀H₄₆N₁₂O₅Na⁺

Using pET28a-LIC we performed a plasmid prep. (EHMT1 (2IGQ) was a gift from Cheryl Arrowsmith (Addgene plasmid # 25504; <http://n2t.net/addgene:25504>; RRID: Addgene_25504)) Agar plates were made using the formula 40 g LB Agar per 1 L DI water with 100 μ L Kan (Kanamycine Stock: 50 mg/ mL (1000x)).⁹⁴ The LB agar was autoclaved and added to petri dishes once allowed to cool down in the cold room so that it was cool enough to touch. Enough LB agar was added to cover the bottom of the dish. The plate was removed from the cold room and allowed to sit at room temperature (25°C) on the benchtop upside down to prevent condensation from dripping onto the agar. Before streaking the LB Agar plate the pipettor and gloves were sprayed with 70 % ethanol. To plate the bacteria a sterile pipette tip was stabbed in the bacteria and streaked onto half of the plate. The tip was discarded, and the plate was rotated 90° before a new sterile pipette tip was used to streak the plate a 2nd time overlapping a bit with the previously streaked area of the plate. This was repeated once more so that the last quarter of the plate is also streaked. After streaking the plate, the plate was placed upside down in the brown 37°C incubator to incubate overnight.

Once distinct colonies have grown on the agar plate, we prepared four 8 mL culture tubes with LB and the appropriate antibiotic. Before picking colonies the pipettor and gloves were sprayed with 70 % ethanol. To inoculate the culture tubes a sterile pipette tip was stabbed into a single colony and added into the culture tubes. Incubate at 37°C for 12-16 hours because pET28a-LIC is a high copy plasmid.

2.2.2.2 PCR

Obtain a bucket with ice, a PCR kit box and remove the 2x Hot Start Master Mix Eppendorf.⁹⁴ the Nuclease Free water, the template DNA pET28a-LIC EHMT1, the 10 μ M T7 Forward Primer, and the 10 μ M T7 Reverse Primer. Thaw everything on bench top at room temperature except the

template DNA pET28a-LIC EHMT1, the 10 μ M T7 Forward Primer and the 10 μ M T7 Reverse Primer which are thawed on ice. Add 13 μ L nuclease free water is added with sterile pipette tips to a PCR Eppendorf tube. Next add 25 μ L of 2x Hot Start Master Mix to the PCR Eppendorf tube and vortex to mix. Next add 10 μ L of the Template DNA (pET28a-LIC EHMT1) to the Eppendorf tube. Thereafter add 1 μ L of both the 10 μ M T7 Forward Primer and the 10 μ M T7 Reverse Primer. Vortex to mix well. We placed the PCR Eppendorf tube the Bio Rad T100 thermocycler we ran the pre saved method labeled T7_PCR. T7_PCR's cycling parameters are listed in table 1.

Segment	Cycles	Temperature	Time
1	1	94	30 seconds
2	30	94	30 seconds
		65	1 minute
		68	7 minutes
3	1	68	5 minutes
4	1	4	∞

Table 1. T7_PCR's cycling parameters

In a separate Eppendorf tube, we added 40 μ L of the PCR reaction mixture. Next, we added 5 volumes Buffer PB to 1 volume of the PCR reaction (200 μ L of Buffer PB) and vortexed the mixture. We placed a QIAquick column in a provided 2 mL collection tube. To bind DNA, the sample was applied to the QIAquick column and centrifuged for 30–60 seconds. The flow-through was discarded and the QIAquick column was placed back into the same Eppendorf tube. 750 μ L of Buffer PE was added to the QIAquick column and centrifuged for 30–60 seconds. We discarded the flow-through and placed the QIAquick column back into the same tube. Then the the QIAquick column was centrifuged once more in the 2 mL collection tube for 1 min to remove the residual wash buffer. Then each QIAquick column was placed in a clean 1.5 mL microcentrifuge tube. To elute the DNA, we added 50 μ L of Buffer EB (10 mM Tris·Cl, pH 8.5) or water (pH 7.0–8.5) to the center of the QIAquick membrane and centrifuged the column for 1 min. To increase DNA

concentration, we added 30 μL of elution buffer to the center of the QIAquick membrane, let the column stand for 1 min and then centrifuged. We checked the concentration of the protein using a Thermo scientific Nanodrop 2000 spectrophotometer.

2.2.2.3 Transforming Cells

In a pre-chilled 1.5 mL microcentrifuge tube that is in ice we added the 2 μL of purified plasmid of DNA directly into BL21 DE3 competent cells.⁹⁴ The mixture was gently stirred and quickly returned to ice, where it was let sit for 5 minutes. The cells were heat shocked in a hot water bath at 42°C for 30 seconds. The cells were then allowed to sit on ice for 2 more minutes. Next, we added 80 μL of room temperature S.O.C. medium. The microcentrifuge tube was shaken at 250 rpm at 37°C for 60 minutes prior to being plated a on Kanamycin plate

In four 2 L culture flasks 47.6 g of Terrific Broth modified (TB) were dissolved in 1L of di-ionized water by gently swirling. To each flask 4 mL of glycerol was added. The flasks were covered with aluminum foil autoclave tape and then autoclaved for 15 minutes. After autoclaving the flasks were stored at room temperature away from sun light.

2.2.2.4 Protein Purification

The cultures were poured into large centrifuge containers and balanced before being spun down for 40 minutes at 1400 G's.⁹⁴ A small sample was taken before centrifugation so that it could be compared to the sample after it has been centrifuged. Once the samples are finished centrifuging a sample of the supernatant was taken and saved. The rest of the supernatant was poured off and the pellets were scooped out, and resuspended in protease buffer with 50 mg of Lysozyme. This mixture was let to sit for 30 minutes so that the Lysozyme was given time to work to break down the cell wall. 5 μL of nuclease was added to break down DNA. This solution was sheered through

a syringe to make sure there were no clumps before running it on the Avestin Emulsiflex C3 (also referred to as French pressure cell press or French press). The pressed solution was put into centrifuge tubes that were graded for over 5000 rpm rating and then balanced again. The samples were centrifuged for 1 hour at 18000 rpm at 4°C. When finished another sample of the supernatant was taken and saved. 2 mL of equilibrated beads suspended in protease buffer were added to the samples and then shaken for 1 hour. The solution was loaded onto a Ni-NTA column and then eluted off using varying concentrations of imidazole washes. The washes were performed with 0, 10, 20, 30, 40, 50, 60, 70, 80, 90, 100% solutions of elution buffer to wash buffer. (Wash Buffer

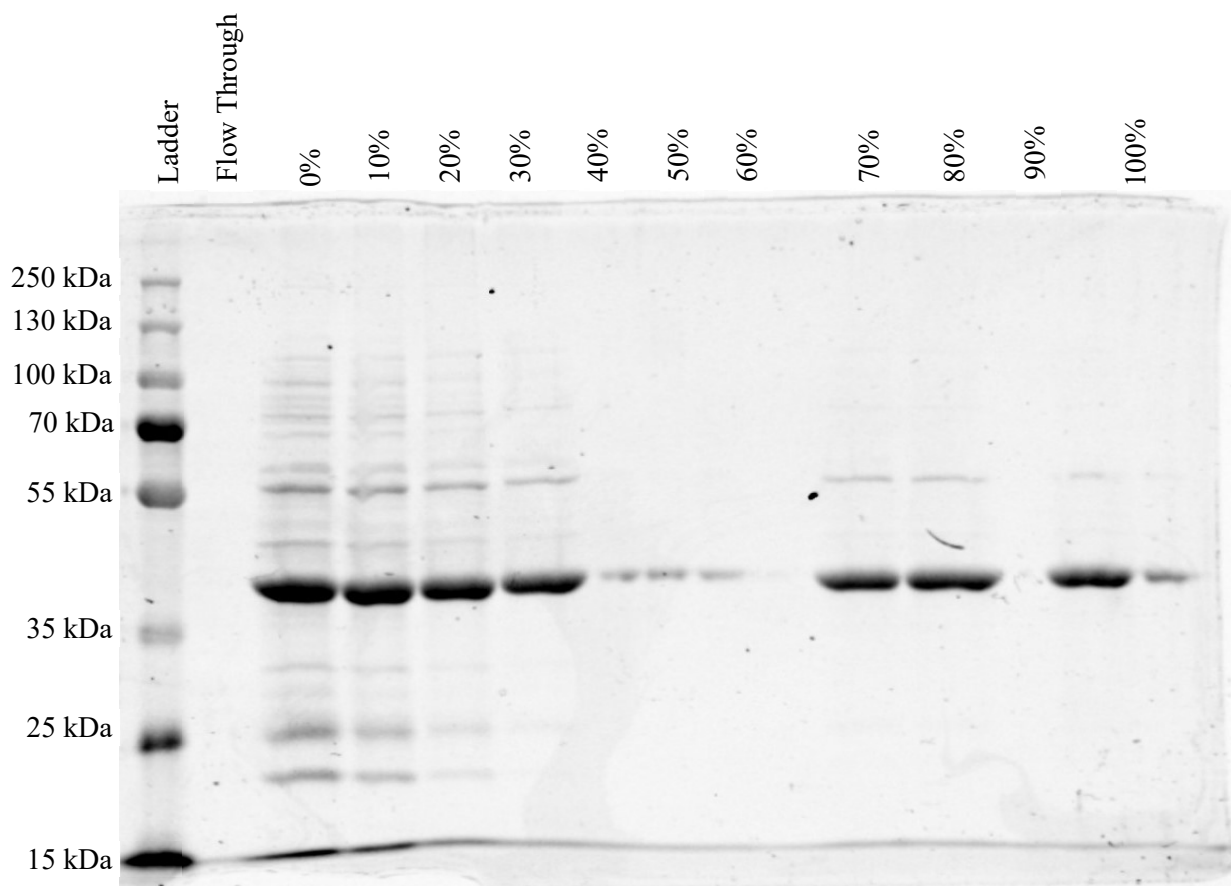


Figure 3. 10% SDS page gel of the elutions from the Ni-NTA column. Elutions using a percent of elution buffer: wash buffer. The elutions using between 40% and 100% elution buffer were considered pure, while the fractions eluted off with 0% through 30% washes were considered impure.

1 L: 20 mM Tris pH = 8.00, 250 mM NaCl, 5 % glycerol, and 50 mM imidazole. Elution Buffer
1 L: 20 mM Tris pH = 8.00, 250 mM NaCl, 5 % glycerol, and 250 mM imidazole.)

After this column was run, we deemed all of the fraction eluted with concentration between 40% and 100% enough via agarose electrophoresis gel. (Fig. 16) We also deemed the fractions eluted between 0 and 30% not pure enough yet, but we would recolumn them to obtain more pure protein. Both of these groups were put into dialysis bags and allowed to dialyze for 48 hours to remove imidazole. The impure samples were recolumned after dialysis, while the pure samples were concentrated using a Vivaspin 20 centrifugal concentrator run at 4950 rpm at 4°C for 15 minutes at a time. We got the pure EHMT1 solution down to a concentration of 228 μM ^{95 PDB:2IGQ}

2.3 Noncompetitive Protein Pulldown Assay

We diluted a stock of Probe 3 to 10 nM using DMSO as well as diluting the EHMT1 stock to 228 μM . Solutions of Probe 3 and EHMT1 in PBS buffer with varying concentrations were made and incubated in a warm water bath at 37°C for 10 minutes. The solution is then was irradiated in a CL-1000 Ultraviolet Crosslinker while on ice at 365 nm for 1 hour.⁸ While the samples irradiate high-capacity streptavidin agarose resin beads were equilibrated in PBS buffer. Once the samples have finished incubating the samples added to a protein concentrator and centrifuged at 14000 g for 5 minutes, then 100 μL of PBS buffer were added and centrifuging was repeated. This step was added to remove unbound probe so that it would not compete with the bound probe for the streptavidin beads. To remove the protein-probe complex from the filter of the concentrator we put the filter into a clean concentrator tube and centrifuge it at 1000 g for 2 minutes. Once the beads were equilibrated and the samples were filtered, we would resuspend the samples in 16 μL of PBS buffer add the samples to the beads and incubate for 1 hour on a Thermocycler shaking at 1500 rpm at room temperature. The samples were then spun down at 13000 rpm for 3 minutes at

3°C and the supernatant was removed, and saved, and then 300 µL of PBS buffer was added to the samples. The samples were then vortexed, and then this process was repeated twice more with the supernatants being saved. 20 µL of 25 mM Biotin in BPS containing .4% SDS (w/v) was added to each sample and then they were incubated at 95°C for 5 minutes while shaking on the Thermocycler at 1500rpm or 10 minutes at 800 rpm at 95°C. The samples and all saved supernatants from the three washes were then put onto a Supervac to reduce their volumes. They were then resuspended in 10 µL of PBS with 5 µL of Laemmli buffer and heated at 100°C for 10 minutes. The samples were then added to a 10% SDS page gel for 70 minutes at 120 Volts. The gels were then analyzed using western blot procedure.

This same protein pull assay down method was completed with ADA in place of EHMT1. The pure ADA that was used in these experiments was purchased from Sigma-Aldrich as a 10 mg/mL (245 µM) stock solution.

2.4 Competitive Protein Pulldown Assay

The competitive assay is run with the same protocol as the noncompetitive protein pulldown assay except instead of adding Probe 3 to the initial Eppendorf tubes SAM was added in place of it and it was incubated for 5 minutes in the hot water bath at 37°C. After this Probe 3 was added and the samples were incubated again at 37°C for 10 minutes. The rest of the assay is the same as the noncompetitive protein pulldown assay.

The same competitive protein pulldown assay was completed ADA in place of EHMT1 and Inosine in place of SAM.

3. Results & Discussion

3.1 Synthesis of Probe 1

In our initial synthetic plan (Figure 17), the synthesis of probe 1 started with commercially available 8-brominosine. The 2', 3', and 5'-position hydroxyl groups were protected with acetic

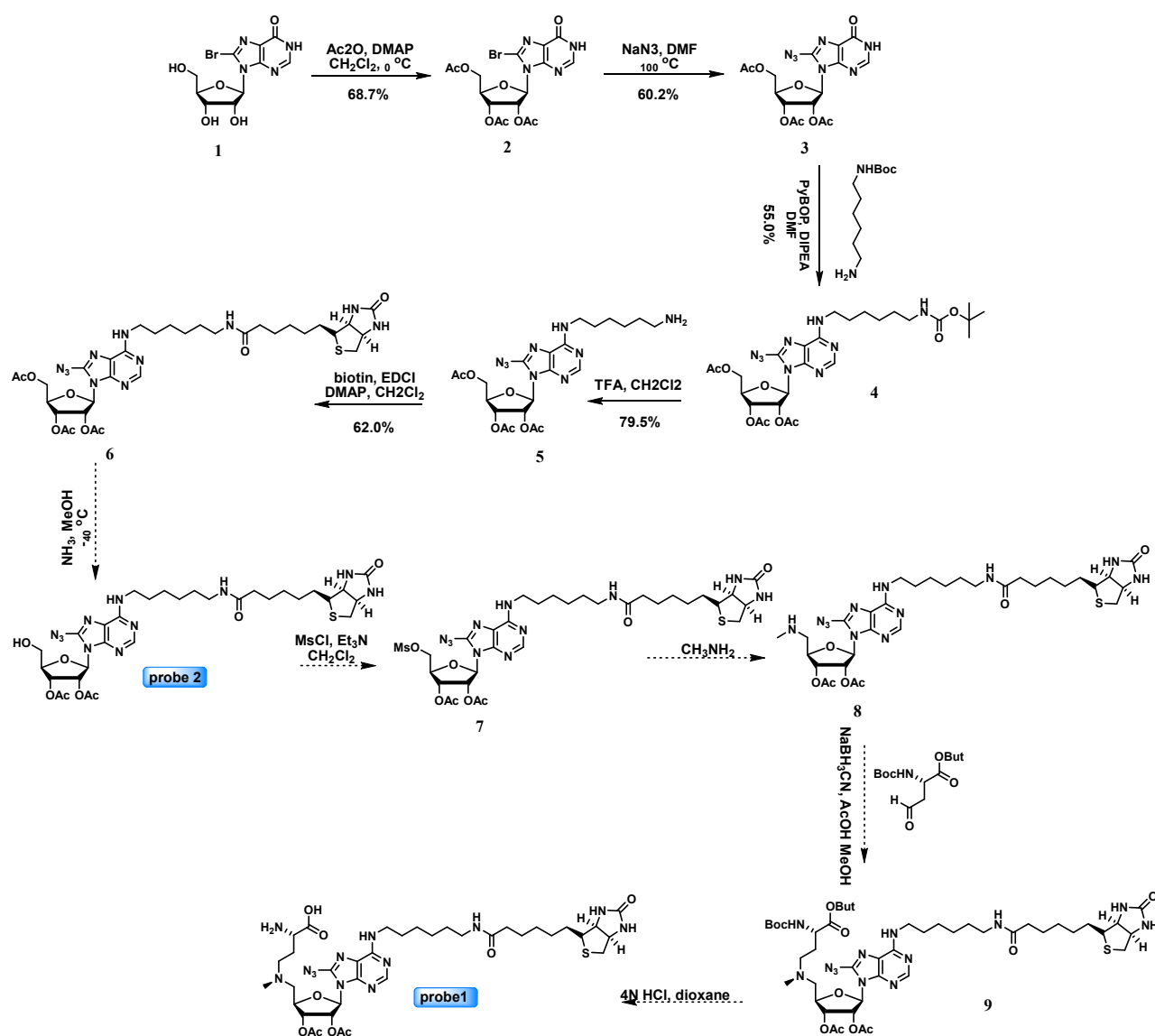


Figure 17. Synthetic scheme 1. This scheme was unsuccessful because the selective deprotection of the 5-position acetyl group was unable to be performed

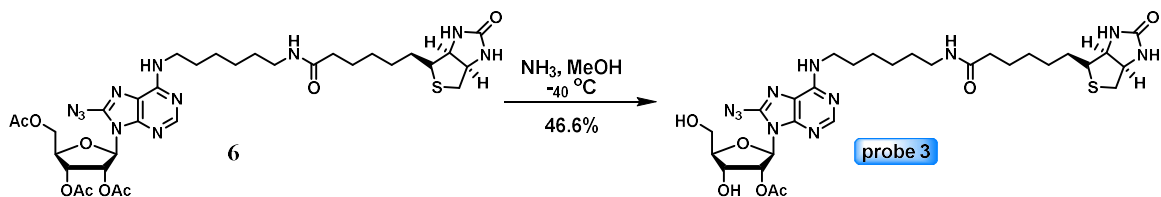


Figure 18. The serendipitous synthesis of probe 3.

anhydride to afford intermediate 2 in 68.7% yield. The bromine in intermediate 2 can then be easily replaced by azido group through nucleophilic substitution reaction with sodium azide in DMF at $100\text{ }^\circ\text{C}$. This step resulted in the formation of intermediate 3 in 60.2% yield. Mono-protected 1,6-diaminohexane was coupled with intermediate 3 under standard amide coupling condition using PyBOP as the coupling agent. Intermediate 4 was thus obtained in 55.0% yield. The Boc protecting group in intermediate 4 was removed with the treatment of TFA in dichloromethane, leading to the formation of intermediate 5 in 79.5% yield. This deprotection step revealed a free amino group which can then be coupled to biotin *via* another round of amide coupling reaction using EDCI as the coupling agent. The second coupling reaction appended biotin to the core structure to afford intermediate 6 in 62.0% yield.

In our original plan, the 5'-acetyl group in compound 6 could be selectively removed under a previously described condition to form probe 2 (Figure 17).⁶ This would allow the “warhead” portion to be conjugated to the riboside through the 5'-position. However, this selective deprotection was not successful. Instead of the desired mono-deprotected product, a mono-protected product, probe 3 (Figure 18), was obtained in 46.6% yield. The reaction conditions were further modified to achieve the desired product. However, changing the reaction temperature (to $-20\text{ }^\circ\text{C}$ or $0\text{ }^\circ\text{C}$) or changing the stoichiometry of the reactants only led to significant and complex decomposition of the starting material. Although not the desired compound, probe 3 was proven

to be extremely useful for the establishment and optimization of the labeling and affinity enrichment assay which will be discussed later in this chapter.

The unsuccessful initial synthetic efforts prompted us to seek an alternative synthetic route.

Scheme 2, seen in figure 19, also started with commercially available 8-bromoinosine, but the first step was the protection of the 2' and 3'-position hydroxy groups on the ribose ring as an acetonide.

This reaction was carried out in a mixture of acetone and 2,2-dimethoxypropane with *p*-

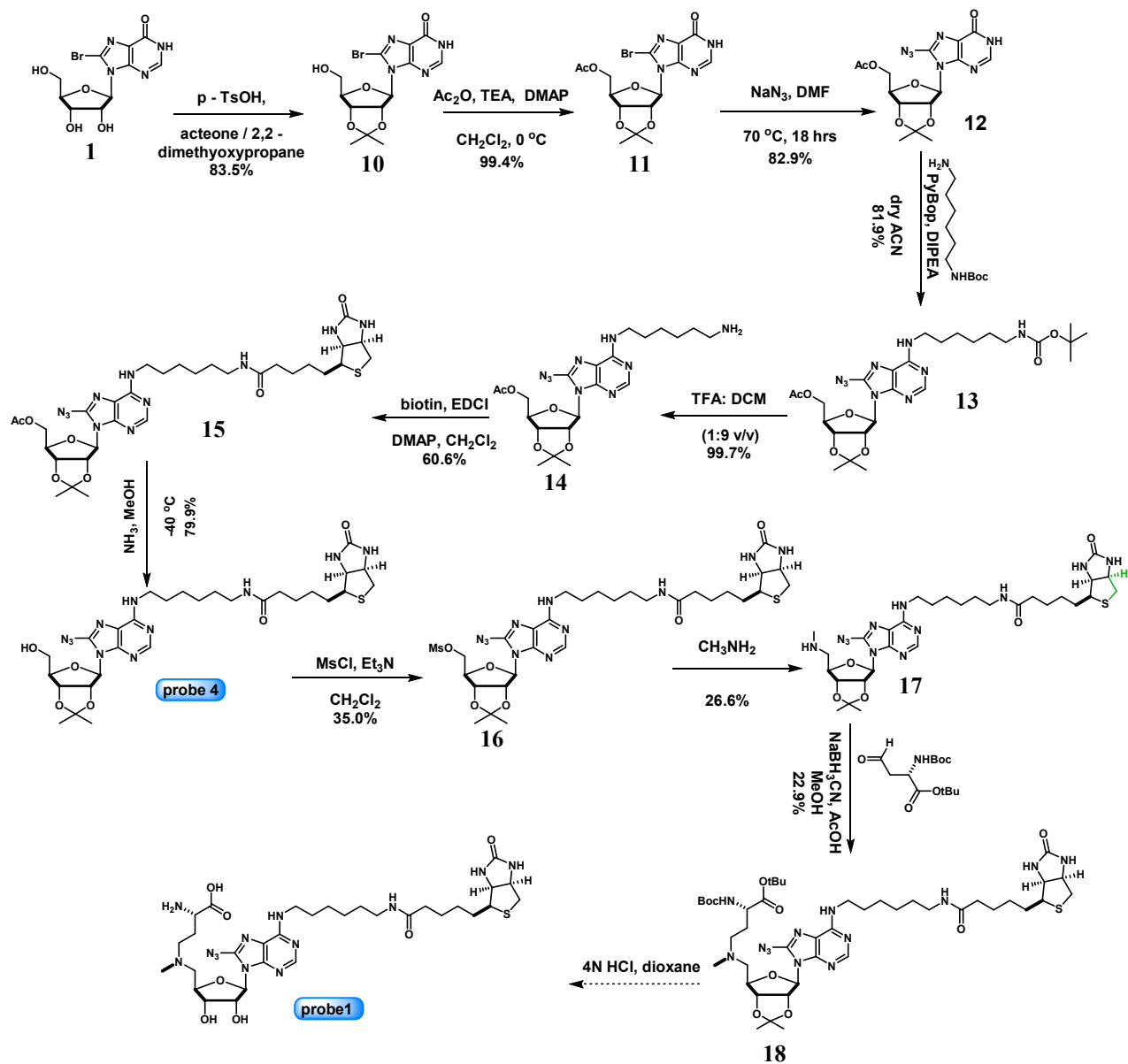


Figure 19. Synthetic scheme 2. This scheme was successful in forming probe 1.

toluenesulfonic acid (*p*-TsOH) as the catalyst. Intermediate 1 was obtained in 83.5% yield. The 5'-position hydroxyl group in intermediate 1 was, once again, protected with acetic anhydride to afford intermediate 2, with an obtained yield of 99.4%. The fully-protected 8-bromoinosine derivative, intermediate 2, was then subjected to the nucleophilic substitution using sodium azide to form intermediate 3 in nearly 82.9% yield. Intermediate 3 was then coupled to mono-*N*-Boc-1,6-diaminohexane, followed by Boc deprotection and coupling to biotin. The reaction conditions of these three steps were similar to the ones in synthetic plan 1. They gave decent to good yields, leading to the formation of intermediate 6. The selective deprotection of the 5'-position acetyl group was straightforward using ammonia in methanol at -40°C. The successful selective deprotection resulted in the formation of probe 4 in 79.9% yield. The free hydroxyl group in probe 4 was activated as a mesylate by reacting with methanesulfonyl chloride (MsCl) in the presence of trimethylamine (TEA). Intermediate 7 was obtained in 35.0% yield. Mesylate 7 was used for the next step without further purification. The amination of 7 using methylamine led to the formation of intermediate 8. A reductive amination between intermediate 8 and *tert*-butyl (*S*)-2-[*N*-(*tert*-butoxycarbonyl) amino]-4-oxobutanoate (compound 9) in the presence of NaBH₃CN and acetic acid led to the formation of an advanced intermediate 10 in 22.9% yield. Ultimately, the global deprotection of intermediate 10 will give rise to probe 1. As of now, we are still in the process of optimizing the reaction conditions of the final step.

3.2 EHMT1 Expression and Purification

When we obtained our pET28a-LIC vector we attempted to transfect a Rosetta DE3 cell line. The Rosetta DE3 cells did not grow, forcing us to use another cell line for this transformation. The second cell line we used was the BL21 DE3, and these cells grew and were cultured successfully.⁹⁶ These cells were then lysed, the this was then cells were pelleted. The pellets were separated from the cell supernatant, resuspended in buffer and then lysozymes and nucleases were used to break down excess cell wall and DNA respectively. This was then sheared using a syringe and the emulsiflex. This solution was then equilibrated with nickel beads, to allow for the his-tagged EHMT1 to bind. This was then loaded onto a column and was washed with a wash solution to remove any unbound protein. An imidazole solution with increasing concentrations was then

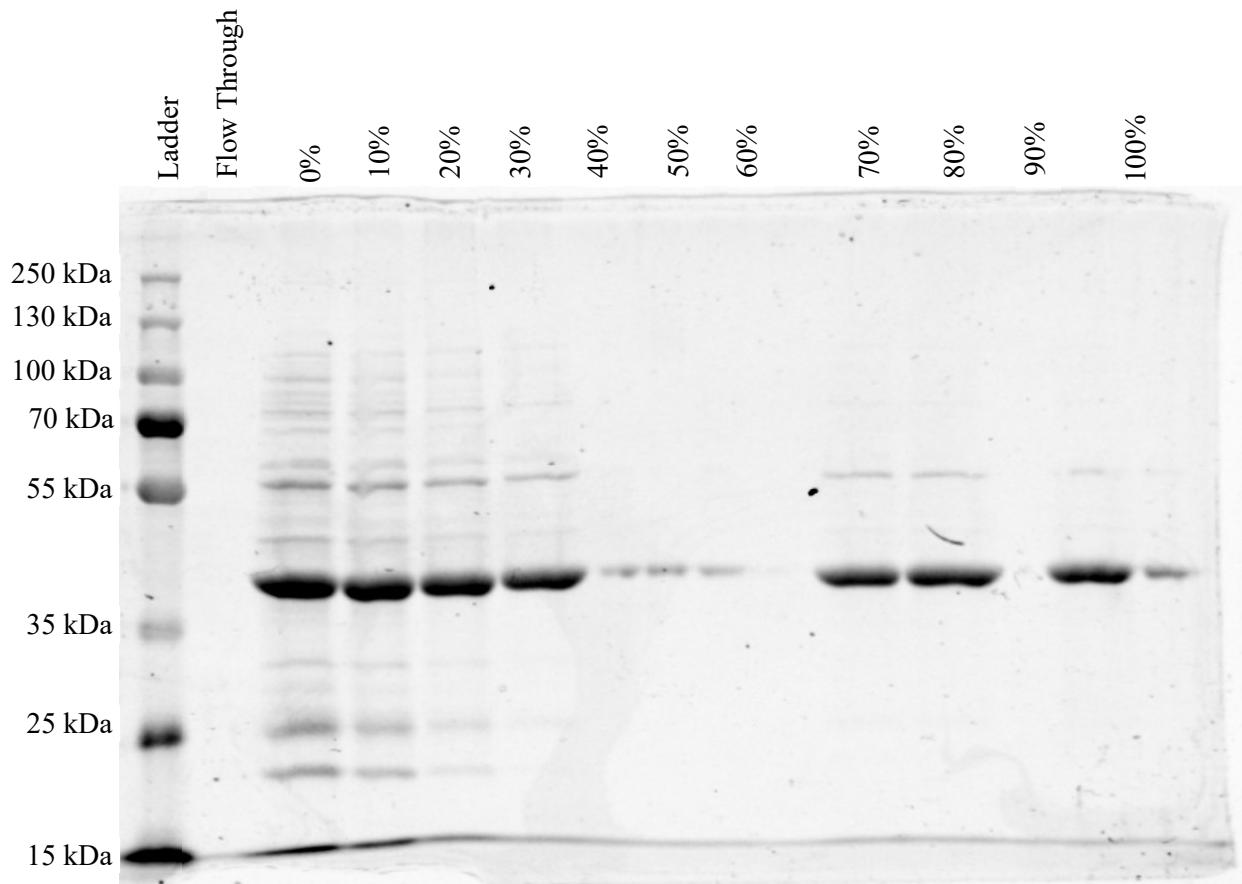


Figure 20. 10% SDS page gel of the elutions from the Ni-NTA column. Elutions using a percent of elution buffer: wash buffer. The elutions using between 40% and 100% elution buffer were considered pure, while the fractions eluted off with 0% through 30% washes were considered impure.

used to elute off the bound EHMT1 off of the column. The samples were resolved using SDS-PAGE gel.

3.3 Photoaffinity Labeling and Affinity Enrichment of EHMT1 Assay

In parallel to the synthesis, we also dedicated efforts to establish and optimize the photoaffinity labeling and the subsequent affinity enrichment assay using synthetic probes. With probe 1 still in the making, we used probe 3 for the assay development.

3.3.1 Optimization of Irradiation Time

SAM-based probe 3 targets the active sites of MTases. When the photoactivatable azido group of the probe is in the vicinity of the protein and is UV irradiated, the two become covalently conjugated. The irradiation time was optimized first. In this study, a 365 nm UV lamp was used because optimal photocrosslinking was observed for aryl azide at this wavelength as suggested by the literature.⁸ 500 μ M of Probe 3 was incubated with recombinant EHMT1 10.26 μ M for 10 min. Subsequently, the samples were irradiated with varying amounts of time (from 15 min to 90 min) at 365 nm. The samples were then resolved by SDS-PAGE and analyzed by western blot using an anti-biotin antibody (Fig. 21). The labeling was detected after merely 15 min's irradiation. And the labeling intensity reached plateau within 60 min.

With this knowledge moving forward all photocrosslinking experiments were completed with a 60-min irradiation time.

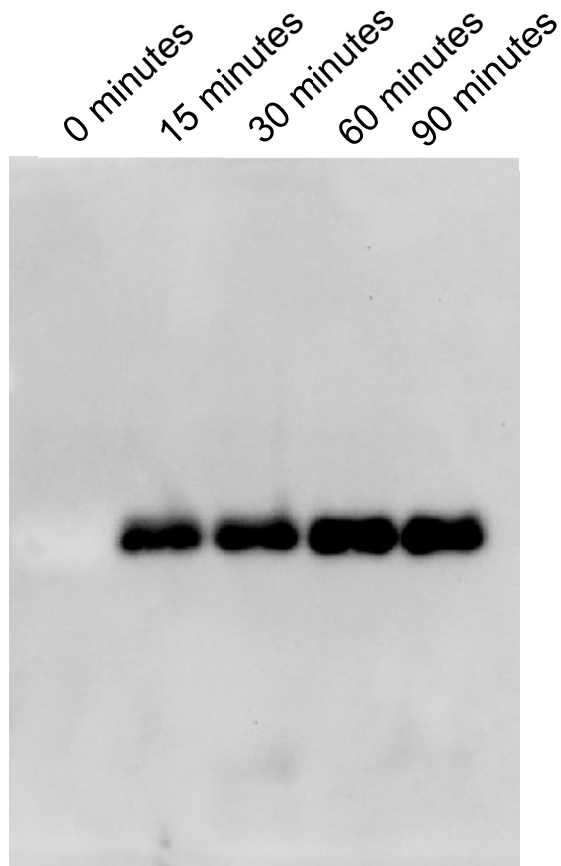


Figure 21. Western blot of time dependent binding. We see the bands get darker as irradiation time increases, but hits a peak at 60 minutes.

3.3.2 Optimization of Probe Concentration

Following the optimization of the irradiation time, the concentration of the probe was also optimized. To determine the most optimal concentrations of the probe, EHMT1 was incubated with varying concentrations of probe 3 (0, 25, 50, 125, 250 or 500 μM) and then irradiated at 356 nm for 60 min. The samples were then resolved by SDS-page gel and analyzed by western blot (Fig. 22). Probe 3 was able to label recombinant EHMT1 in a concentration-dependent manner. Below 250 μM , there were negligible levels of labeling. The labeling started to be detected at 250 μM concentration, and intensified at 500 μM dosage. For the following affinity enrichment assay, only concentrations higher than 250 μM were used.

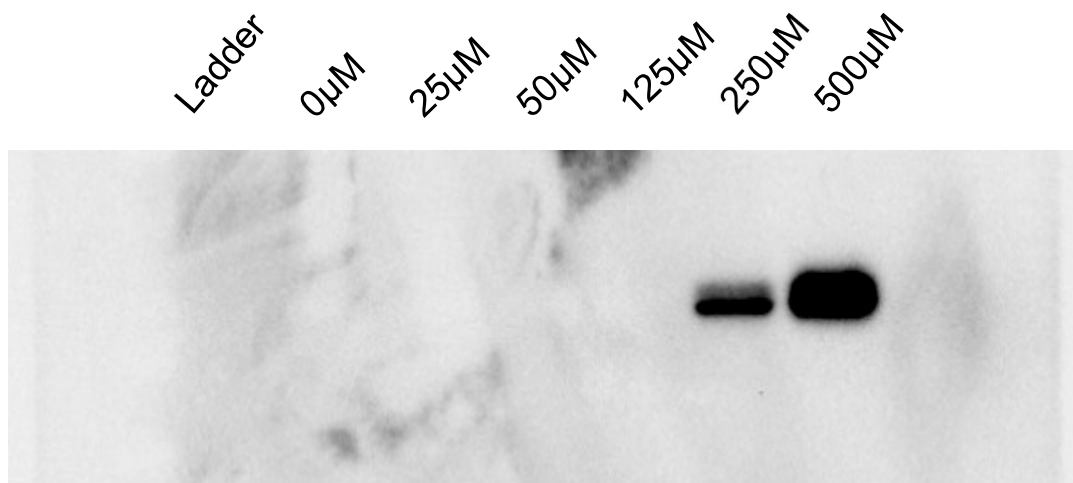


Figure 22. Western blot from concentration dependent study. Bands become visible at 250 μM of probe 3. This band became more intense as probe 3 concentration was increased to 500 μM . Seeing a lack of bands in 25 μM , 50 μM , and 125 μM concentrations of probe 3 led us to believe this concentration was too low to label EHMT1, and following this study we did not run concentrations of probe lower than 250 μM .

3.3.3 Improvement of Enrichment and Elution

Following the concentration-dependent study, we attempted to run our first complete pull-down assay. EHMT1 was incubated with 0, 250, or 500 μM probe 3 before being irradiated for 60 min. After photocrosslinking, the samples were incubated with streptavidin beads for 1 hour on a shaker to allow the biotinylated proteins to be captured by the beads. The supernatants containing unbound proteins were then separated from the beads. After thorough rinsing, the EHMT1-Probe 3 complex was then eluted off of the beads with a 2 mM solution of biotin in PBS buffer. The samples were then resolved by SDS-PAGE and analyzed by western blot using an anti-biotin antibody. From this experiment we saved every wash, elution, and the beads to determine if the probe protein complex was lost during any step.

Figure 23 illustrates the western blots from the pull-down experiment. At both 250 and 500 μM concentrations, biotinylated EHMT1 was detected in a concentration-dependent fashion in the elutions, albeit at relatively low intensity. However, significant amount of labeled EHMT1 was

detected in the supernatants and on the beads, suggesting that not all the biotinylated proteins were captured and not all captured proteins were completely eluted off. To improve the capture capacity, the incubation time of EHMT1-probe 3 complex with the beads was increased from 1 h to 3 h. To

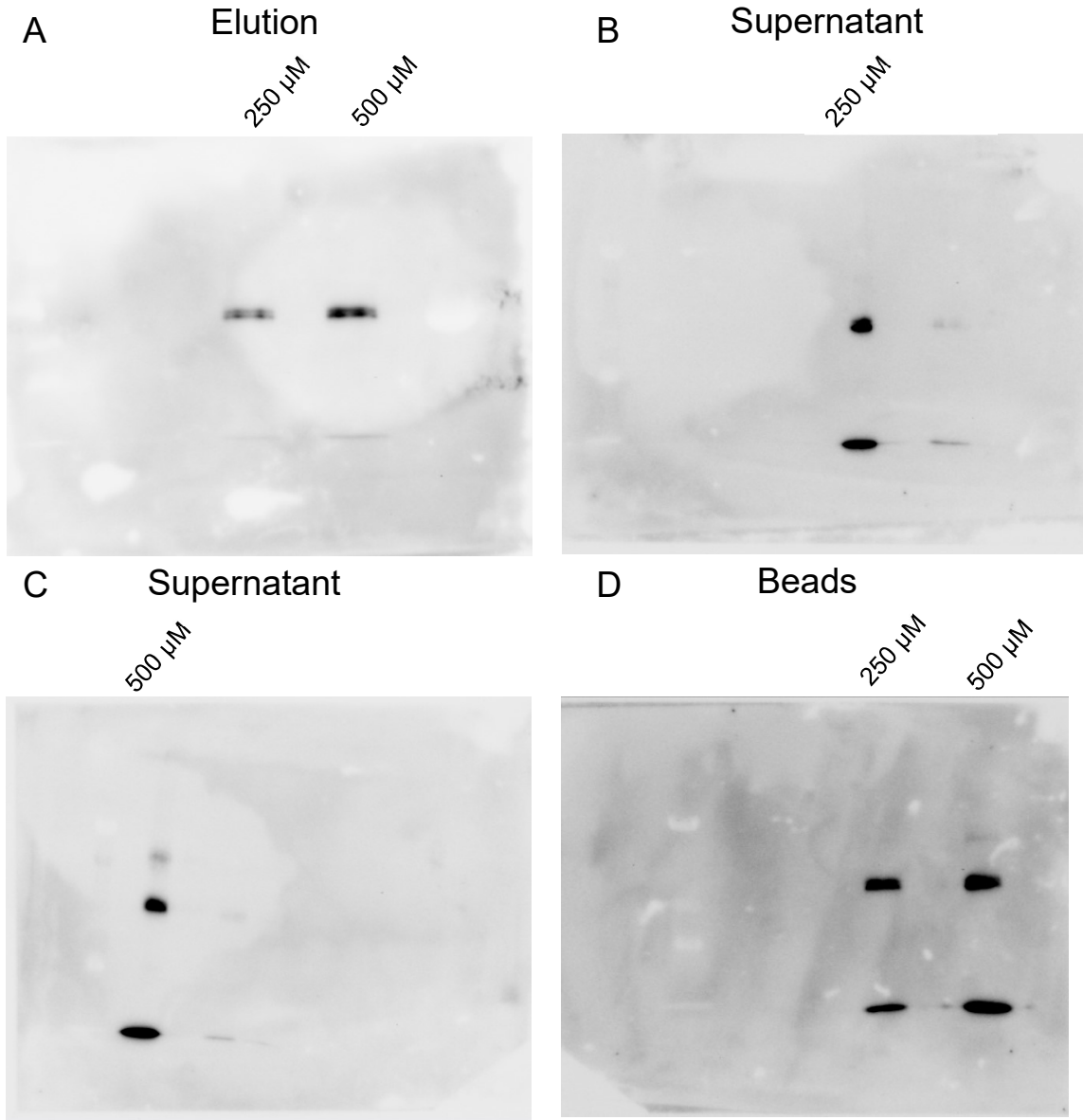


Figure 23. A. The elution gel we see faint bands in the 250 μM and 500 μM of concentration of probe 3. B. The supernatant gel 1 with the 250 μM concentration of Probe 3 sample. The dark band here is problematic because all EHMT1-probe 3 complex should have bound to the streptavidin beads, and the same goes for C. The supernatant gel 2 with the 500 μM concentration Probe 3 sample. D. The beads gel also has dark bands on it where it should not. We would have expected all EHMT1-probe 3 complex to have eluted off of the streptavidin beads during the elution wash.

improve elution efficiency, the concentration of biotin in the elution solution was increased from 2 mM to 25 mM. These modifications greatly improved the affinity enrichment and elution because almost all the labeled EHMT1 was captured and almost completely eluted off of the beads.

3.3.4 Pull-down Assay Lacking a Filtration Step

A revised version of the complete pull-down assay was performed including optimized irradiation time, optimized probe concentrations, improved enrichment and elution strategies.

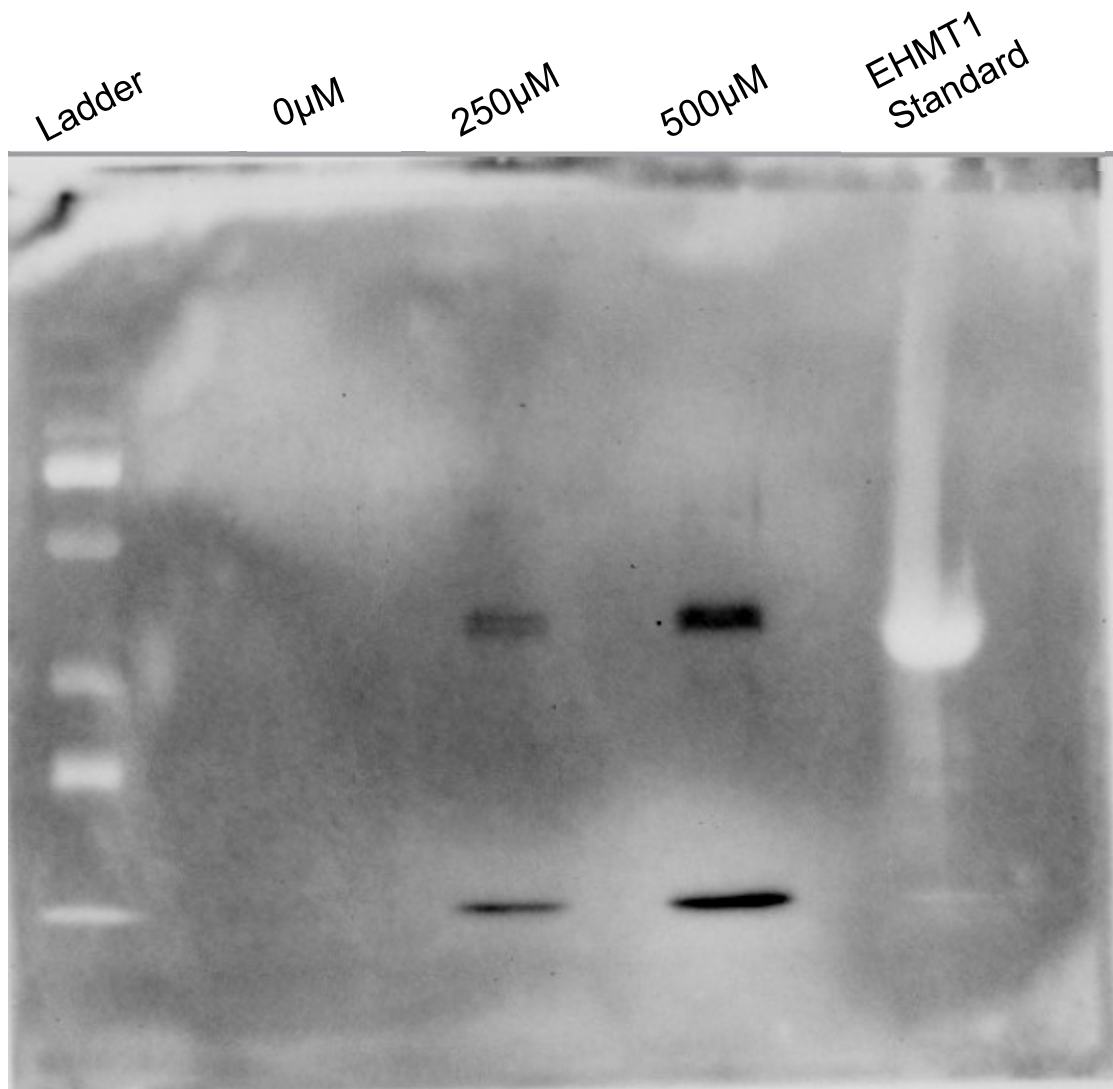


Figure 24. The experiment without a filtration step. The top bands that we see are at 37 KDa and the bottom bands are where the gel was allowed to run down to. We see band intensity increase as Probe 3 concentration increases which is promising,

EHMT1 was incubated with probe 3 and irradiated for 1 h at 365 nm. Streptavidin beads were then introduced into the samples for 3 h's incubation. Subsequently, the supernatants containing the unbound proteins were removed. The beads were thoroughly rinsed with buffer and then incubated with elution buffer containing 25 mM biotin. The eluted samples were resolved by SDS-PAGE and analyzed by western blot as described above.

Concentration-dependent labeling and enrichment of EHMT1 was observed in the elution samples (Fig. 24.). However, in addition to the biotinylated EHMT1 (~37 kDa), another band running close to the bottom of the blot was also detected. We reasoned that the lower running band was most likely the free probe 3. In the initial incubation, high micromolar concentrations of probe 3 were used. Some of the unbound probes were carried over to the elution samples. This can be problematic because the free probes could compete with the biotinylated proteins for binding to reduce the efficiency of the enrichment. To reconcile this, after the photoaffinity labeling, a filtration step was added to remove the free probes. Centrifugal filter units with 10 kDa cutoff were used to eliminate the small molecules, but to retain the proteins. After the filtration, the samples were subjected to the affinity enrichment as described above.

3.3.5 Optimized Pull-down Assay

After the above-mentioned alterations and adjustments, an optimized photoaffinity labeling and affinity enrichment assay was established. Briefly, the synthetic probe was incubated with EHMT1. After 1 h's UV irradiation, the samples were filtered to remove unbound probes. The filtered samples were then incubated with high-capacity streptavidin beads. Unbound proteins were separated from the beads. After thorough rinsing, the beads were incubated with excess

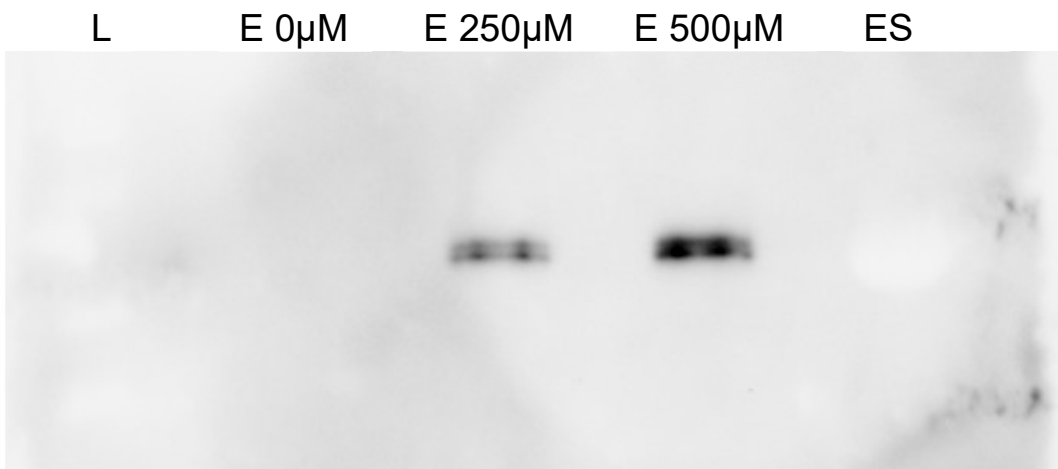


Figure 25. Affinity enrichment assay. L was the protein ladder to make sure the gel ran to completion. E 0 μM is a protein standard, we expect to see no band in this lane because EHMT1 does not have biotin tag for anti-biotin antibodies to bind to. E 250 μM has that concentration of Probe 3 present in the solution. We see a band here meaning probe 3 has covalently bound to EHMT1 via photocrosslinking. The band at E 500 μM is for probe 3 concentration is darker than the 250 μM implying the increased concentration led to increased binding. Finally, the ES is the enzyme standard lane.

amount of biotin to dissociate the proteins from the beads. Finally, the elutions were analyzed by western blot as mentioned previously.

Figure 25 shows a western blot for an optimized pull-down assay. Probe 3 labeled EHMT1 in a dose-dependent manner, as evidenced by the bands at ~ 37 kDa. More importantly, the lower running bands corresponding to the unbound probe were not detected, suggesting the successful removal of these small molecules from the samples. Additionally, biotinylated proteins were not observed in supernatants, washes or on the beads, further proving the effective enrichment and elution.

Taken together, the photoaffinity labeling and enrichment assay using SAM-based chemical probes has been established and optimized. Probe 3, indeed, labeled EHMT1, although at high micromolar concentrations (no less than 250 μM). The relatively weak affinity of probe 3 to MTase stemmed from its structural features. Probe 3, lacking the “warhead” portion, is an adenosine

analog rather than a SAM derivative. We hypothesized that probe 3 would prefer to bind to adenosine binding proteins, and probe 1, a true SAM analog, would have a higher affinity to MTases. This type of selectivity is ideal for probe development.

3.4 Pull-down Assay Using an Adenosine Binding Protein

Adenosine deaminase (ADA) was used for the following experiments. ADA is an enzyme that catalyzes the deamination of adenosine into inosine.⁹⁷ A deficiency in ADA in humans leads to t-lymphocyte development deficiency.⁹⁸ In addition to ADA being a well-known adenosine binding protein it is also commercially available. Being commercially available allows us to save time skipping the protein purification.

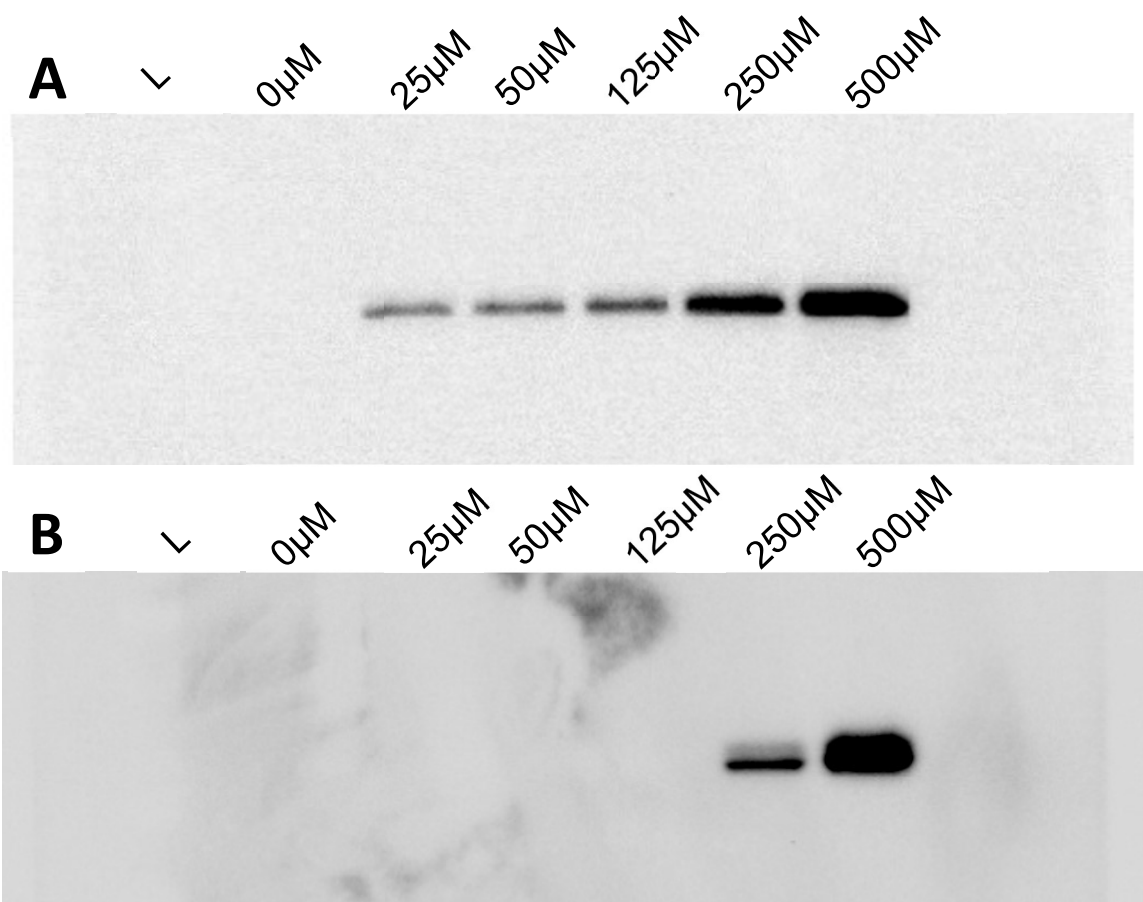


Figure 26. Chemiluminescence western blot images of the affinity enrichment gels. A) is a competitive binding of Probe 3 competing with inosine binding to ADA. B) is a competitive binding of Probe 3 competing with SAM binding to EHMT1. The lanes labeled L were where the ladder was run. Lanes labeled with concentration are stating the concentration of Probe 3 present in that sample.

Recombinant ADA was incubated with probe 3 at various concentrations (0, 25, 50, 125, 250 or 500 μM) before being irradiated at 365 nm for 1 h. After removal of free probes using centrifugal filter units, the samples were incubated with streptavidin beads for affinity capture. The supernatants were then removed, and the beads were rinsed and incubated with biotin elution buffer. The eluted proteins were analyzed by immunoblotting (Fig. 26.). Probe 3, as expected, demonstrated higher affinity to ADA. It labeled this protein in a nice concentration-dependent manner. Even at the lowest concentration, 25 μM , the labeling could still be detected.

3.5 Competitive Labeling Assay

One of the major issues in photoaffinity labeling is the non-specific labeling which may create background noise or false positive results. In order to rule out the possibility of off-target effect, competition analysis using known EHMT1 or ADA inhibitors was also performed. SAM, the endogenous co-substrate of MTases, was used as the competitor for EHMT1. The protein was incubated with SAM before the addition of probe 3. Subsequently, the samples were subjected to the filtration, capture, rinsing and elution protocols as described before (Figure 27. A). With probe 3 alone, EHMT1 was labeled in a concentration-dependent manner, consistent with prior results.

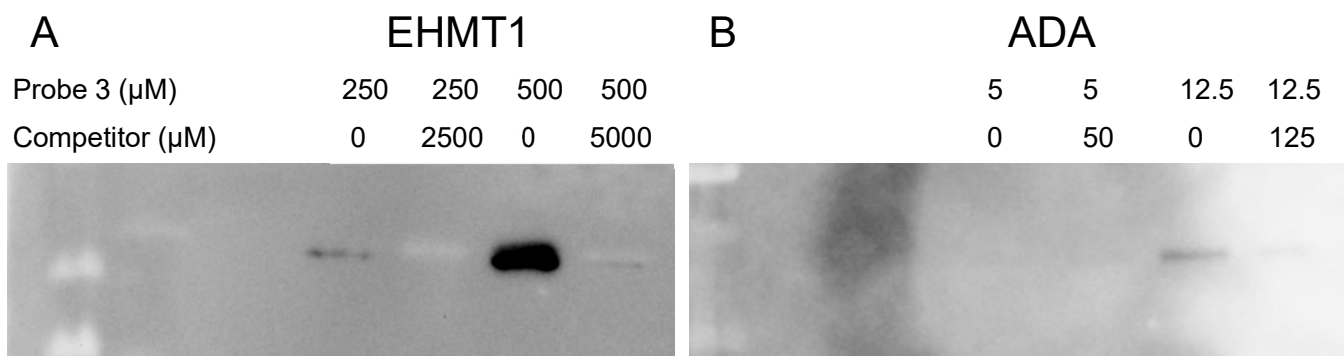


Figure 27. A. Western blot we obtained from the competitive pull-down assay with Probe 3 and EHMT1. A faint band is observed with 250 μM of Probe 3 in the absence of the competitor SAM. In the presence of ten times concentration of SAM the 250 μM of Probe 3 is out competed and the band disappears. The band intensity at 500 μM of Probe 3 is more intense, but again when ten times concentration of the competitor is added the band disappears. B. Western blot we obtained from the competitive pull-down assay with Probe 3 and ADA. A faint band is observed at 12.5 μM of Probe 3, but when 10 times concentration of competitor cladribine is present the band again disappears.

The introduction of excess amounts of SAM, the labeling of EHMT1 by probe 3 was almost completely abolished, suggesting the on-target activity of our probe.

For ADA, a known inhibitor, cladribine,^{99,93} was chosen for the competitive labeling experiments. Cladribine is a purine analog that is resistant to ADA breakdown, this causes it to accumulate in cells. Probe 3 alone at 12.5 μM demonstrated robust labeling of ADA (Figure 27, B). In the presence of 10 times excess amount of cladribine, the labeling was significantly reduced, once again suggesting the on-target effect of the synthetic probe.

3.6 Spiked in Cell Lysate Labeling

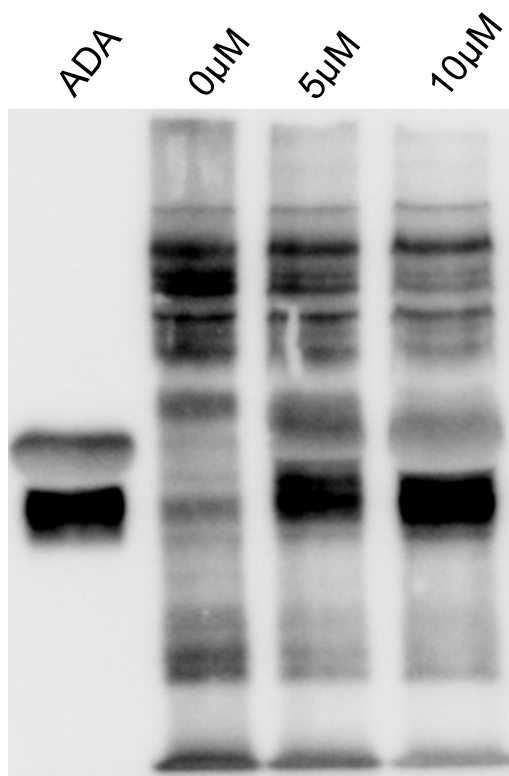


Figure 28. In the first lane we have an ADA standard to show what where on the blot we would expect to see our pulled down protein to be at. With 0 μM of Probe 3 we still see some protein being pulled down, we can attribute this to proteins that bind naturally to streptavidin beads. With the addition of 5 μM of Probe 3 we see a faint band appear where we could expect ADA to be on the blot. With 10 μM of Probe 3 the band is now very intense where we would expect to see ADA on the blot.

We wanted to make sure we could use this protein pull-down to see if we could separate a specific type or protein from a cell lysate. For this experiment we spiked in 10 μM of ADA into the cell lysate from the EHMT1. We incubated probe 3 with the cell lysate and then performed and then irradiated it for 3 hours. We then loaded these samples onto the SDS-page gel and ran western blot procedures to obtain our blot.

In Figure 28 we see the blot obtained from the spiked in protein cell lysate affinity labeling assay. We ran a lane with pure ADA to show where the band would be present so that we could see it in comparison to other bands that might be present. We see some protein noise that is present from the cell lysate in lane with 0 μM of probe 3. In lane with 5 μM of probe 3 we see a faint band where we would expect the ADA band to be. The lane with 10 μM of probe 3 we see a very distinct intense band. This leads us to believe that we can selectively pull-down proteins that our probes bind to.

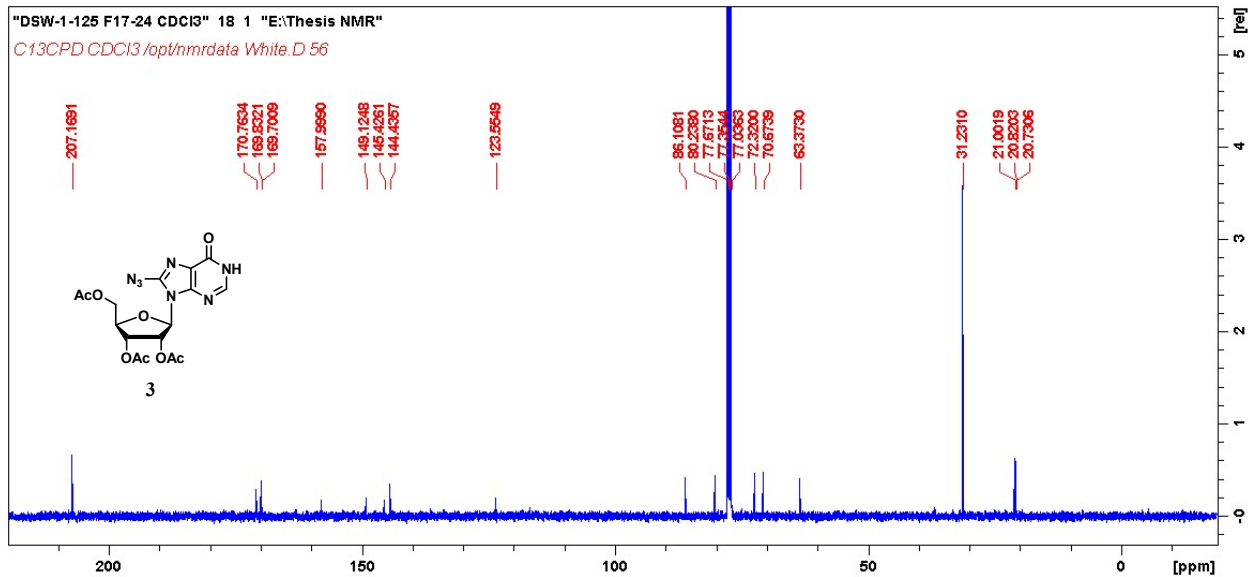
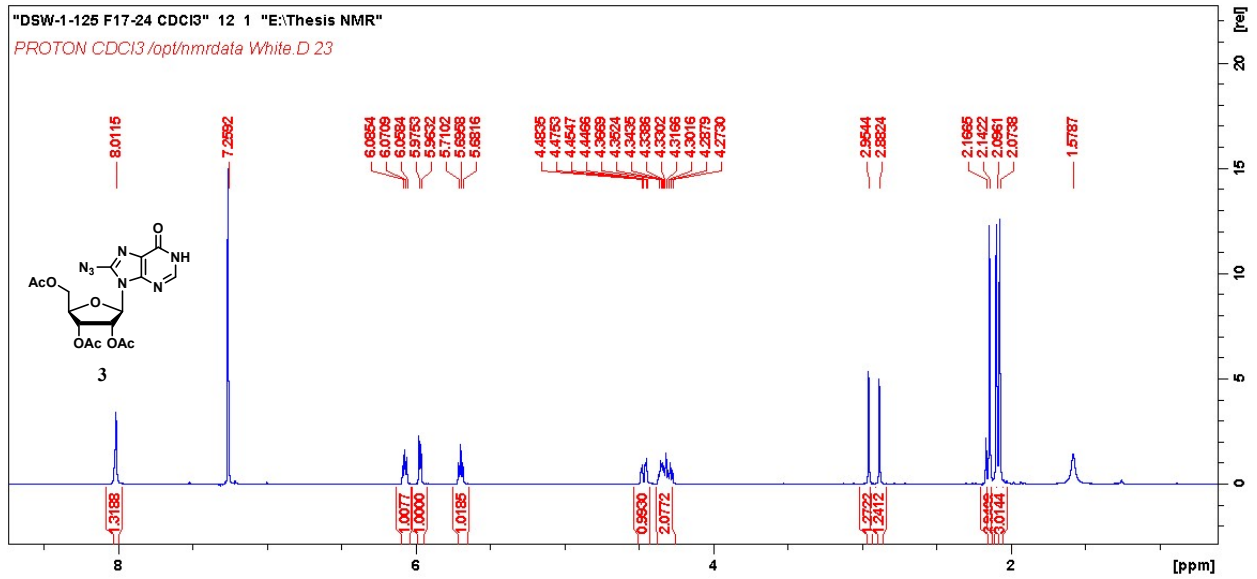
3.7 Conclusion

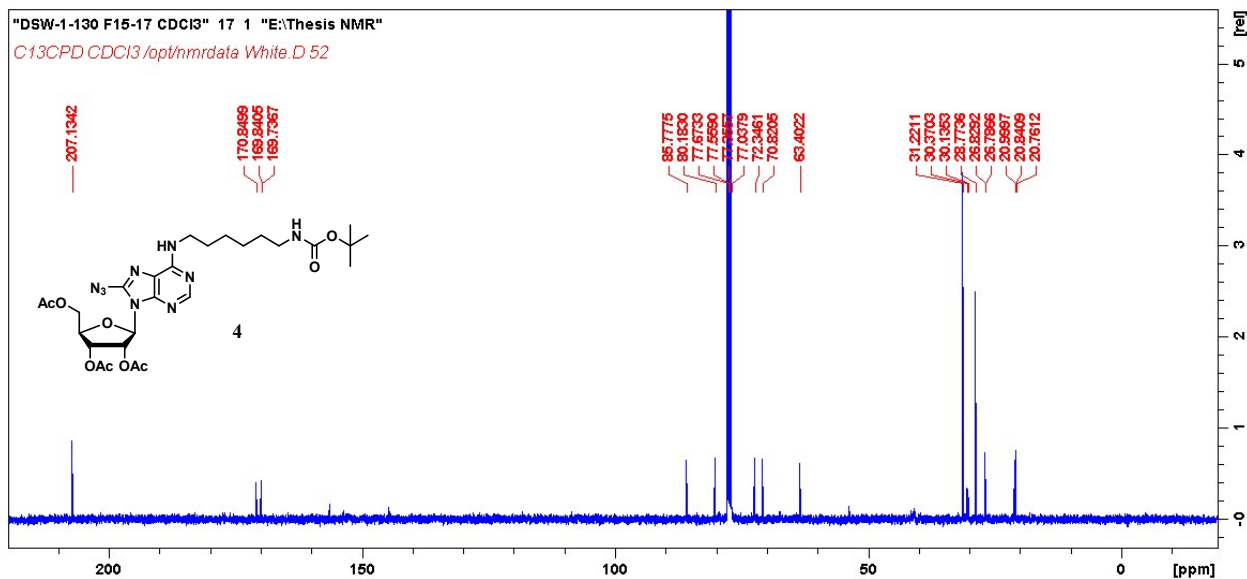
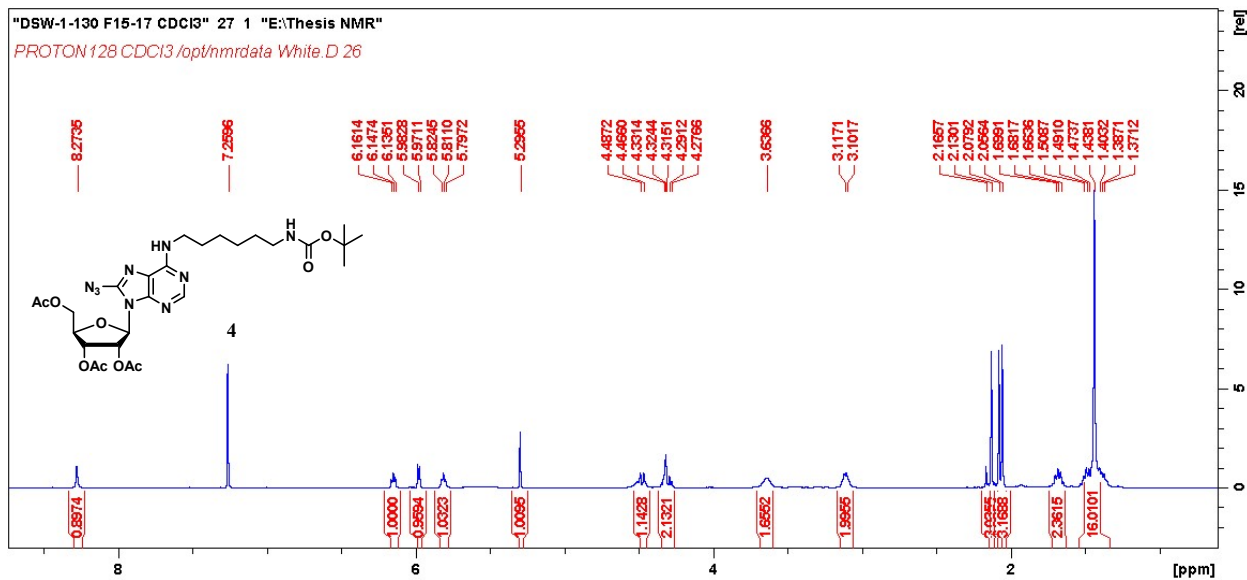
This project aimed to synthesize probe 1 and create an assay for the profiling of MTases. We synthesized an intermediate of probe 1, probe 3. Studying the biological activity of probe 3 will provide us an important understanding of how we expect probe 1 to function when it is successfully synthesized. We optimized a protein pull-down assay to study the activity of probe 3 using both a MTase and an adenosine binding protein. We have determined that probe 3 was able to bind to our model MTase EHMT1. Following this we completed a competition assay using SAM as a competitor to rule out photocrosslinking caused by nonspecifically interacting between probe 3 and EHMT1. Due to requiring a high concentration of probe 3 to pull-down EHMT1 we used an adenosine binding protein, ADA, to show probe 1 should have a higher affinity when completed. We performed the same pulldown and competitive assays with ADA as we had with

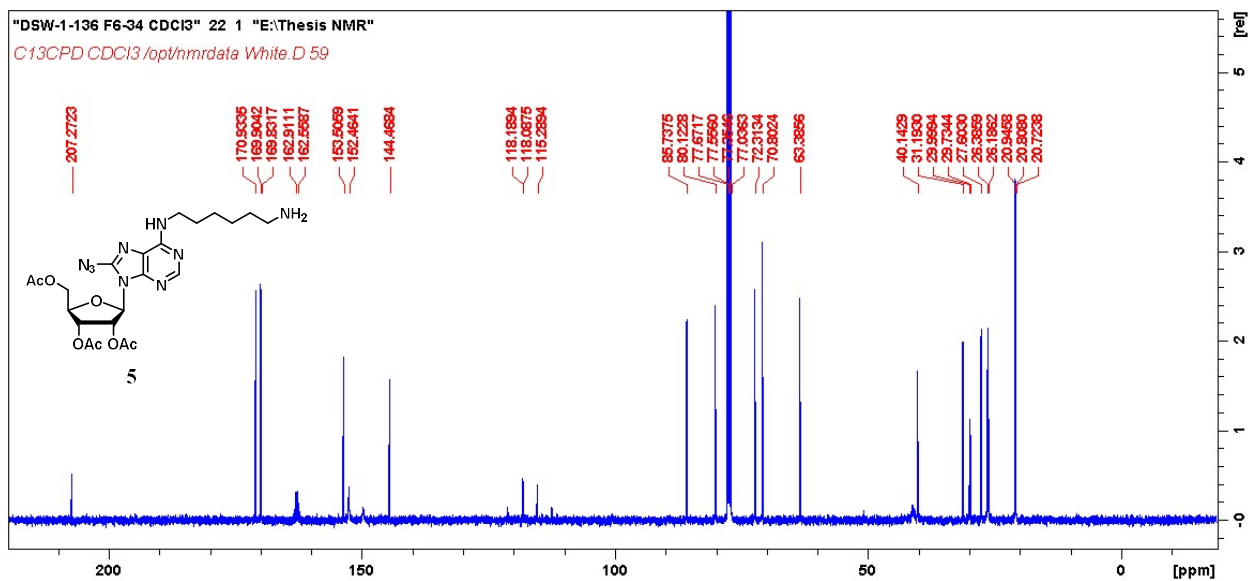
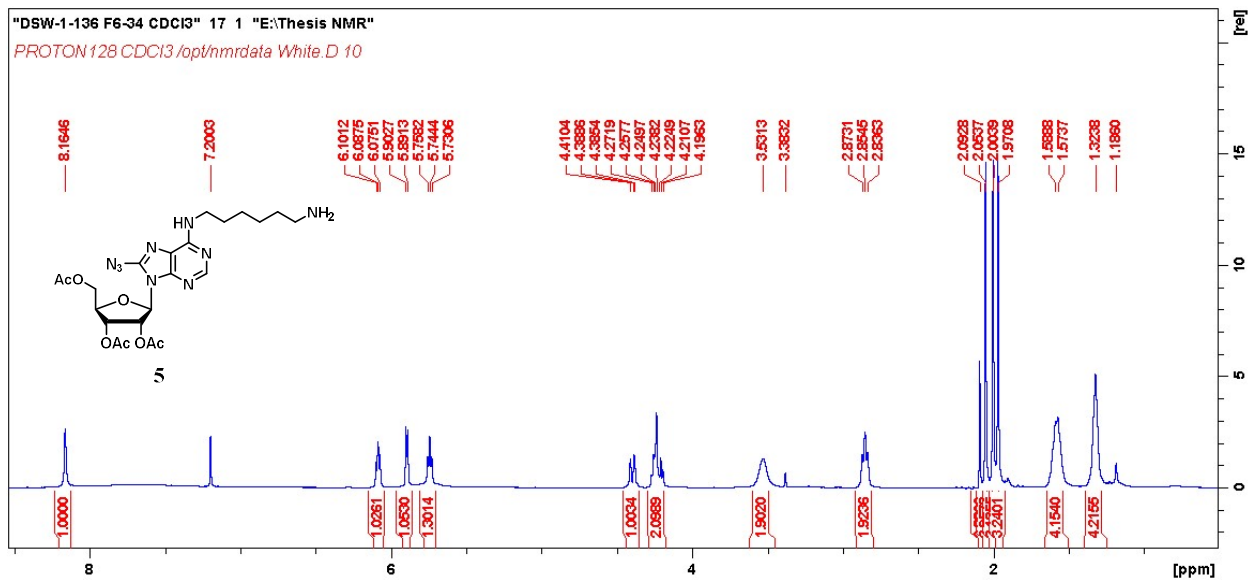
EHMT1. From these studies we found that probe 3 would bind to ADA at a much lower concentration than it would to EHMT1, we reasoned that this must occur because probe 3 is an adenosine analog not a SAM analog. In our final experiments we performed protein labeling with ADA spiked into cell lysate. We saw that we were able to selectively separate ADA from the cell lysate. This means in the future we should be able to use probe 1 to selectively pull-down MTases from their endogenous cell lysate.

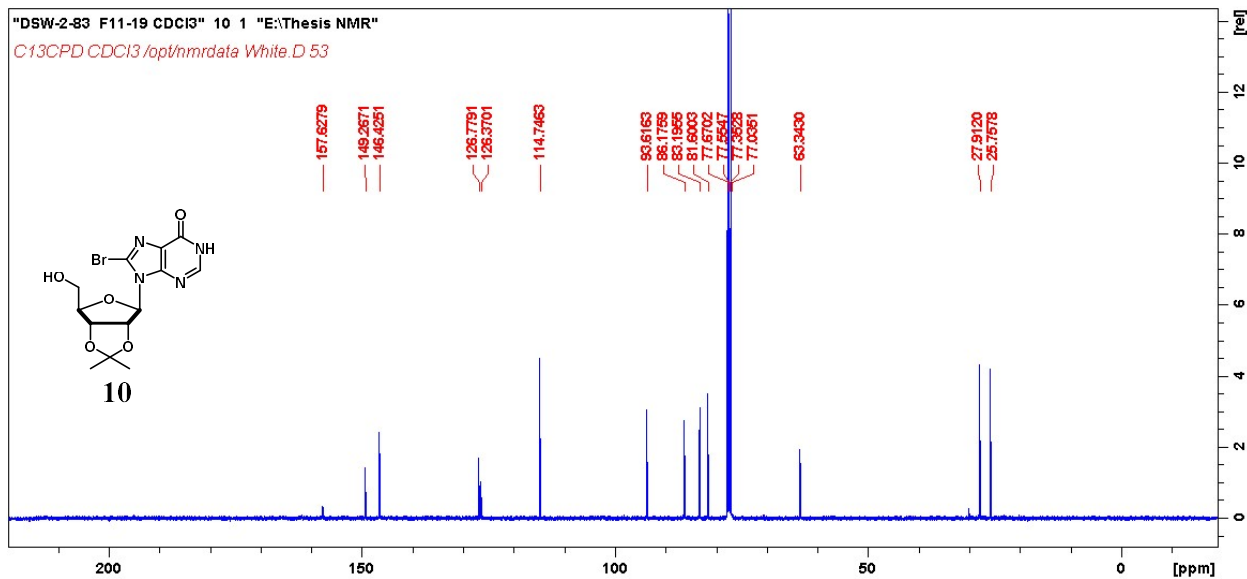
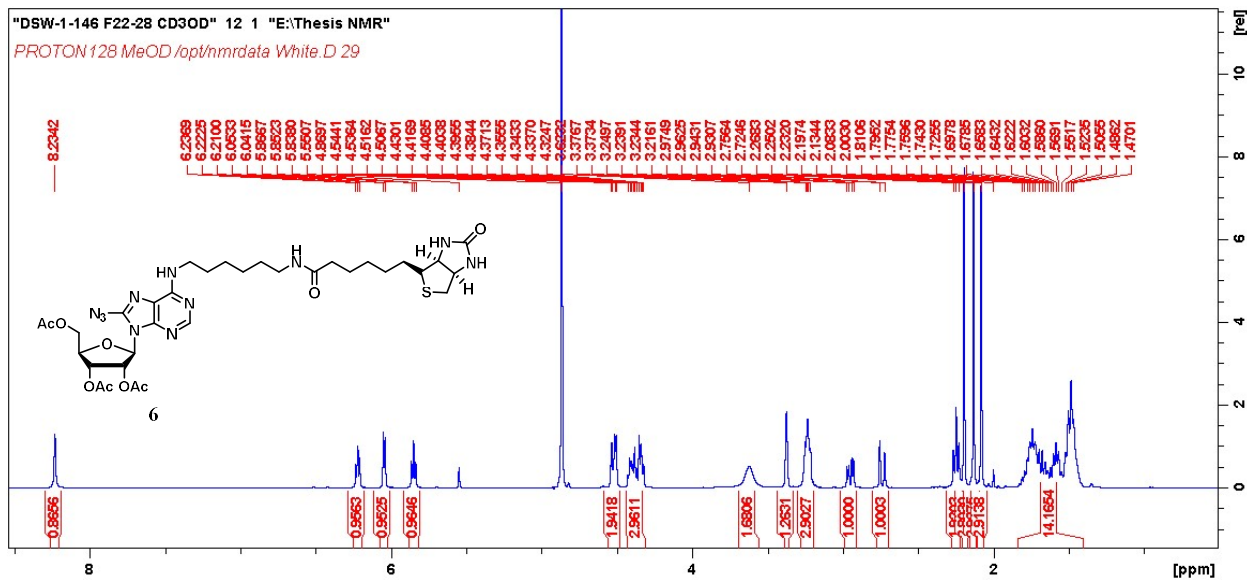
A future study we would like to perform a protein pull-down using a MTase at its endogenous concentration. An additional study that could be completed to improve our probe would be to perform a docking analysis. We could attempt to further optimize the positions of the azide photocrosslinking group as well as linker region containing the biotin tag to improve binding to MTases. Finally, a proteomic profiling study will be completed by Dr. Stan Steven from the University of Southern Florida in the future to determine if our probes will bind to any other proteins.

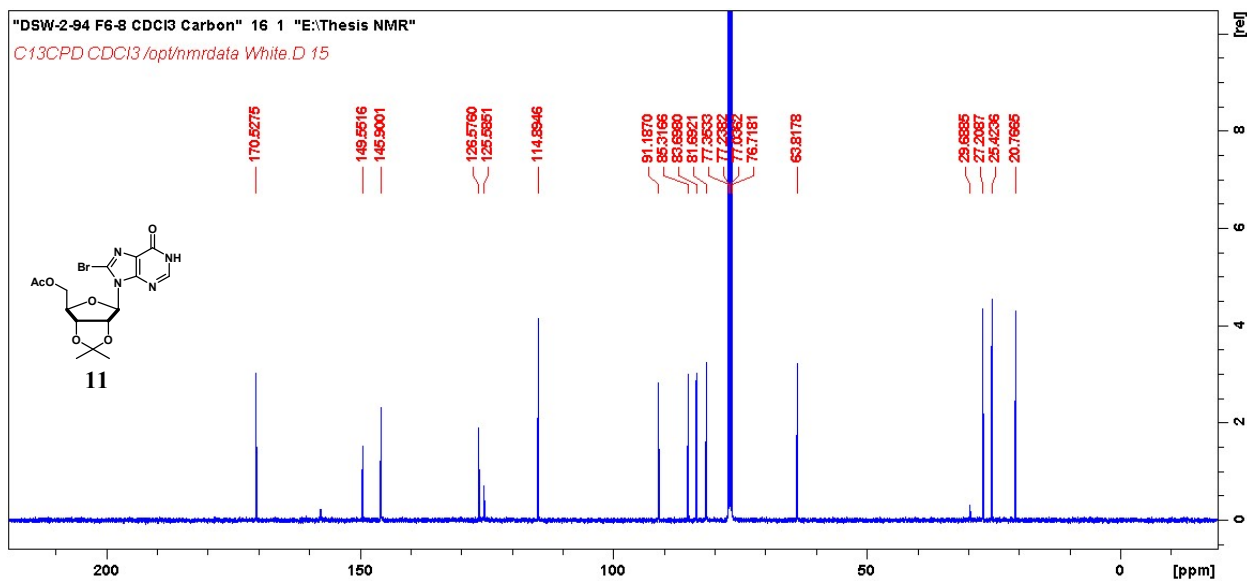
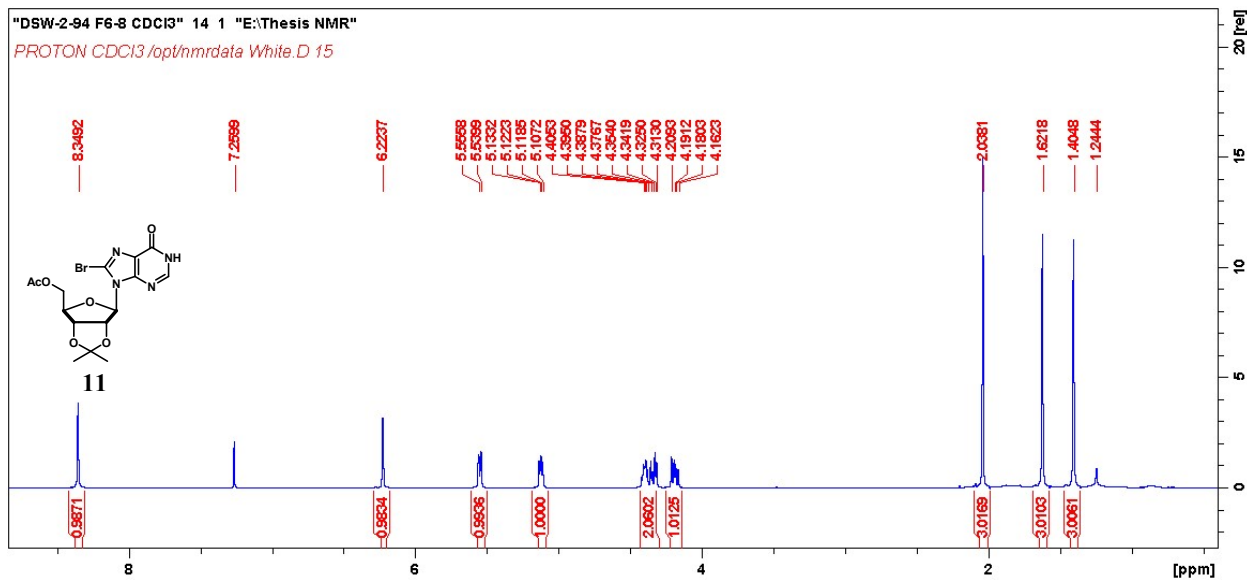
4. NMR Spectrums

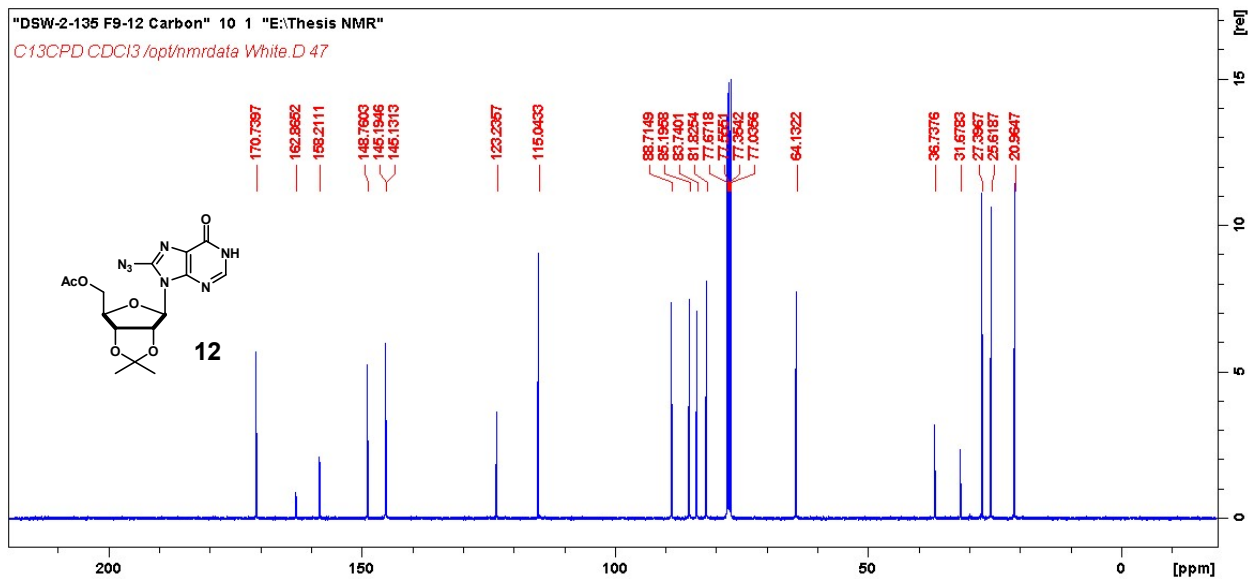
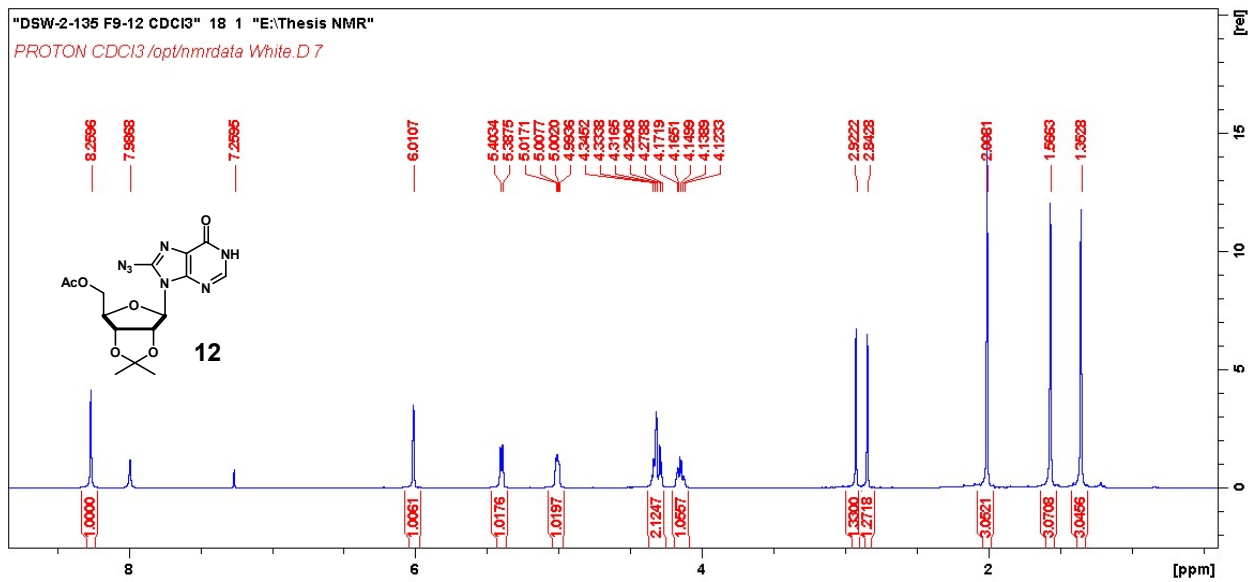


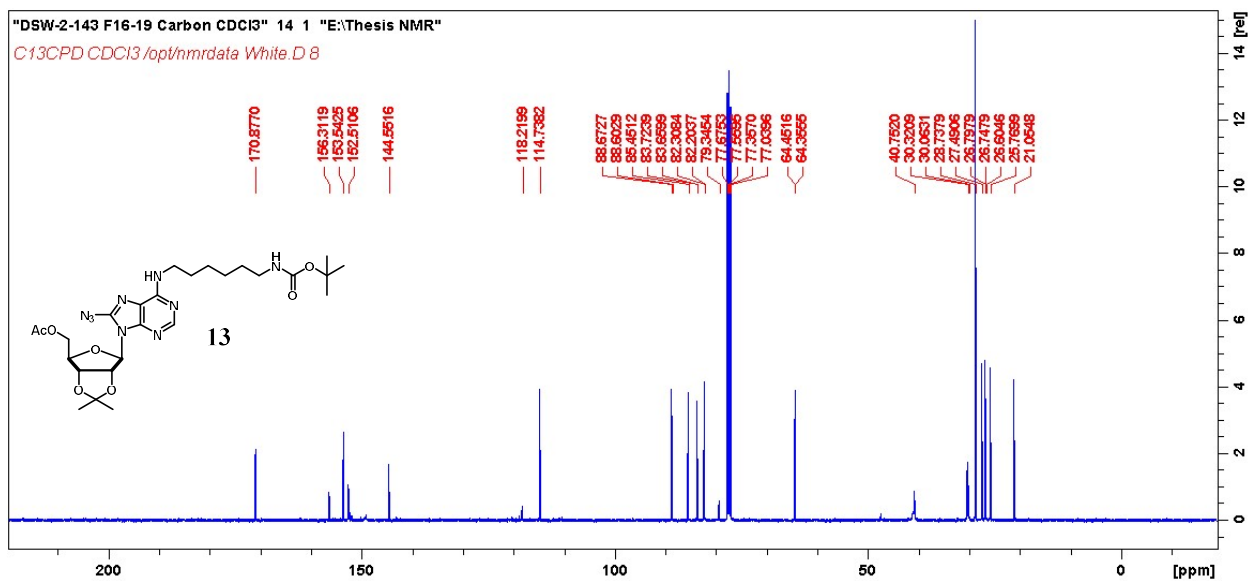
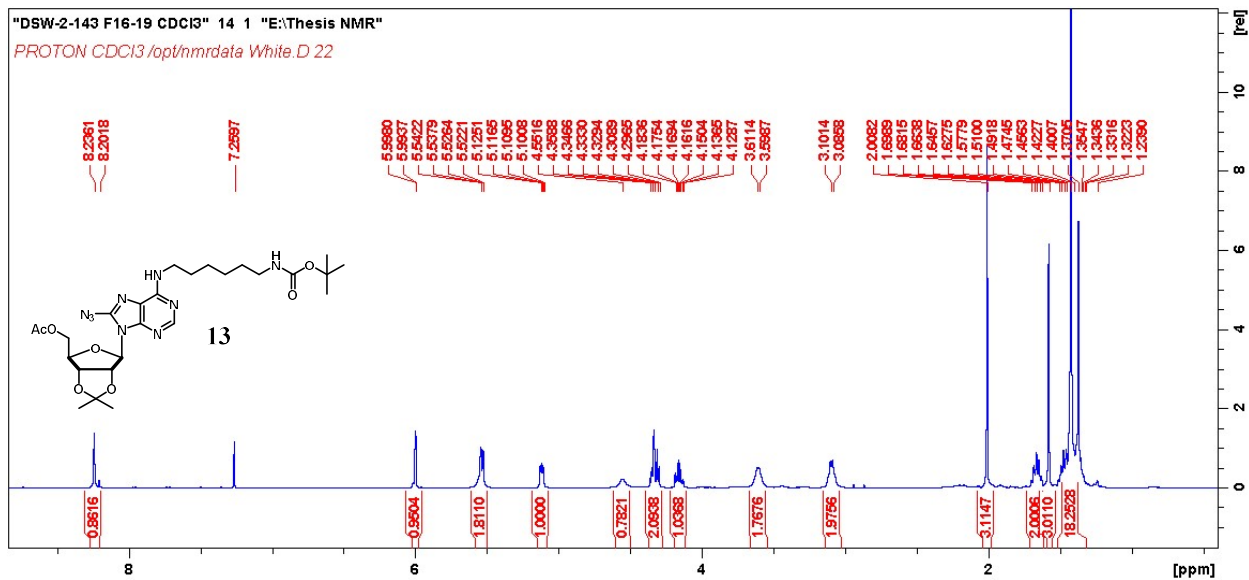


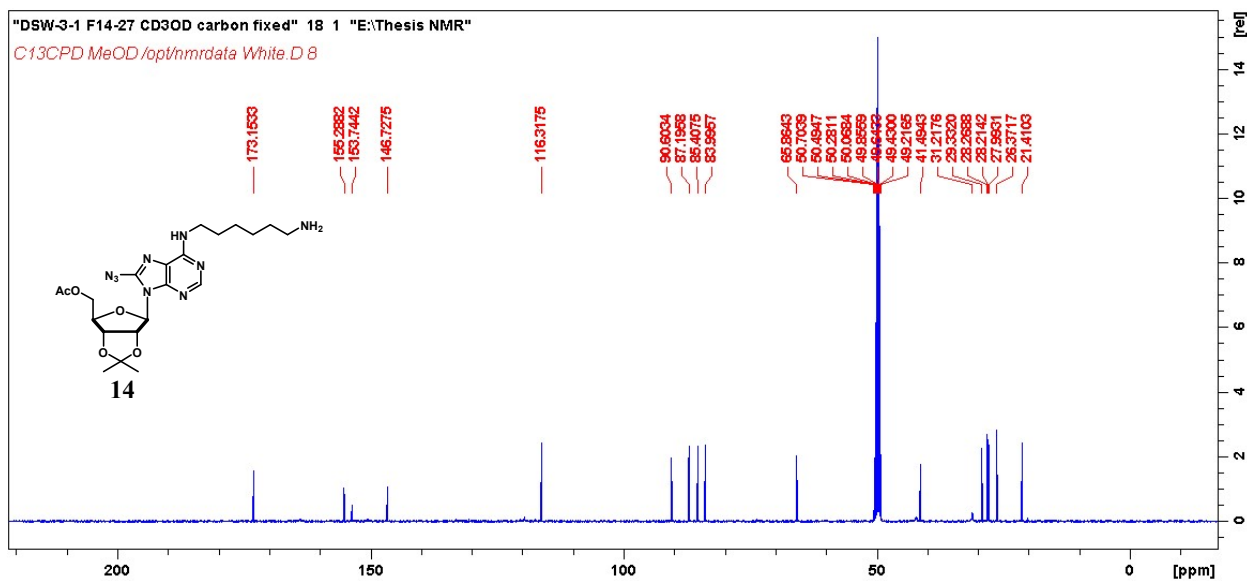
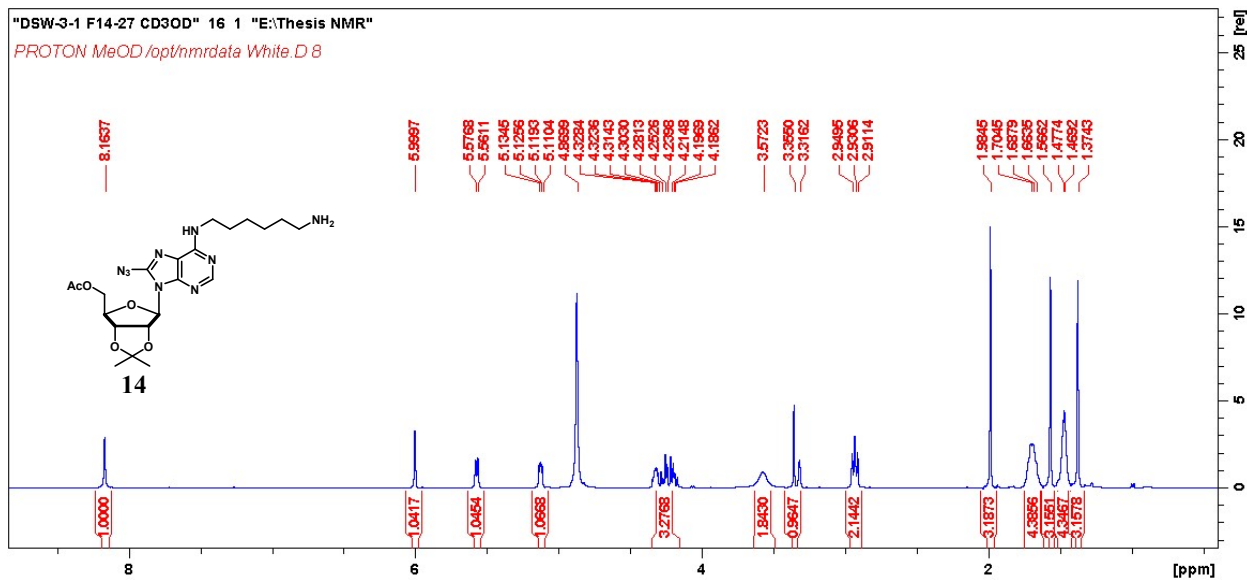


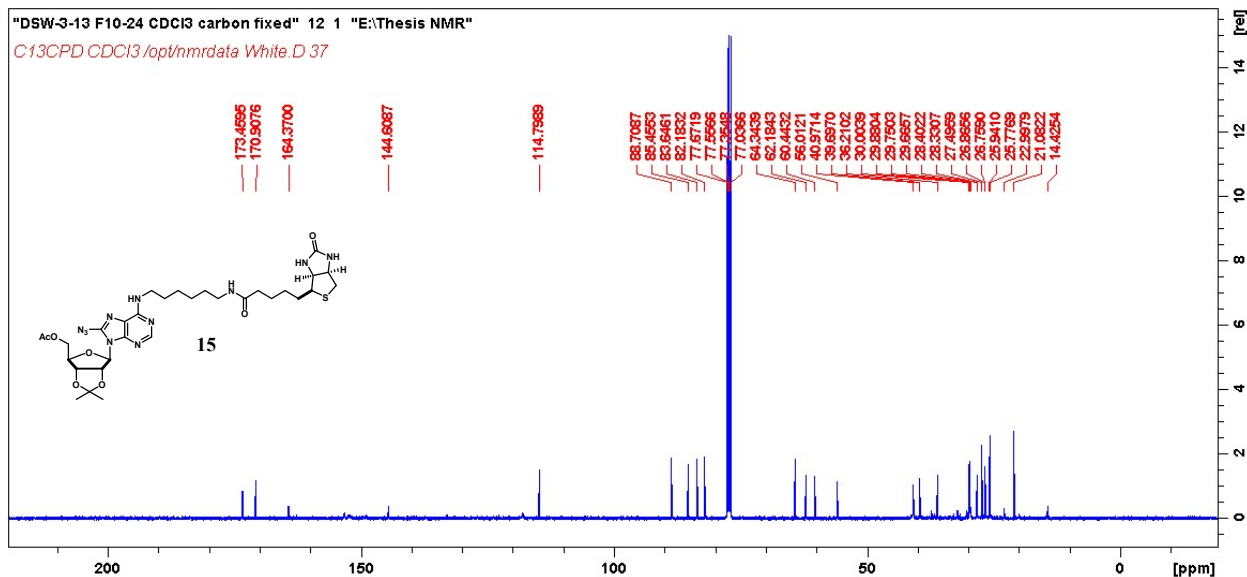
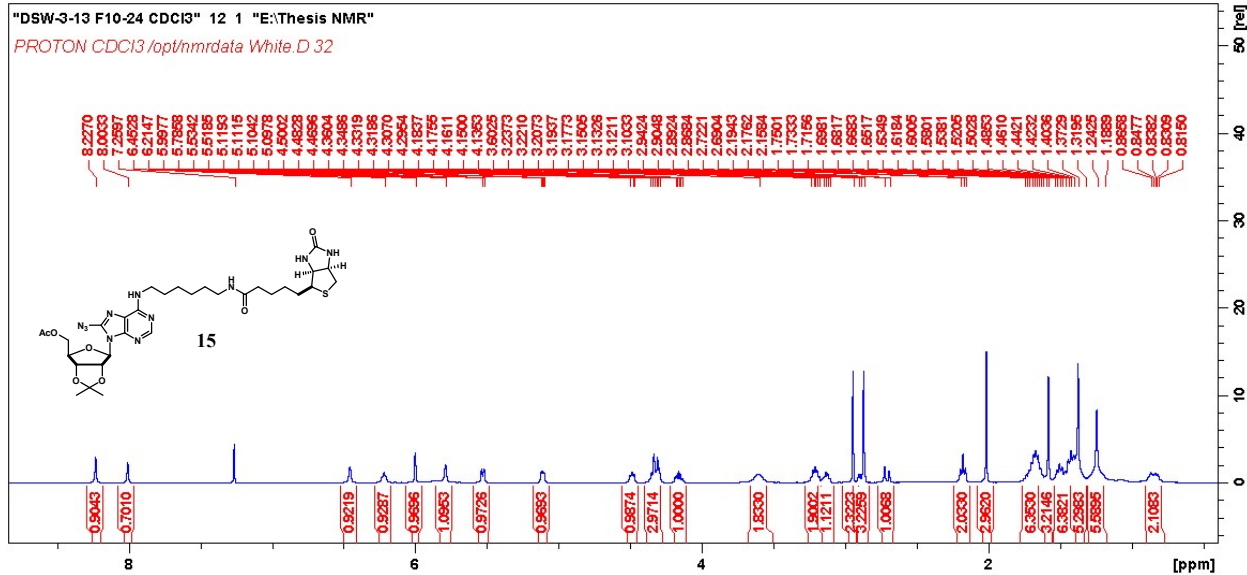


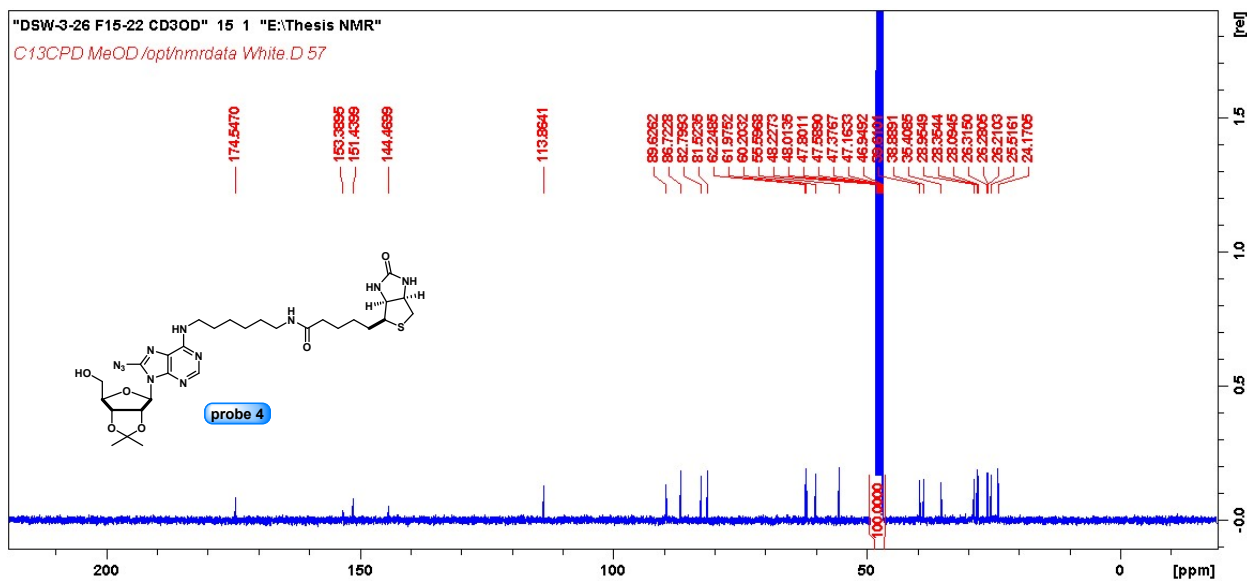
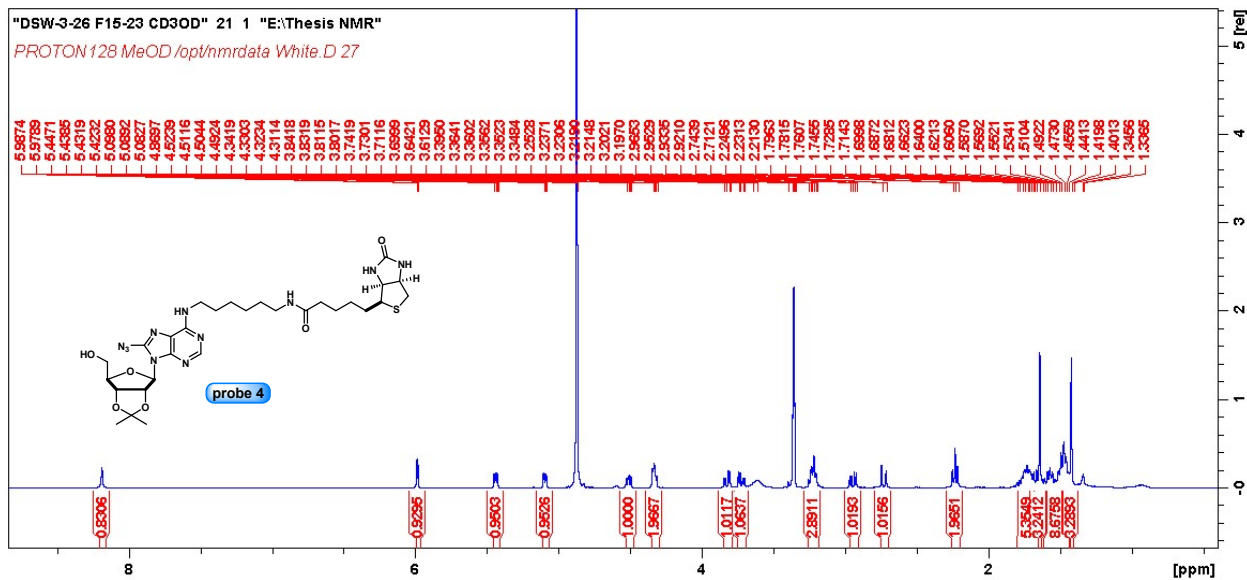


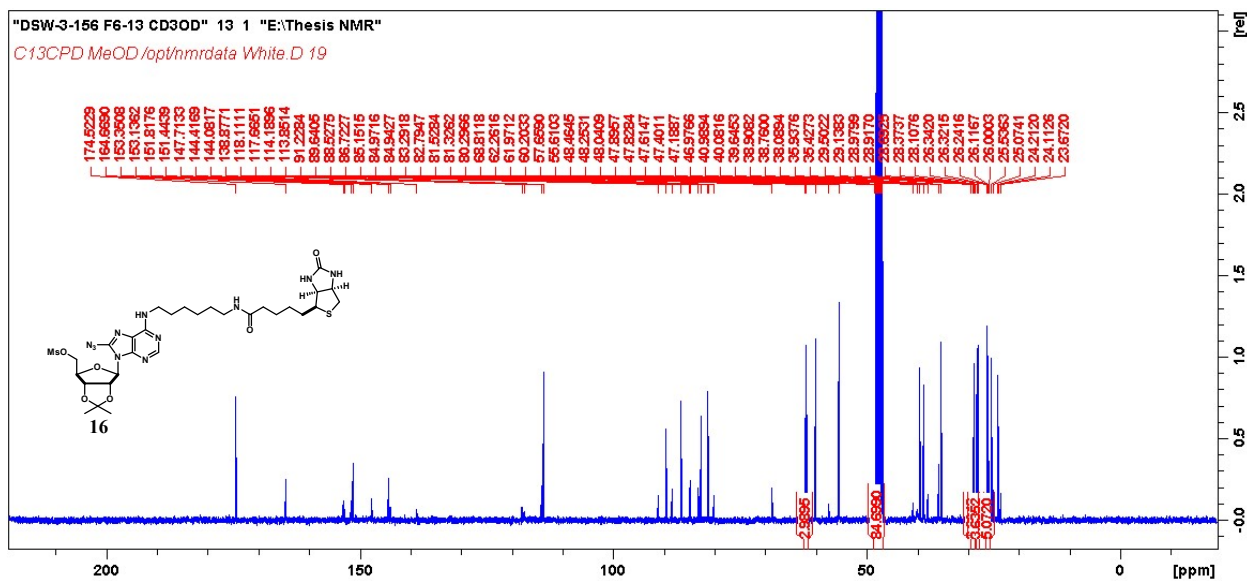
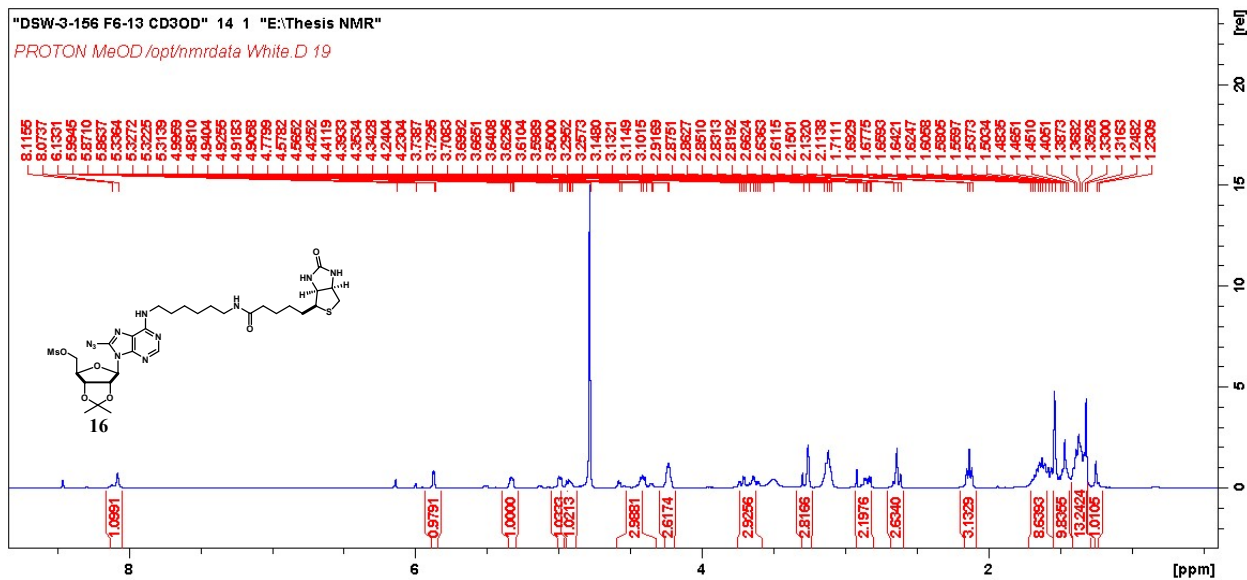


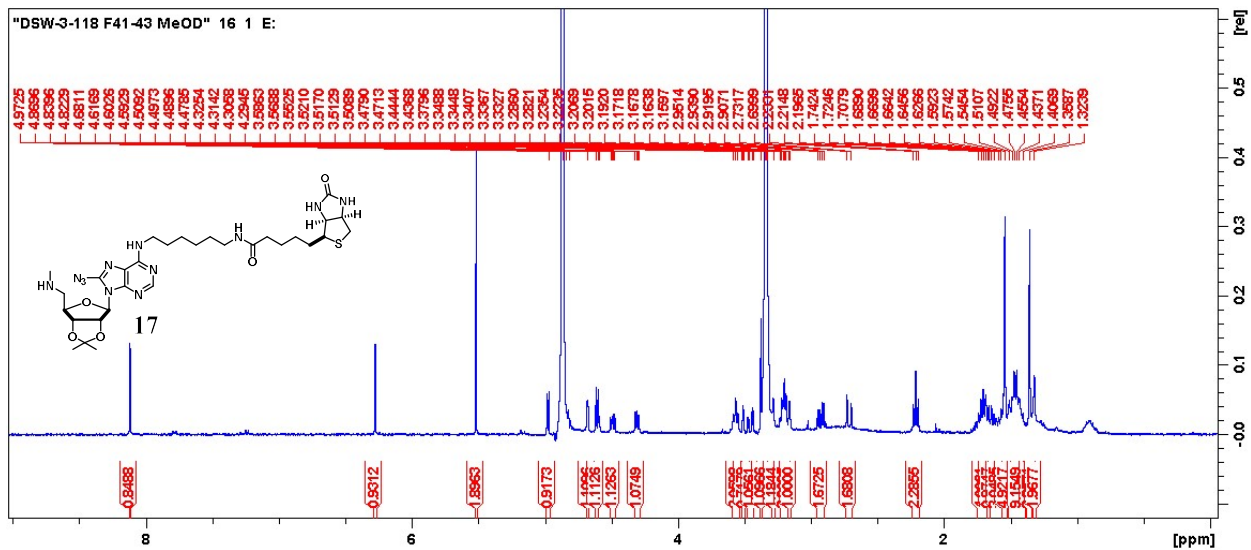












References

- (1) Kaniskan, H. Ü.; Martini, M. L.; Jin, J. Inhibitors of Protein Methyltransferases and Demethylases. *Chem. Rev.* **2018**, *118* (3), 989–1068.
<https://doi.org/10.1021/acs.chemrev.6b00801>.
- (2) Mack, J. P. G.; Slaytor, M. B. Affinity Chromatography of an S-Adenosylmethionine-Dependent Methyltransferase Using Immobilized S-Adenosylhomocysteine. Purification of the Indolethylamine N-Methyltransferases of *Phalaris Tuberosa*. *J. Chromatogr. A* **1978**, *157* (C), 153–159. [https://doi.org/10.1016/S0021-9673\(00\)92331-8](https://doi.org/10.1016/S0021-9673(00)92331-8).
- (3) Metere, A.; Graves, C. E. Factors Influencing Epigenetic Mechanisms: Is There a Role for Bariatric Surgery? *High-Throughput* **2020**, *9* (1), 1–6. <https://doi.org/10.3390/ht9010006>.
- (4) Petrossian, T. C.; Clarke, S. G. Uncovering the Human Methyltransferasome. *Mol. Cell. Proteomics* **2011**, *10* (1), 1–12. <https://doi.org/10.1074/mcp.M110.000976>.
- (5) Hymbaugh Bergman, S. J.; Comstock, L. R. N-Mustard Analogs of S-Adenosyl-L-Methionine as Biochemical Probes of Protein Arginine Methylation. *Bioorganic Med. Chem.* **2015**, *23* (15), 5050–5055. <https://doi.org/10.1016/j.bmc.2015.05.001>.
- (6) Mahajan, S.; Manetsch, R.; Merkler, D. J.; Stevens, S. M. Synthesis and Evaluation of a Novel Adenosine-Ribose Probe for Global-Scale Profiling of Nucleoside and Nucleotide-Binding Proteins. *PLoS One* **2015**, *10* (2), 1–17.
<https://doi.org/10.1371/journal.pone.0115644>.
- (7) Dalhoff, C.; Lukinavičius, G.; Klimašauskas, S.; Weinhold, E. Synthesis of S-Adenosyl-L-Methionine Analogs and Their Use for Sequence-Specific Transalkylation of DNA by Methyltransferases. *Nat. Protoc.* **2006**, *1* (4), 1879–1886.
<https://doi.org/10.1038/nprot.2006.253>.

- (8) Murale, D. P.; Hong, S. C.; Haque, M. M.; Lee, J. S. Photo-Affinity Labeling (PAL) in Chemical Proteomics: A Handy Tool to Investigate Protein-Protein Interactions (PPIs). *Proteome Sci.* **2017**, *15* (1), 1–34. <https://doi.org/10.1186/s12953-017-0123-3>.
- (9) Ramadan, M.; Bremner-hay, N. K.; Carlson, S. A.; Comstock, L. R. Synthesis and Evaluation of N 6-Substituted Azide- and Alkyne- Bearing N -Mustard Analogs of S - Adenosyl- L -Methionine. *Tetrahedron* **2014**, *70*, 5291–5297.
- (10) Swarbrick, J. M.; Potter, B. V. L. Total Synthesis of a Cyclic Adenosine 5'-Diphosphate Ribose Receptor Agonist. *J. Org. Chem.* **2012**, *77* (9), 4191–4197. <https://doi.org/10.1021/jo202319f>.
- (11) Waddington, C. H. The Epigenotype. 1942. *Int. J. Epidemiol.* **2012**, *41* (1), 10–13. <https://doi.org/10.1093/ije/dyr184>.
- (12) Callinan, P. A.; Feinberg, A. P. The Emerging Science of Epigenomics. *Hum. Mol. Genet.* **2006**, *15 Spec No* (1), 95–101. <https://doi.org/10.1093/hmg/ddl095>.
- (13) Goldberg, A. D.; Allis, C. D.; Bernstein, E. Epigenetics: A Landscape Takes Shape. *Cell* **2007**, *128* (4), 635–638. <https://doi.org/10.1016/j.cell.2007.02.006>.
- (14) McGinty, R. K.; Tan, S. Nucleosome Structure and Function. *Chem. Rev.* **2015**, *115* (6), 2255–2273. <https://doi.org/10.1021/cr500373h>.
- (15) Andrews, A. J.; Luger, K. Nucleosome Structure(s) and Stability: Variations on a Theme. *Annu. Rev. Biophys.* **2011**, *40* (1), 99–117. <https://doi.org/10.1146/annurev-biophys-042910-155329>.
- (16) Bird, A. DNA Methylation Patterns and Epigenetic Memory. *Genes Dev.* **2002**, *16* (1), 6–21. <https://doi.org/10.1101/gad.947102>.
- (17) Li, E.; Zhang, Y. DNA Methylation in Mammals. *Cold Spring Harb. Perspect. Biol.* **2014**,

- 6 (5). <https://doi.org/10.1101/cshperspect.a019133>.
- (18) Kobayashi, H.; Arima, T. Genomic Imprinting in Mammals. *J. Mamm. Ova Res.* **2006**, *23* (4), 143–149. <https://doi.org/10.1274/jmor.23.143>.
- (19) Luger, K.; Mäder, A. W.; Richmond, R. K.; Sargent, D. F.; Richmond, T. J. Crystal Structure of the Nucleosome Core Particle at 2.8 Å Resolution. *Nature* **1997**, *389* (6648), 251–260. <https://doi.org/10.1038/38444>.
- (20) Bannister, A. J.; Kouzarides, T. Regulation of Chromatin by Histone Modifications. *Cell Res.* **2011**, *21* (3), 381–395. <https://doi.org/10.1038/cr.2011.22>.
- (21) Ferri, E.; Petosa, C.; McKenna, C. E. Bromodomains: Structure, Function and Pharmacology of Inhibition. *Biochem. Pharmacol.* **2016**, *106*, 1–18. <https://doi.org/10.1016/j.bcp.2015.12.005>.
- (22) Zhang, G.; Pradhan, S. Mammalian Epigenetic Mechanisms. *IUBMB Life* **2014**, *66* (4), 240–256. <https://doi.org/10.1002/iub.1264>.
- (23) Yun, M.; Wu, J.; Workman, J. L.; Li, B. Readers of Histone Modifications. *Cell Res.* **2011**, *21* (4), 564–578. <https://doi.org/10.1038/cr.2011.42>.
- (24) ALLFREY, V. G.; FAULKNER, R.; MIRSKY, A. E. Acetylation and Methylation of Histones and Their Possible Role in The. *Proc. Natl. Acad. Sci. United States* **1964**, *51* (1938), 786–794. <https://doi.org/10.1073/pnas.51.5.786>.
- (25) Choudhary, C.; Kumar, C.; Gnad, F.; Nielsen, M. L.; Rehman, M.; Walther, T. C.; Olsen, J. V.; Mann, M. Lysine Acetylation Targets Protein Complexes and Co-Regulates Major Cellular Functions. *Science (80-.)*. **2009**, *325* (5942), 834–840. <https://doi.org/10.1126/science.1175371>.
- (26) Ng, S. S.; Yue, W. W.; Oppermann, U.; Klose, R. J. Dynamic Protein Methylation in

- Chromatin Biology. *Cell. Mol. Life Sci.* **2009**, *66* (3), 407–422.
<https://doi.org/10.1007/s00018-008-8303-z>.
- (27) Bedford, M. T.; Clarke, S. G. Protein Arginine Methylation in Mammals: Who, What, and Why. *Mol. Cell* **2009**, *33* (1), 1–13. <https://doi.org/10.1016/j.molcel.2008.12.013>.
- (28) Li, B.; Carey, M.; Workman, J. L. The Role of Chromatin during Transcription. *Cell* **2007**, *128* (4), 707–719. <https://doi.org/10.1016/j.cell.2007.01.015>.
- (29) Krogan, N. J.; Dover, J.; Khorrami, S.; Greenblatt, J. F.; Schneider, J.; Johnston, M.; Shilatifard, A. COMPASS, a Histone H3 (Lysine 4) Methyltransferase Required for Telomeric Silencing of Gene Expression. *J. Biol. Chem.* **2002**, *277* (13), 10753–10755.
<https://doi.org/10.1074/jbc.C200023200>.
- (30) Krogan, N. J.; Kim, M.; Tong, A.; Golshani, A.; Cagney, G.; Canadien, V.; Richards, D. P.; Beattie, B. K.; Emili, A.; Boone, C.; Buratowski, S.; Greenblatt, J.; Shilatifard, A. Methylation of Histone H3 by Set2 in *Saccharomyces Cerevisiae* Is Linked to Transcriptional Elongation by RNA Polymerase II Downloaded from [Http://Mcb.Asm.Org/](http://Mcb.Asm.Org/) on September 18 , 2012 by IMPERIAL COLLEGE LONDON
Methylation of Histone H3 by Set2 in *Saccharom.* **2003**, *23* (12), 4207–4218.
<https://doi.org/10.1128/MCB.23.12.4207>.
- (31) Tiffon, C. The Impact of Nutrition and Environmental Epigenetics on Human Health and Disease. *Int. J. Mol. Sci.* **2018**, *19* (11). <https://doi.org/10.3390/ijms19113425>.
- (32) Alegría-Torres, J. A.; Baccarelli, A.; Bollati, V. Epigenetics and Lifestyle. *Epigenomics* **2011**, *3* (3), 267–277. <https://doi.org/10.2217/epi.11.22>.
- (33) Tobi, E. W.; Lumey, L. H.; Talens, R. P.; Kremer, D.; Putter, H.; Stein, A. D.; Slagboom, P. E.; Heijmans, B. T. DNA Methylation Differences after Exposure to Prenatal Famine

- Are Common and Timing- and Sex-Specific. *Hum. Mol. Genet.* **2009**, *18* (21), 4046–4053. <https://doi.org/10.1093/hmg/ddp353>.
- (34) Breiding, M. J. Readers, Writers and Erasers: Chromatin as the Whiteboard of Heart Disease. *Physiol. Behav.* **2014**, *63* (8), 1–18.
<https://doi.org/10.1161/CIRCRESAHA.116.303630.Readers>.
- (35) Biswas, S.; Rao, C. M. Epigenetic Tools (The Writers, The Readers and The Erasers) and Their Implications in Cancer Therapy. *Eur. J. Pharmacol.* **2018**, *837* (August), 8–24.
<https://doi.org/10.1016/j.ejphar.2018.08.021>.
- (36) Filippakopoulos, P.; Picaud, S.; Mangos, M.; Keates, T.; Lambert, J. P.; Barseyte-Lovejoy, D.; Felletar, I.; Volkmer, R.; Müller, S.; Pawson, T.; Gingras, A. C.; Arrowsmith, C. H.; Knapp, S. Histone Recognition and Large-Scale Structural Analysis of the Human Bromodomain Family. *Cell* **2012**, *149* (1), 214–231.
<https://doi.org/10.1016/j.cell.2012.02.013>.
- (37) Sanchez, R.; Zhou, M. M. The PHD Finger: A Versatile Epigenome Reader. *Trends Biochem. Sci.* **2011**, *36* (7), 364–372. <https://doi.org/10.1016/j.tibs.2011.03.005>.
- (38) Arrowsmith, C. H.; Bountra, C.; Fish, P. V.; Lee, K.; Schapira, M. Epigenetic Protein Families: A New Frontier for Drug Discovery. *Nat. Rev. Drug Discov.* **2012**, *11* (5), 384–400. <https://doi.org/10.1038/nrd3674>.
- (39) Cheng, Y.; He, C.; Wang, M.; Ma, X.; Mo, F.; Yang, S.; Han, J.; Wei, X. Targeting Epigenetic Regulators for Cancer Therapy: Mechanisms and Advances in Clinical Trials. *Signal Transduct. Target. Ther.* **2019**, *4* (1). <https://doi.org/10.1038/s41392-019-0095-0>.
- (40) Estey, E. H. Epigenetics in Clinical Practice: The Examples of Azacitidine and Decitabine in Myelodysplasia and Acute Myeloid Leukemia. *Leukemia* **2013**, *27* (9), 1803–1812.

- <https://doi.org/10.1038/leu.2013.173>.
- (41) Grant, S.; Easley, C.; Kirkpatrick, P. Vorinostat. *Nat. Rev. Drug Discov.* **2007**, *6* (1), 21–22. <https://doi.org/10.1038/nrd2227>.
- (42) Ganesan, A.; Arimondo, P. B.; Rots, M. G.; Jeronimo, C.; Berdasco, M. The Timeline of Epigenetic Drug Discovery: From Reality to Dreams. *Clin. Epigenetics* **2019**, *11* (1), 1–17. <https://doi.org/10.1186/s13148-019-0776-0>.
- (43) Cochran, A. G.; Conery, A. R.; Sims, R. J. Bromodomains: A New Target Class for Drug Development. *Nat. Rev. Drug Discov.* **2019**, *18* (8), 609–628. <https://doi.org/10.1038/s41573-019-0030-7>.
- (44) Andrieu, G.; Belkina, A. C.; Denis, G. V. Clinical Trials for BET Inhibitors Run Ahead of the Science. *Drug Discov. Today Technol.* **2016**, *19*, 45–50. <https://doi.org/10.1016/j.ddtec.2016.06.004>.
- (45) Zhang, G.; Smith, S. G.; Zhou, M. M. Discovery of Chemical Inhibitors of Human Bromodomains. *Chem. Rev.* **2015**, *115* (21), 11625–11668. <https://doi.org/10.1021/acs.chemrev.5b00205>.
- (46) Gilham, D.; Wasiak, S.; Tsujikawa, L. M.; Halliday, C.; Norek, K.; Patel, R. G.; Kulikowski, E.; Johansson, J.; Sweeney, M.; Wong, N. C. W. RVX-208, a BET-Inhibitor for Treating Atherosclerotic Cardiovascular Disease, Raises ApoA-I/HDL and Represses Pathways That Contribute to Cardiovascular Disease. *Atherosclerosis* **2016**, *247*, 48–57. <https://doi.org/10.1016/j.atherosclerosis.2016.01.036>.
- (47) Wapenaar, H.; Dekker, F. J. Histone Acetyltransferases: Challenges in Targeting Bi-Substrate Enzymes. *Clin. Epigenetics* **2016**, *8* (1), 1–11. <https://doi.org/10.1186/s13148-016-0225-2>.

- (48) Milite, C.; Feoli, A.; Viviano, M.; Rescigno, D.; Cianciulli, A.; Balzano, A. L.; Mai, A.; Castellano, S.; Sbardella, G. The Emerging Role of Lysine Methyltransferase SETD8 in Human Diseases. *Clin. Epigenetics* **2016**, *8* (1). <https://doi.org/10.1186/s13148-016-0268-4>.
- (49) Hamamoto, R.; Komatsu, M.; Takasawa, K.; Asada, K.; Kaneko, S. Epigenetics Analysis and Integrated Analysis of Multiomics Data, Including Epigenetic Data, Using Artificial Intelligence in the Era of Precision Medicine. *Biomolecules* **2020**, *10* (1). <https://doi.org/10.3390/biom10010062>.
- (50) Hunter, P. The Second Coming of Epigenetic Drugs. *EMBO Rep.* **2015**, *16* (3), 276–279. <https://doi.org/10.15252/embr.201540121>.
- (51) Wong, K. K. DNMT1: A Key Drug Target in Triple-Negative Breast Cancer. *Semin. Cancer Biol.* **2020**, No. May. <https://doi.org/10.1016/j.semcancer.2020.05.010>.
- (52) Mizuno, S. I.; Chijiwa, T.; Okamura, T.; Akashi, K.; Fukumaki, Y.; Niho, Y.; Sasaki, H. Expression of DNA Methyltransferases DNMT1, 3A, and 3B in Normal Hematopoiesis and in Acute and Chronic Myelogenous Leukemia. *Blood* **2001**, *97* (5), 1172–1179. <https://doi.org/10.1182/blood.V97.5.1172>.
- (53) Morgan, A. E.; Davies, T. J.; McAuley, M. T. The Role of DNA Methylation in Ageing and Cancer. *Proc. Nutr. Soc.* **2018**, *77* (4), 412–422. <https://doi.org/10.1017/S0029665118000150>.
- (54) Lyko, F. The DNA Methyltransferase Family: A Versatile Toolkit for Epigenetic Regulation. *Nat. Rev. Genet.* **2018**, *19* (2), 81–92. <https://doi.org/10.1038/nrg.2017.80>.
- (55) Tuorto, F.; Herbst, F.; Alerasool, N.; Bender, S.; Popp, O.; Federico, G.; Reitter, S.; Liebers, R.; Stoecklin, G.; Gröne, H.; Dittmar, G.; Glimm, H.; Lyko, F. The TRNA

- Methyltransferase Dnmt2 Is Required for Accurate Polypeptide Synthesis during Haematopoiesis . *EMBO J.* **2015**, *34* (18), 2350–2362.
<https://doi.org/10.15252/emj.201591382>.
- (56) Subramaniam, D.; Thombre, R.; Dhar, A.; Anant, S. DNA Methyltransferases: A Novel Target for Prevention and Therapy. *Front. Oncol.* **2014**, *4 MAY* (May), 1–13.
<https://doi.org/10.3389/fonc.2014.00080>.
- (57) Morera, L.; Lübbert, M.; Jung, M. Targeting Histone Methyltransferases and Demethylases in Clinical Trials for Cancer Therapy. *Clin. Epigenetics* **2016**, *8* (1), 16.
<https://doi.org/10.1186/s13148-016-0223-4>.
- (58) Han, D.; Huang, M.; Wang, T.; Li, Z.; Chen, Y.; Liu, C.; Lei, Z.; Chu, X. Lysine Methylation of Transcription Factors in Cancer. *Cell Death Dis.* **2019**, *10* (4).
<https://doi.org/10.1038/s41419-019-1524-2>.
- (59) GUAN, X.; ZHONG, X.; MEN, W.; GONG, S.; ZHANG, L.; HAN, Y. Analysis of EHMT1 Expression and Its Correlations with Clinical Significance in Esophageal Squamous Cell Cancer. *Mol. Clin. Oncol.* **2014**, *2* (1), 76–80.
<https://doi.org/10.3892/mco.2013.207>.
- (60) Bremer, S. C. B.; Conradi, L. C.; Mechie, N. C.; Amanzada, A.; Mavropoulou, E.; Kitz, J.; Ghadimi, M.; Ellenrieder, V.; Ströbel, P.; Hessmann, E.; Gaedcke, J.; Bohnenberger, H. Enhancer of Zeste Homolog 2 in Colorectal Cancer Development and Progression. *Digestion* **2019**. <https://doi.org/10.1159/000504093>.
- (61) Qi, W.; Chan, H. M.; Teng, L.; Li, L.; Chuai, S.; Zhang, R.; Zeng, J.; Li, M.; Fan, H.; Lin, Y.; Gu, J.; Ardayfio, O.; Zhang, J. H.; Yan, X.; Fang, J.; Mi, Y.; Zhang, M.; Zhou, T.; Feng, G.; Chen, Z.; Li, G.; Yang, T.; Zhao, K.; Liu, X.; Yu, Z.; Lu, C. X.; Atadja, P.; Li,

- E. Selective Inhibition of Ezh2 by a Small Molecule Inhibitor Blocks Tumor Cells Proliferation. *Proc. Natl. Acad. Sci. U. S. A.* **2012**, *109* (52), 21360–21365.
<https://doi.org/10.1073/pnas.1210371110>.
- (62) Scheer, S.; Ackloo, S.; Medina, T. S.; Schapira, M.; Li, F.; Ward, J. A.; Lewis, A. M.; Northrop, J. P.; Richardson, P. L.; Kaniskan, H. Ü.; Shen, Y.; Liu, J.; Smil, D.; McLeod, D.; Zepeda-Velazquez, C. A.; Luo, M.; Jin, J.; Barsyte-Lovejoy, D.; Huber, K. V. M.; De Carvalho, D. D.; Vedadi, M.; Zaph, C.; Brown, P. J.; Arrowsmith, C. H. A Chemical Biology Toolbox to Study Protein Methyltransferases and Epigenetic Signaling. *Nat. Commun.* **2019**, *10* (1), 1–14. <https://doi.org/10.1038/s41467-018-07905-4>.
- (63) Wood, K.; Tellier, M.; Murphy, S. DOT1L and H3K79 Methylation in Transcription and Genomic Stability. *Biomolecules* **2018**, *8* (1), 1–16. <https://doi.org/10.3390/biom8010011>.
- (64) Zurita-Lopez, C. I.; Sandberg, T.; Kelly, R.; Clarke, S. G. Human Protein Arginine Methyltransferase 7 (PRMT7) Is a Type III Enzyme Forming ω -N G-Monomethylated Arginine Residues. *J. Biol. Chem.* **2012**, *287* (11), 7859–7870.
<https://doi.org/10.1074/jbc.M111.336271>.
- (65) Chan-Penebre, E.; Kuplast, K. G.; Majer, C. R.; Boriack-Sjodin, P. A.; Wigle, T. J.; Johnston, L. D.; Rioux, N.; Munchhof, M. J.; Jin, L.; Jacques, S. L.; West, K. A.; Lingaraj, T.; Stickland, K.; Ribich, S. A.; Raimondi, A.; Scott, M. P.; Waters, N. J.; Pollock, R. M.; Smith, J. J.; Barbash, O.; Pappalardi, M.; Ho, T. F.; Nurse, K.; Oza, K. P.; Gallagher, K. T.; Kruger, R.; Moyer, M. P.; Copeland, R. A.; Chesworth, R.; Duncan, K. W. A Selective Inhibitor of PRMT5 with in Vivo and in Vitro Potency in MCL Models. *Nat. Chem. Biol.* **2015**, *11* (6), 432–437. <https://doi.org/10.1038/nchembio.1810>.
- (66) Mai, V.; Comstock, L. R. Synthesis of an Azide-Bearing N-Mustard Analogue of S-

- Adenosyl-L-Methionine. *J. Org. Chem.* **2011**, *76* (24), 10319–10324.
<https://doi.org/10.1021/jo2019637>.
- (67) Kaminskas, E.; Farrell, A. T.; Wang, Y.; Sridhara, R.; Pazdur, R. FDA Drug Approval Summary: Azacitidine (5-azacytidine, VidazaTM) for Injectable Suspension. *Oncologist* **2005**, *10* (3), 176–182. <https://doi.org/10.1634/theoncologist.10-3-176>.
- (68) Pappano, W. N.; Guo, J.; He, Y.; Ferguson, D.; Jagadeeswaran, S.; Osterling, D. J.; Gao, W.; Spence, J. K.; Pliushchev, M.; Sweis, R. F.; Buchanan, F. G.; Michaelides, M. R.; Shoemaker, A. R.; Tse, C.; Chiang, G. G. The Histone Methyltransferase Inhibitor A-366 Uncovers a Role for G9a/GLP in the Epigenetics of Leukemia. *PLoS One* **2015**, *10* (7), 1–13. <https://doi.org/10.1371/journal.pone.0131716>.
- (69) F.S. Collins, E.S. Lander, J. Rogers, et al. International Human Genome Sequencing Consortium, Finishing the Euchromatic Sequence of the Human Genome. *Nature* **2004**, *431* (7011), 931–945.
- (70) Marinov, G. K.; Williams, B. A.; McCue, K.; Schroth, G. P.; Gertz, J.; Myers, R. M.; Wold, B. J. From Single-Cell to Cell-Pool Transcriptomes: Stochasticity in Gene Expression and RNA Splicing. *Genome Res.* **2014**, *24* (3), 496–510.
<https://doi.org/10.1101/gr.161034.113>.
- (71) Ponomarenko, E. A.; Poverennaya, E. V.; Ilgisonis, E. V.; Pyatnitskiy, M. A.; Kopylov, A. T.; Zgoda, V. G.; Lisitsa, A. V.; Archakov, A. I. The Size of the Human Proteome: The Width and Depth. *Int. J. Anal. Chem.* **2016**, *2016*. <https://doi.org/10.1155/2016/7436849>.
- (72) Eisenberg, D.; Marcotte, E. M.; Xenarios, I.; Yeates, T. O. Protein Function in the Post-Genomics Era. *Nature* **2000**, *405* (6), 823–826.
- (73) Chandramouli, K.; Qian, P.-Y. Proteomics: Challenges, Techniques and Possibilities to

- Overcome Biological Sample Complexity. *Hum. Genomics Proteomics* **2009**, *1* (1).
<https://doi.org/10.4061/2009/239204>.
- (74) Saghatelian, A.; Cravatt, B. F. Assignment of Protein Function in the Postgenomic Era. *Nat. Chem. Biol.* **2005**, *1* (3), 129. <https://doi.org/10.1038/nchembio0805-130>.
- (75) Zuhl, A. M.; Mohr, J. T.; Bachovchin, D. A.; Niessen, S.; Hsu, K. L.; Berlin, J. M.; Dochnahl, M.; López-Alberca, M. P.; Fu, G. C.; Cravatt, B. F. Competitive Activity-Based Protein Profiling Identifies Aza- β -Lactams as a Versatile Chemotype for Serine Hydrolase Inhibition. *J. Am. Chem. Soc.* **2012**, *134* (11), 5068–5071.
<https://doi.org/10.1021/ja300799t>.
- (76) Speers, A. E.; Cravatt, B. F. Chemical Strategies for Activity-Based Proteomics. *ChemBioChem* **2004**, *5* (1), 41–47. <https://doi.org/10.1002/cbic.200300721>.
- (77) Breiding, M. J. Activity-Based Protein Profiling for Mapping and Pharmacologically Interrogating Proteome-Wide Ligandable Hotspots Allison. *Physiol. Behav.* **2014**, *63* (8), 1–18. <https://doi.org/10.1016/j.copbio.2016.08.003>.Activity-Based.
- (78) Deng, H.; Lei, Q.; Wu, Y.; He, Y.; Li, W. Activity-Based Protein Profiling: Recent Advances in Medicinal Chemistry. *Eur. J. Med. Chem.* **2020**, *191*, 112151.
<https://doi.org/10.1016/j.ejmech.2020.112151>.
- (79) Bennis, H. J.; Wincott, C. J.; Tate, E. W.; Child, M. A. Activity- and Reactivity-Based Proteomics: Recent Technological Advances and Applications in Drug Discovery. *Curr. Opin. Chem. Biol.* **2021**, *60*, 20–29. <https://doi.org/10.1016/j.cbpa.2020.06.011>.
- (80) Wang, S.; Tian, Y.; Wang, M.; Wang, M.; Sun, G. B.; Sun, X. B. Advanced Activity-Based Protein Profiling Application Strategies for Drug Development. *Front. Pharmacol.* **2018**, *9* (APR), 1–9. <https://doi.org/10.3389/fphar.2018.00353>.

- (81) Demko, Z. P.; Sharpless, K. B. A Click Chemistry Approach to Tetrazoles by Huisgen 1,3-Dipolar Cycloaddition: Synthesis of 5-Sulfonyl Tetrazoles from Azides and Sulfonyl Cyanides. *Angew. Chemie - Int. Ed.* **2002**, *41* (12), 2110–2113.
[https://doi.org/10.1002/1521-3773\(20020617\)41:12<2110::AID-ANIE2110>3.0.CO;2-7](https://doi.org/10.1002/1521-3773(20020617)41:12<2110::AID-ANIE2110>3.0.CO;2-7).
- (82) Horisawa, K. Specific and Quantitative Labeling of Biomolecules Using Click Chemistry. *Front. Physiol.* **2014**, *5* (Nov), 1–6. <https://doi.org/10.3389/fphys.2014.00457>.
- (83) Martell, J.; Weerapana, E. Applications of Copper-Catalyzed Click Chemistry in Activity-Based Protein Profiling. *Molecules* **2014**, *19* (2), 1378–1393.
<https://doi.org/10.3390/molecules19021378>.
- (84) Greenbaum, D. C.; Arnold, W. D.; Lu, F.; Hayrapetian, L.; Baruch, A.; Krumrine, J.; Toba, S.; Chehade, K.; Brömme, D.; Kuntz, I. D.; Bogoy, M. Small Molecule Affinity Fingerprinting: A Tool for Enzyme Family Subclassification, Target Identification, and Inhibitor Design. *Chem. Biol.* **2002**, *9* (10), 1085–1094. [https://doi.org/10.1016/S1074-5521\(02\)00238-7](https://doi.org/10.1016/S1074-5521(02)00238-7).
- (85) Jessani, N.; Cravatt, B. F. The Development and Application of Methods for Activity-Based Protein Profiling. *Curr. Opin. Chem. Biol.* **2004**, *8* (1), 54–59.
<https://doi.org/10.1016/j.cbpa.2003.11.004>.
- (86) Wang, K.; Yang, T.; Wu, Q.; Zhao, X.; Nice, E. C.; Huang, C. Chemistry-Based Functional Proteomics for Drug Target Deconvolution. *Expert Rev. Proteomics* **2012**, *9* (3), 293–310. <https://doi.org/10.1586/epr.12.19>.
- (87) Liu, Y.; Patricelli, M. P.; Cravatt, B. F. Activity-Based Protein Profiling: The Serine Hydrolases. *Proc. Natl. Acad. Sci. U. S. A.* **1999**, *96* (26), 14694–14699.
<https://doi.org/10.1073/pnas.96.26.14694>.

- (88) Jessani, N.; Liu, Y.; Humphrey, M.; Cravatt, B. F. Enzyme Activity Profiles of the Secreted and Membrane Proteome That Depict Cancer Cell Invasiveness. *Proc. Natl. Acad. Sci. U. S. A.* **2002**, *99* (16), 10335–10340. <https://doi.org/10.1073/pnas.162187599>.
- (89) Seidah, N. G.; Chrétien, M. Eukaryotic Protein Processing: Endoproteolysis of Precursor Proteins. *Curr. Opin. Biotechnol.* **1997**, *8* (5), 602–607. [https://doi.org/10.1016/S0958-1669\(97\)80036-5](https://doi.org/10.1016/S0958-1669(97)80036-5).
- (90) Leslie, C. C. Cytosolic Phospholipase A2: Physiological Function and Role in Disease. *J. Lipid Res.* **2015**, *56* (8), 1386–1402. <https://doi.org/10.1194/jlr.R057588>.
- (91) Yves, D.; Suzan, I.; Anthony, M. Proteases and Protease Inhibitors in Tumor Progression. *Chem Bio Serpins* **1997**, 89–97.
- (92) Niphakis, M. J.; Cravatt, B. F. Enzyme Inhibitor Discovery by Activity-Based Protein Profiling. *Annu. Rev. Biochem.* **2014**, *83*, 341–377. <https://doi.org/10.1146/annurev-biochem-060713-035708>.
- (93) Shi, C.; Tiwari, D.; Wilson, D. J.; Seiler, C. L.; Schnappinger, D.; Aldrich, C. C. Bisubstrate Inhibitors of Biotin Protein Ligase in Mycobacterium Tuberculosis Resistant to Cyclonucleoside Formation. *ACS Med. Chem. Lett.* **2013**, *4* (12), 1213–1217. <https://doi.org/10.1021/ml400328a>.
- (94) Rao, R. A.; Ketkar, A. A.; Kedia, N.; Krishnamoorthy, V. K.; Lakshmanan, V.; Kumar, P.; Mohanty, A.; Kumar, S. D.; Raja, S. O.; Gulyani, A.; Chaturvedi, C. P.; Brand, M.; Palakodeti, D.; Rampalli, S. KMT 1 Family Methyltransferases Regulate Heterochromatin–Nuclear Periphery Tethering via Histone and Non-histone Protein Methylation. *EMBO Rep.* **2019**, *20* (5), 1–20. <https://doi.org/10.15252/embr.201643260>.
- (95) Avvakumov, G. V.; Walker, J. R.; Xue, S.; Finerty, P. J.; Mackenzie, F.; Newman, E. M.;

- Dhe-Paganon, S. Amino-Terminal Dimerization, NRDP1-Rhodanese Interaction, and Inhibited Catalytic Domain Conformation of the Ubiquitin-Specific Protease 8 (USP8). *J. Biol. Chem.* **2006**, *281* (49), 38061–38070. <https://doi.org/10.1074/jbc.M606704200>.
- (96) Małecki, J.; Ho, A. Y. Y.; Moen, A.; Dahl, H. A.; Falnes, P. Human METTL20 Is a Mitochondrial Lysine Methyltransferase That Targets the β Subunit of Electron Transfer Flavoprotein (ETF β) and Modulates Its Activity. *J. Biol. Chem.* **2015**, *290* (1), 423–434. <https://doi.org/10.1074/jbc.M114.614115>.
- (97) Flinn, A. M.; Gennery, A. R. Adenosine Deaminase Deficiency: A Review. *Orphanet J. Rare Dis.* **2018**, *13* (1), 5–11. <https://doi.org/10.1186/s13023-018-0807-5>.
- (98) Sauer, A. V.; Brigida, I.; Carriglio, N.; Aiuti, A. Autoimmune Dysregulation and Purine Metabolism in Adenosine Deaminase Deficiency. *Front. Immunol.* **2012**, *3* (AUG), 1–19. <https://doi.org/10.3389/fimmu.2012.00265>.
- (99) Campagna-Slater, V.; Mok, M. W.; Nguyen, K. T.; Feher, M.; Najmanovich, R.; Schapira, M. Structural Chemistry of the Histone Methyltransferases Cofactor Binding Site. *J. Chem. Inf. Model.* **2011**, *51* (3), 612–623. <https://doi.org/10.1021/ci100479z>.